University of Alberta

Source Apportionment of Chiral Persistent Organic Pollutants

by

Brian Justin Asher

A thesis submitted to the Faculty of Graduate Studies and Research
in partial fulfillment of the requirements for the degree of

Doctor of Philosophy

Chemistry

Fall 2011
Edmonton, Alberta

Abstract

This thesis explores the fate of chiral compounds in the environment, with a focus on the utility of enantiomer measurements for elucidating pollutant sources.

The enantiomer distributions of several chiral polychlorinated biphenyls (PCBs) were measured in the water column of the Hudson River Estuary, and the atmosphere above it, to provide evidence for the relative contribution of fresh versus historical sources. Racemic distributions were observed in air for all chiral congeners detected, but nonracemic distributions for PCB 95 occurred throughout the water column. The results suggest that the source of this congener, and potentially other congeners, to the local aquatic food web is weathered historical contamination. In contrast, the source of PCBs to the local atmosphere is likely fresh releases from the surrounding dense urban centre.

The choice of peak integration technique and its effect on the measurement of chiral contaminants was studied. The common valley drop method was shown to bias calculated enantiomer fractions to a greater extent than a deconvolution method. Typical biases when using the valley drop method were shown to have a dramatic effect on environmental calculations that employ the enantiomer fraction.

The enantiomer distributions and concentrations of PCBs in soil and air were determined in the region surrounding a hazardous waste incinerator in Alberta, Canada. Concentrations and homologue patterns showed that the incinerator was the primary source of PCBs to the region. Enantiomer

distributions in air were largely racemic, yet nonracemic signatures were observed in soil. This data suggests that atmospheric PCBs in the region likely originate from recent emissions from the incinerator, and not revolatilization of historically deposited contaminants from soil.

By examining concentrations, as well as isomer and enantiomer distributions of perfluorooctane sulfonate (PFOS) in several aquatic species, the impact of precursor compounds on concentrations of PFOS in the aquatic food web of Lake Ontario was deduced. Racemic distributions were observed in some forage fish, but nonracemic distributions were observed in invertebrate species as well as lake trout. Since the biotransformation of precursors to PFOS is known to be enantioselective, the observed nonracemic signatures in some aquatic species points to an influence of precursors on the local aquatic organisms body burdens of PFOS.

Acknowledgement

I gratefully acknowledge each of my co-supervisors, Charles Wong and Jonathan Martin for their mentorship and support during my graduate studies. At different times, you provided me with thoughtful responses and advice to my sometimes-naïve questions. From each of you, I learned a unique perspective and style, which positively influenced my development as a scientist, and I consider myself enriched from having worked with both of you.

A special thanks goes to my fellow grad students in the Wong group: Matt Ross, Sherri MacLeod, Nick Warner, Derek Bleackley, Ev McClure, Vicki Cooper, Josh Morrissey and Lisa Nikolai. Matt and Sherri, I'll always cherish our countless long discussions about science, politics, and life.

Thanks to James Harynuk, Lisa D'Agostino, Jenilee Way, Kathy Yackulic, Yuan Wang, and Jon Benskin at the University of Alberta, Lisa Rodenburg, Shu Yan, and Songyan Du from Rutgers University, Amila De Silva, Christine Spencer, Derek Muir, and Sean Backus at Environment Canada, all of whom played important roles in my work. An extra thanks goes to those who I coerced into putting up with snow, mud, and stuck trucks as we wandered through the forest searching for air samplers. Thanks also to members of the Martin group at U of A and the Wong group at U of W for helpful feedback and preparation.

Funding which supported my research was provided by the Natural Sciences and Engineering Research Council (NSERC), and the Canada Research Chairs Program to Dr. Wong. The Hudson River Estuary work was additionally funded by the New Jersey Department of Environmental Protection and the

Hudson River Foundation. Thank you to NSERC for awarding me two postgraduate scholarships, Alberta Ingenuity for awarding me a studentship, the University of Alberta, for the Walter H. Johns graduate fellowships, and the Society of Environmental Toxicology and Chemistry for student travel awards and a Student Training Exchange Opportunity award.

To Mom and Dad, thank you for leading me down this path and for reminding me what I'm capable of. Your encouragement and unconditional love truly motivated me when I felt discouraged.

To my incredible wife, best friend, and love: Echo, thank you for walking with me, every step of the way, on this trek. You were my de-stresser, my sounding board, and my perspective away from the lab, the books, and the laptop. I truly could not have done this without your patience, understanding, and love.

Table of Contents

List of Figures

List of Tables

List of Symbols, Nomenclature, or Abbreviations

ANOVA	analysis of variance
A_s	peak asymmetry
CAO	Coastal Atlantic Ocean
CSIA	compound specific isotope analysis
CYP	cytochrome p-450
DDE	1,1-bis-(4-chlorophenyl)-2,2-dichloroethene
DDT	1,1,1-trichloro-2,2-di(4-chlorophenyl)ethane
D_{eff}	effective diffusivity
d_f	film thickness
d_p	particle diameter
d.w.	dry weight
DFR	deviation from racemic
DM	deconvolution method
DRE	destruction and removal efficiency
ECD	electron capture detector
ECF	electrochemical fluorination
EF	enantiomer fraction
ER	enantiomer ratio
GC-MS	gas chromatography-mass spectrometry
GC-MS/MS	gas chromatography-tandem mass spectrometry
GEMG	Guassian-exponentially modified Guassian function
HCB	hexachlorobenzene
HCH	hexachlorocyclohexane
HPLC	high performance liquid chromatography
HRE	Hudson River Estuary
k_m	biotransformation rate constant
Kow	octanol-water partition coefficient
N-EtFOSA	N-ethyl perfluorooctane sulfonamide
N-EtFOSE	N-ethyl perfluorooctane sulfonamidoethanol
N-MeFOSA	N-methyl perfluorooctane sulfonamide
NR	nonracemic
PAH	polycyclic aromatic hydrocarbon
PCA	principal component analysis
PCB	polychlorinated biphenyl
PCDD	polychlorinated dibenzodioxin

PCDF	polychlorinated dibenzofuran
PFC	perfluorinated compound
PFNA	perfluorononanoic acid
PFOA	perfluorooctanoic acid
PFOS	perfluorooctane sulfonate
PFOSA	perfluorooctane sulfonamide
PFOSi	perfluorooctane sulfinate
PMF	positive matrix factorization
POP	persistent organic pollutant
POSF	perfluorooctane sulfonyl fluoride
PreFOS	perfluorooctane sulfonate precursor
PUF	polyurethane foam
QFF	quartz fibre filter
r^2	coefficient of determination
R_s	peak resolution
σ_{EF}	standard deviation of enantiomer fraction
S/N	signal to noise ratio
SD	standard deviation
SHTC	Swan Hills Treatment Centre
TSM	total suspended matter
VDM	valley drop method

Chapter 1: Sources of Persistent Organic Pollutants

A portion of this chapter has been previously published as Martin, J.W., Asher, B.J., Beesoon, S., Benskin, J.P., and Ross, M.S. PFOS or PreFOS? Are perfluorooctane sulfonate precursors (PreFOS) important determinants of human and environmental perfluorooctane sulfonate (PFOS) exposure? Journal of Environmental Monitoring (2010) 12, 1979-2004. BJA's contribution to this paper is captured in Section 1.3.5.

1.1 Persistent organic pollutants

The research in this body of work focuses on two separate chemical compounds or classes of compound: polychlorinated biphenyls (PCBs) and perfluorooctanesulfonate (PFOS). While the molecular structures, physical and chemical properties, biological effects, and historical uses of these compounds are vastly different, both belong to a notorious group of chemicals, known collectively as *persistent organic pollutants*, or POPs. POPs are considered high priority chemical contaminants typically based on several critical factors. These include their resistance to degradation, their ability to bioaccumulate in the tissues of organisms, and their potential to have adverse impacts on the health of humans and the environment. Additionally, POPs have the ability to undergo long-range transport, leading to their distribution across the globe, including the contamination of remote regions far from where they are manufactured, used, and disposed. Due to concerns about these compounds, policy makers at both the national and international level have committed to the elimination of these compounds from production and use, and to the reduction of their concentrations in the environment.

Most notably, the Stockholm Convention on Persistent Organic Pollutants is an international treaty that came into force in May 2004, and was ratified by 173 countries including Canada as of April 2011. Participating countries agreed to eliminate or reduce levels of (initially) twelve priority POPs, with 9 additional pollutants (including PFOS) added in May 2009 [1]. Examples of these compounds include the pesticides DDT and α- and β-hexachlorocyclohexane

(HCH), industrial chemicals like PCBs, and unintentional byproducts such as polychlorinated dibenzodioxins and polychlorinated dibenzofurans (PCDD/Fs). While production and use of many of these compounds has been halted or significantly restricted – some have been for decades – most are still widely distributed in the environment. For example, production of PCBs was halted in North America in the late 1970s, but existing stocks of these compounds are ubiquitous. PCBs are still present in transformers and other electrical equipment, as well as building materials in urban regions [2]. In the environment, they are bound to soil and sediment at contaminated sites, and are still at significant concentrations in flora and fauna around the world. Similarly, DDT, which was also banned in North America in the 1970s, is still present in significant concentrations in Canadian and US agricultural soil, and continues to contribute to elevated atmospheric concentrations at sites near historical applications of the pesticide [3, 4].

Eliminating existing stocks and "hot spots" of contamination is not trivial. For policies such as the Stockholm Convention to be effective, these sources of POPs must be identified. Scientists face many challenges in this regard, including apportioning the importance of multiple point and diffuse sources, distinguishing historical contamination versus recent emissions, and determining the contribution of related precursor compounds to current contaminant levels. Knowledge of continuing sources of POPs will allow policy makers to make informed choices about how best to reduce environmental contamination.

Furthermore, a thorough understanding of where POPs originate from will enable us to make more accurate predictions of future contamination levels.

This thesis describes the measurement of enantiomer signatures of chiral contaminants as a tool to help resolve some of these challenges. A multitude of other techniques for determining sources of POPs in the environment have been employed, and are briefly discussed in the following section. This is followed by a brief discussion on the properties, and environmental fate and effects of the two classes of contaminants studied in this thesis—PCBs and PFOS, and the role of chirality for these classes. Finally, the outline of the studies comprising this thesis is detailed.

1.2 Methods of Source Determination

1.2.1 Temperature models

A continuing source of contaminants to the atmosphere is the volatilization of previously deposited contaminants from environmental surfaces such as soil and water [5, 6]. As a result, atmospheric concentrations of semivolatile contaminants frequently show a dependence on atmospheric temperature, modeled by the Clausius-Clapeyron equation:

$$\ln P = a_0 + \frac{\Delta H_{SA}}{RT} \qquad \text{Equation 1-1}$$

where P represents the partial pressure of the contaminant, a_0 is a constant (intercept), ΔH_{SA} is the contaminant's enthalpy of volatilization from environmental surfaces to air, R is the gas constant, and T is the air temperature. Although the slope of the ln P versus 1/T relationship, based on environmental

data, generally does not correspond to a thermodynamically meaningful ΔH_{SA} (and is often reported simply as the Clausius-Clapeyron slope, a_1 instead), Wania et al. suggested that such a slope has utility for source determination [7]. Steeper slopes (i.e. a greater dependence on temperature) indicate a predominance of local contaminant sources, via volatilization from environmental surfaces, while shallow slopes indicate that atmospheric concentrations are dominated by long-range advective-diffusive transport [7]. Such a relationship has been shown to be unreliable under various scenarios, including when a significant number of measurements are at low (near-freezing) temperatures, when contaminant concentrations are low, and when data sets are small ($n<25$) [8].

1.2.2 Contaminant ratios

Environmental chemical analysis most often produces concentration data for several related analytes simultaneously, and the relative concentrations of these compounds are often used as evidence when determining contaminant sources. Specifically, the ratio of multiple components of a commercial mixture, such as the ratio of α- and γ-HCH concentrations, have been used to differentiate between recent and historical pesticide applications (technical HCH formulations are 70% α-HCH, while more recent-use lindane is >99% γ-HCH [9]). Thus, a low α/γ ratio is indicative of a source comprised of recent lindane use. For example, Haugen et al. showed seasonal variation in the α/γ ratio in the air of southern Norway, corresponding to usage patterns of lindane in western Europe [10]. Likewise, Qiu et al. analysed the ratio of *o,p'*-DDT to *p,p'*-DDT to apportion the

DDT-impurity in the current-use pesticide Dicofol as a contributing source of DDT to Chinese air [11]. More recently, De Silva et al. used isomer profiling to distinguish between sources of perfluorooctanoate (PFOA) [12]. PFOA is manufactured by two methods: electrochemical fluorination (ECF), which produces approximately 22% branched isomers, and telomerization, which produces exclusively linear compounds. In that study, analysis of the percent branched compositions in polar bears was used to infer differences in the relative contributions of ECF inputs between a Canadian and Greenland location [12]. In addition to different components of technical mixtures, the ratios of parent compounds to metabolites have been used to determine contaminant sources. For example, the ratio of DDT to its dechlorinated breakdown product DDE can be used to verify recent pesticide applications. Tavares et al. used this principle to deduce recent DDT application at some sites in All Saints Bay, Brazil [13]. One difficulty in using contaminant ratios for source profiling is that the compounds that are subject to these ratios can have important differences in their environmental distribution as well as their rates of degradation, confounding the interpretation of these ratios. For example, α-HCH has a longer atmospheric lifetime than γ-HCH, possibly due to differences in rates of reaction with hydroxyl radicals, resulting in skewed ratios in Arctic air [9].

1.2.3 Chemometrics

Chemometrics is a general term used to describe a set of statistical techniques used for extracting potentially useful information from complex

chemical analysis data sets. Many environmental monitoring studies collect large amounts of chemical concentration data (sometimes dozens or even hundreds of different chemical species are simultaneously quantified), physical parameters such as soil or water characteristics, and environmental parameters such as temperature data and wind speed. Several different statistical methods can be employed to transform this large number of parameters into a greatly reduced number of contributions. Chemometrics is a broad and burgeoning field which has been extensively reviewed elsewhere [14, 15] and is only briefly discussed here, in the context of environmental source apportionment. Most commonly, principal component analysis (PCA) is used to extract orthogonal contributions, called "principal components," which can account for the majority of the variance in the data. Interpretation of these principal components can be used to deduce both point and diffuse sources, particularly if the compositions of the sources are well characterized. For example, Harrison et al. measured airborne polycyclic aromatic hydrocarbons (PAHs) along with metal species and used PCA followed by multiple linear regression analysis to apportion several sources of these compounds to Birmingham, U.K. air, including vehicle emissions, and oil and coal combustion [16]. The use of PCA for source apportionment is limited, however, as the method has difficulty in handling missing data and non-detects, and the interpretation of the determined principal components (i.e. attributing them to specific sources in the case of source apportionment) is difficult [14].

More recent and robust chemometric techniques, such as positive matrix factorization (PMF) [17], chemical mass balance modeling [18], and potential

source contribution function receptor modeling [19] have been applied to source apportionment problems. For example, Du et al. used PMF analysis to identify several important sources of PCBs in the Delaware River, including sediment resuspension, combined sewer overflows, and waste water treatment plants as major contributors [20]. Li et al. applied the U.S. EPA's widely used chemical mass balance receptor model and accompanying software (CMB8.2) to apportion sources of PAHs in lake sediment quantitatively [21]. Finally, the potential source contribution function is a probabilistic model that divides up a study site into grid cells, and uses receptor concentrations and air parcel back trajectories to estimate source "hot spots," which has been demonstrated for determining sources of numerous POPs, including organochlorine pesticides [22] and PCBs [23]. A significant advantage of chemometric techniques is that they can be applied quickly and easily with appropriate software. However, these techniques also require a large number of samples to be effective. Furthermore, the resulting mathematical models can often be complex, and are subject to misinterpretation.

1.2.4 Compound specific stable isotope analysis (CSIA)

This technique is based on the principle that the isotope signatures of an environmental contaminant will be reflective of the specific conditions during its manufacture. Thus, small differences in isotope signatures between manufacturers can be used to "fingerprint" a contaminant's source. CSIA has been used successfully to match duck samples from the Housatonic River in Massachusetts to the Aroclor mixture responsible for its contamination [24]. In

addition, ^{13}C isotopes have been used to identify the industrial source of PAHs to sediment from the St. Lawrence River [25]. Because of the high precision required to acquire isotope data suitable for source apportionment, CSIA requires the use of specialized instrumentation, namely an isotope-ratio mass spectrometer, capable of enhanced mass resolution. Unfortunately, poor sensitivity of CSIA instrumentation (i.e., limits of detection of ng injected compared to pg and lower for typical mass spectrometry for trace environmental analysis) remains a major drawback to its widespread application, and has limited its use in all but the most highly contaminated sites [26].

1.3 Background on two contaminants: PCBs and PFOS

1.3.1 Polychlorinated Biphenyls – Background, Sources, and Properties

Owing to their heavy use throughout most of the twentieth century, PCBs are among the most prevalent and highly concentrated anthropogenic contaminants worldwide. PCBs are a class of 209 different chemicals (referred individually as "congeners"), based on the theoretical number of unique combinations of chlorine atoms (between one and ten) that can be substituted on a biphenyl backbone (Figure 1-1). For simplicity, PCB congeners are generally referred to using the systematic numbering (1 to 209) convention developed by Ballschmiter and Zell (e.g. 2,2',3,3',6,6'-hexachlorobiphenyl is given the name PCB 136) [27]. Among industrial uses, these compounds were primarily used as dielectric fluids in electrical transformers and capacitors. PCBs were also used as coolants and in heat transfer fluid applications, as well as additives in inks and

pigments, sealants, and carbonless copy paper. The industrial utility of these compounds is due to a number of important physical and chemical properties, including high dielectric constants and significant stability to thermal and chemical degradation. In North America, PCBs were primarily manufactured by Monsanto Chemical Company, and were sold, not as pure compounds, but as mixtures of dozens of congeners called Aroclors with varying weight percentages of chlorine. Manufacturing of PCBs also occurred in other countries, including Russia, Japan, China, Germany, Czechoslovakia, and the United Kingdom. An estimated 1.3×10^9 kg were produced worldwide between 1930 and 1993 with the majority (70%) of this amount composed of the tri-, tetra-, and pentachlorinated congeners [28]. While Canada did not engage in the manufacture of PCBs, *ca.* 40,000 tonnes were imported, with about 24,000 tonnes accounted for in in-use applications, storage, and those destroyed by incineration. The remaining 16,000 tonnes were released by either direct disposal into the environment, or via vapourization from transformers, capacitors, sealants, and releases from other PCB applications [29].

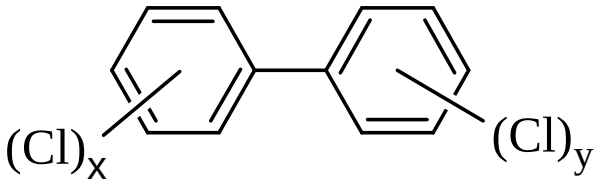

Figure 1-1: *General structure of a PCB molecule with the general formula* $C_{12}H_{10-n}Cl_n$

Like many environmental contaminants, some of the physical and chemical properties that made PCBs so useful have contributed to their global

environmental problems. These compounds are hydrophobic – values of log K_{ow} for PCBs range from 4 to 8, and generally increase with an increased degree of chlorination [30]. As a result, PCBs associate readily with soil, sediment, and biological material. In addition, PCBs have been shown to bioaccumulate, increasing to higher concentrations at higher trophic levels in food webs [31, 32]. In the environment, PCBs are resistant to photolysis, hydrolysis, and biodegradation, leading to their overall persistence. PCBs are also considered to be semi-volatile, as their vapour pressure is high enough to allow their long-range transport to regions far from their manufacture use, and disposal. In addition, the cold condensation effect has led to increased accumulation of semi-volatile compounds with latitude in polar regions [33] and with altitudes in mountain ranges [34], leading to significant contamination of once-pristine regions.

1.3.2 Health Effects of PCBs.

PCBs, while not considered to be acutely toxic, have been shown to cause numerous adverse health effects in both human and wildlife populations. Many PCB congeners, particularly those that are coplanar – containing zero or one *ortho* chlorines – are well known to exhibit "dioxin-like" activity. Along with chlorinated dioxins and furans, these compounds act as agonists of the aryl-hydrocarbon receptor in organisms, resulting in the induction of CYP enzymes, a mechanism believed to be responsible for carcinogenicity, among other toxic effects [35]. Numerous case-control studies have linked PCB exposure to cancer, including non-Hodgkin's lymphoma in the occupationally exposed [36] and in

general populations [37]. Increased mortality in several cancers of the gastrointestinal tract have been found in capacitor manufacturing workers [38]. In addition, several Aroclors, when administered to rats, induce liver and stomach tumours [39, 40]. PCBs are considered a probable human carcinogen by both the Environmental Protection Agency [41] and the International Agency for Research on Cancer. In addition to carcinogenicity, PCBs are neurotoxic, as demonstrated by a study showing reduced intellectual capacity in children who had been exposed *in utero* via maternal ingestion of PCB-contaminated Lake Michigan fish [42] – a disturbing effect that has been replicated in other studies [43, 44]. Other toxic effects in humans include endocrine disrupting effects [45] and immune system dysfunction [46]. Numerous studies have demonstrated the negative health impacts of PCBs to wildlife as well. Examples include: a negative correlation between reproductive output and PCB concentration (among other organochlorine compounds) in Glaucous gulls [47]; endocrine disrupting effects in seals which were fed highly PCB-contaminated fish [48]; and reproductive and endocrine effects in laboratory-exposed mink [49].

1.3.3 Perfluorooctane sulfonate – Background, Sources, and Properties

Perfluorooctane sulfonate (PFOS) has emerged as a global contaminant of significant research interest. PFOS was produced, primarily by the 3M Company, throughout the latter half of the 20th century, with an estimated global production volume of 96,000 tonnes [50]. Synthesis of PFOS was conducted by means of electrochemical fluorination, producing a mixture of approximately 70% linear

and 30% branched compounds [51]. Applications of PFOS have utilized its surface activity, as the surfactant molecule has both hydrophobic and lipophobic characteristics, with high chemical stability. Uses of PFOS include water and oil repellant coatings on textiles and paper, metal plating, and as a major ingredient in fire-fighting foams. PFOS ($CF_3(CF_2)_7SO_3^-$) is part of a larger class of chemicals generally referred to as perfluoroalkyl compounds (PFCs), which include the prevalent PFOA, other perfluorocarboxylic acids, perfluoroalkyl sulfonates of differing chain length, and several classes of precursor compounds (compounds capable of transforming in the environment to perfluorocarboxylates and perfluoroalkylsulfonates, respectively). However, the focus in this section will be on PFOS and its precursors.

The structure of PFOS is very different from legacy pollutants, such as PCBs, DDTs, and HCHs, leading to its unusual properties and environmental distribution compared to other POPs. In the environment, PFOS readily dissociates into its anionic form, given its low pK_a. As a result, the compound has essentially negligible vapour pressure and high water solubility. Since PFOS is a surfactant, its K_{ow} cannot be accurately determined using standard methods. However, several studies have shown that PFOS is indeed bioaccumulative, with elevated biomagnification factors measured in both laboratory and field studies [52-54]. PFOS is also extremely persistent in the environment. To date, no study has demonstrated measurable degradation (biotic or abiotic) of these compounds under environmentally relevant conditions.

1.3.4 Health Effects of PFOS

Human blood samples from around the world have been found to contain PFOS, usually at concentrations higher than all other PFCs [55, 56]. Since PFOS is not metabolized, and undergoes significant enterohepatic recirculation as well as binding to blood proteins, long elimination half-lives in humans (in excess of 5 years) have been observed [57]. Chronic toxicity studies on monkeys resulted in observed immune system dysfunction, reduced body weight, increased liver weight, and disruption in serum levels of cholesterol and triiodothyronin [58]. In addition PFOS has been shown to be capable of peroxisome proliferation [59], as well as inhibit gap junction cellular communication in rats [60]. PFOS has also been implicated as a developmental toxicant, as rats exposed prenatally had significantly reduced survival after birth [61]. Similar developmental effects have also been observed in wildlife including reduced hatchability of white leghorn chicken eggs [62], reduced survival in quails [63], and delayed metamorphosis and reduced growth in frogs [64].

1.3.5 PFOS and "PreFOS"

Numerous studies have confirmed that PFOS is globally distributed, having been detected in wildlife around the world, including in foodwebs close to urbanized centres, as well as remote locations such as the arctic [53, 65, 66]. Yet despite this ubiquity, the sources of PFOS to humans and wildlife, are not fully understood. Similar to other PFCs, PFOS can enter the environment via either direct emission through the manufacture and end use of PFOS-containing

products, or via indirect sources such as the degradation of PFOS precursors. PFOS precursors, referred to here as "PreFOS," such as perfluorooctanesulfonamide (PFOSA), are higher molecular weight derivatives that can degrade, biotically or abiotically, to PFOS. These compounds are widely detected in the environment, and several studies have demonstrated their transformation to PFOS, which have been comprehensively summarized elsewhere [67]. For example, PFOS was shown to be formed from a sulfonamide PreFOS molecule via aerobic biotransformation in activated sludge [68]. The formation of PFOS from PreFOS has also been observed *in vitro* with rat liver slices [69] and *in vivo* with female rats [70].

These findings lead to an important debate: To what extent do precursors contribute to the levels of PFOS in humans and wildlife? To answer this question as it relates to humans, Vestergren et al. performed exposure modeling to estimate the contribution of precursors and concluded that under a "high" exposure scenario, precursors may account for a large proportion of PFOS exposure [71]. However, thus far, empirical evidence for the environmental importance of PreFOS has come in the form of monitoring studies, by considering the relative concentrations of PFOS and PreFOS in environmental samples, temporal trends in these concentrations, and their statistical correlations. These studies are discussed in the following sections.

1.3.5.1 Relative concentrations of PFOS and Precursors

PFOS and its precursors have been detected worldwide in seawater, river water, air, soil, sediment, and precipitation. In order to elucidate sources of PFOS in the open environment, analysis of the relative concentrations of PFOS and its precursors may provide some insight. Relative concentrations of other PFCs have been used previously to differentiate contaminant sources. For example, Simcik et al. [72] found that the concentration ratio of perfluoroheptanoic acid to perfluorooctanoic acid increased with increasing distance from non-atmospheric sources, and concluded that such a ratio can be used as a tracer of atmospheric contributions of perfluorinated carboxylates. However, an analogous trend for perfluorinated sulfonates was not assessed. Generally, concentrations of PFOS exceed those of PreFOS by one or more orders of magnitude. Concentrations of PFOS in open ocean seawater samples are, as expected, far lower (by 2-3 orders of magnitude) than those of water bodies near urban and industrial regions (e.g. [73]). However, some exceptions to this trend have occurred. Ahrens et al. [74] detected PFCs along a longitudinal gradients in the North and South Atlantic Ocean and observed detectable concentrations for PFOSA, but no other PFCs, south of the equator, including latitudes as far south as 4º S. In this case, the authors suggested that the role of atmospheric transport of this precursor may be important to its detection in this region. Generally, however, PFOS is found to be far more prevalent in water samples than its precursors, namely PFOSA. Reasons for this overall trend are likely due to several factors, including greater production volumes (although the quantities of precursors produced are largely unknown

[50]), and significantly different environmental disposition (sulfonamides are far more likely to volatilize, and to sorb to sediments than sulfonates [75]). Finally, the greater prevalence of PFOS relative to its precursors suggests that oceanic transport, as a mechanism of long range transport to the arctic, is a greater contributor of direct PFOS emissions than precursors.

PFOS and PreFOS have been detected in air samples worldwide. The prevalence of perfluorinated contaminants in air has become a subject of considerable importance, given the compounds' detection in remote regions such as the Arctic and Antarctic, and the need for a thorough understanding of their long-range transport mechanisms. As a result of the negligible volatility of PFOS, most studies of PFCs in air fail to detect PFOS in the gas phase, although Kim et al. [76] detected measurable concentrations in both the gas and particulate phase of air from Albany, NY. In air, PFOS, if measured, is primarily detected in the particulate fraction of air samples, and is generally higher in concentration than its precursors. For example, Barber et al. found average concentrations of 46 pg/m^3 in particulate phase samples from Manchester, UK, higher than the sum of FOSA+FOSE precursors (30 pg/m^3) [77]. Detection of both PFOS and PreFOS on particulate matter in that study, as well as other studies [78-81] suggests that airborne transport of particulate matter may be another means of direct long range transport that warrants further consideration. Most studies, however, consider the movement of PreFOS in the gas-phase to be the major atmospheric transport route, as their volatility dictates that they exist primarily in the gas phase [75]. In addition to PFOSA, other precursors such as *N*-MeFOSE and *N*-EtFOSE are

regularly detected in gas-phase air samples. Evidence for the long-range transport of PreFOS in air is further supported by measurements of these compounds in the arctic atmosphere. Shoeib et al. [78] found average gas-phase concentrations of 8.30 and 1.87 pg/m^3 for *N*-MeFOSE and *N*-EtFOSE, respectively, for cruise samples in the Canadian Archipelago and North Atlantic Ocean, with similar gas-phase concentrations observed in Toronto, Canada, a heavily urbanized centre.

In contrast to abiotic samples, the relative concentrations of PFOS and precursors in biological samples are far more variable. Houde et al. [82] summarized concentrations of PFCs including PFOS and PFOSA in biota for studies up to 2006. Numerous studies have found concentrations of PFOS exceeding PFOSA by one or more orders of magnitude, similar to the abiotic samples discussed above, including in mink samples from the United States [54], polar bears from the Hudson Bay [83] and Greenland [84], numerous bird species from Japan [85], and harbour seals from the northwest Atlantic [86]. There are, however, several studies that have detected concentrations of precursors at approximately equal or greater amounts to those of PFOS. Martin et al. [87] observed higher proportions of PFOSA, and indeed higher overall PFOS concentrations, among benthic organisms such as *diporeia* (280 ng/g PFOS, 180 ng/g PFOSA) and slimy sculpin (450 ng/g PFOS, 150 ng/g PFOSA) compared to higher trophic organisms (e.g. Lake Trout, 170 ng/g PFOS, 16 ng/g PFOSA) in a food web of Lake Ontario. This evidence may indicate a greater contribution of sediment-bound precursors to the levels of PFCs in these organisms. Greater or similar concentrations of precursors compared with the parent PFOS have also

been found in Minke whales and long-finned pilot whales from Greenland [84] and bottlenose dolphins from the Adriatic Sea [88]. Certainly, the presence of high concentrations of precursors in biological or abiotic samples can be taken as evidence that precursors are relatively important contaminants (potentially influenced by localized sources of precursors), especially given precursors' ability to be biotransformed into PFOS [69]. Conversely, a high concentration of precursors relative to PFOS in biological samples may indicate an organism's lack of ability to biotransform the precursor. In addition, relative concentrations of PFOS to precursors in biota may be affected by the presence of local sources, and the dynamics of the local food web. As a result, caution should be exercised when drawing conclusions on the importance of precursors based on the interpretation of concentration data alone.

1.3.5.2 Temporal Trends

Analysis of temporal trends of PFOS and PreFOS environmental concentrations provide some clues as to the relative importance of direct and indirect sources of PFOS. Much of this evidence comes from studies of biological samples in the Arctic. Butt et al. [89] observed significant increases over time in PFOS concentrations in liver samples from ringed seals at two sites in the Canadian arctic, Resolute Bay (1972- 2000; ca.10-fold increase) and Arviat (1992-1998; ca. 4-fold increase). This was followed by a rapid decrease in both PFOS and PFOSA concentrations in the following years up until 2005, which corresponded with the phase-out of POSF production by 3M in 2001. Such a

rapid decline (half lives of 3.2±0.9 and 4.6±9.2 years for PFOS in Arviat and Resolute Bay, respectively) after the phase-out is suggestive of a strong atmospheric source contribution (i.e. volatile precursors) to body burdens of PFOS in local ringed seal. Similarly, northern sea otters in Alaska showed a decrease (by approximately an order of magnitude from peak concentrations) in PFOS and PFOSA concentrations in the years following the phase-out, with PFOSA concentrations at or above PFOS concentrations in the mid to late 90s, and dropping below detection limits (<1.7 ng/g) in the sampling years 2004 to 2007 [90]. This data suggests a cut-off of precursor sources, followed by rapid elimination of PFOSA, via biodegradation to PFOS.

In contrast, several other studies of biological samples in the Arctic and elsewhere have observed temporal trends that failed to demonstrate a similar expected decrease in PFOS and/or precursor concentrations. PFOS concentrations in peregrine falcon eggs in Sweden [91] showed ten-fold increases in PFOS concentrations in the '70s and '80s corresponding to increases in PFOS and PreFOS production during that time, but no significant post-2000 decrease in concentration of these contaminants was observed. Meanwhile, Bossi et al. [92] found concentrations of PFOS in ringed seal livers in East Greenland continue to increase after the phase-out. Likewise, Dietz et al. [93] observed concentrations of PFOS (but not PFOSA) in East Greenland polar bears increase significantly in the years following the phase-out. This observed "time lag" in PFOS concentrations was explained by a greater importance of slow oceanic transport of PFOS for this

region of the arctic, and a far lesser source contribution of atmospheric transport of precursors.

Recent changes in PFOS and precursor concentrations have been observed in nonpolar regions as well. Ahrens et al. [94] observed decreasing concentrations of PFOS and the precursors PFOSA and PFOSi in harbour seals from the German Bight (1999-2008), with similar elimination half-lives (5.6±18.9 and 2.8±0.9 years for PFOS and PFOSA, respectively) to those observed by Butt et al. [89]. Furdui et al. [95] observed an increase in PFOS and PFOSA concentrations from 1979 to 1993 in Lake Ontario lake trout, followed by a decline. A similar trend was observed by Martin et al. [87], who suggested changes in food web structure by invasive zebra mussels in Lake Ontario may be responsible for the concentration change. However, stable nitrogen isotope analysis by Furdui et al. [95] indicated that no trophic changes in lake trout were observed over this time period. The use of temporal trends in assessing the role of atmospheric inputs of precursors at nonpolar (non-remote) regions is problematic, since changes in contaminant levels are primarily affected by local sources of PFCs, and thus the rapidity of these changes are primarily affected by changes in their local usage and disposal. Furthermore, since 3M's phase-out was relatively recent, the majority of temporal trend studies to date have a limited number of time points post-phase-out, reducing the statistical certainty of any observed concentration increase or decrease. Future studies with improved temporal resolution may provide a clearer picture of PFC contamination trends and the role of precursors as a source of PFOS.

1.3.5.3 Correlations between PFOS and PFOSA

Numerous studies have attempted to correlate concentrations of PFOS and PFOSA on an individual sample basis to infer the importance of PFOSA, and by extension precursors in general, to the body burdens of PFOS. Such correlations are generally performed for PFOSA, and not with other precursors, since PFOSA is the most frequently analysed and detected precursor compound. A list of these correlations, with the type of biological sample (as well as correlations involving abiotic samples), its location, and the details of the statistical correlation is listed in Table 1-1. In most cases, the existence of a correlation between PFOS and PFOSA has been used to imply that atmospheric deposition of precursors plays an important role in the levels of PFOS. Strictly speaking, correlations between PFOS and PFOSA do not necessarily mean that PFOS concentrations are due to biodegradation of PFOSA and/or other precursors. Rather, such correlations may simply imply a similar source for the two compounds. This rational has been used previously to suggest that the sources of PFOS are similar to the sources of PFOA and PFNA in specific locations, such as in cormorants from Sardinia Island in the Mediterranean Sea [88], and in fur seals from Antarctica [96]. Caution is advised when interpreting such correlations. Wang et al. found correlations with several other organohalogen contaminants such as PCB congeners [97] in waterbird eggs from South China. This may be indicative of a commonality of contaminant sources in general, driven by proximity to pollution sources such as urbanized centres.

Correlations may therefore be most useful when likely sources of PFOS are remote, such as studies of biological samples in the Canadian arctic. For example, temporal trends that were suggestive of a PreFOS source were also supported by observed correlations between PFOS and PFOSA in ringed seals in the Canadian arctic [89] and northern sea otters from Alaska [90]. However, as evident in Table 1-1, the outcomes of these correlations are often difficult to interpret, further complicated by a multitude of contaminant sources and various capacities for biotransformation of precursors among and within different food webs.

Table 1-1: *Statistical correlations (least squares linear regressions) of PFOS and PFOSA in select studies.*

Medium	Location	Statistical significance	Ref
Mink, Fox	Canada – var. upper latitude locations	Positive, $p<0.05$*	[98]
River otter	Oregon	Positive, $p<0.05$*	[53]
Alewife, smelt, sculpin	Lake Ontario	Positive, $p<0.05$	[87]
Coastal water samples	China, Hong Kong	Positive, $p<0.05$	[99]
Harbour seal	Northwest Atlantic	Positive, $p<0.05$	[86]
Minke whales	Korea	Positive, $p<0.001$	[100]
Yangtzee and Pearl River water	China	Positive, $p<0.001$	[101]
Herring Gull eggs	Great Lakes	Positive, $p<0.0001$	[65]
Northern Sea Otters	Alaska	Positive, $p<0.01$	[90]
Melon-headed whales	Japan	Positive, $p<0.01$	[102]
Ringed seals	Arviat, Nunavut, Canada	Positive, $p<0.05$*	[89]
Bottlenose dolphins	Gulf of Mexico, Atlantic Ocean	Positive, $p<0.005$ at three sites, not significant ($p>0.05$) at one	[103]
Polar bear, loon, ringed seal	Canada – var. Upper latitude locations	Not significant, $p>0.05$*	[98]
Mink, river otter	USA, var. locations	Not significant, $p>0.05$*	[53]
Seawater	German bight	Not significant, $p>0.05$	[104]
Trout, *mysis relicta*	Lake Ontario	Not significant, $p>0.05$	[87]
Adélie penguin eggs	Antarctica	Not significant $p>0.05$	[96]
Common dolphins	Korea	Not significant, $p>0.05$	[100]
Cormorant eggs	Japan, Korea	Not significant, $p>0.05$	[105]
Polar bears	Greenland	Not significant, $p>0.05$	[106]
Grise Fjord ringed seal, various fish	Canada – var. Upper latitude locations	Negative, $p<0.05$*	[98]

* Denotes that a statistical significance, or lack thereof, was reported, but the p-value was not. Therefore, a significance value of 0.05 is assumed.

1.4 Chirality

Chirality is a geometric property which arises when a molecule lacks an internal plane of symmetry, creating two distinct forms called *enantiomers*. Enantiomers are nonsuperimposable mirror images, which rotate plane-polarized light at equal magnitude, but in opposite directions. Chirality commonly occurs when an organic molecule possesses a chiral centre, such as when a carbon atom is attached to four different groups, although other kinds of molecular geometries can result in asymmetry, as discussed below. Enantiomers have identical physical

and chemical properties, but differ in their interaction with asymmetric environments, such as with other chiral compounds, including biomolecules. Biological systems are highly asymmetric – the monomers of some of life's "building-block" molecules, such as amino acids, nucleic acids, and sugars, exist in all-D or all-L forms. In fact, this asymmetry has been regarded as an essential ingredient for the existence of life in the universe [107]. Furthermore, the interactions of the enantiomers of chiral xenobiotic molecules with biological systems can be vastly different, resulting in different rates of biodegradation and different toxicities. The study of chiral compounds is therefore of great interest and utility to environmental scientists.

Chirality is common among environmental pollutants. One quarter of all agrochemicals are chiral [108], including the priority pollutant pesticides *o,p'*-DDT and α-HCH. Other chiral pesticides include current-use herbicides mecoprop and metolachlor, both of which are commonly sold as single-enantiomer formulations, as only one of their respective pairs of enantiomers (more accurately "diastereomers," in the case of metolachlor) possesses herbicidal activity. Chirality occurs in several pharmaceuticals (e.g. ibuprofen, propanolol) and industrial chemicals such as the flame retardant hexabromocyclododecane. Finally, several forms of the compounds that are the focus of this thesis, PCBs and PFOS, are also chiral.

PCB congeners exhibit chirality by way of atropisomerism – conformers that cannot easily interconvert due to hindered rotation about a single bond. Of the 209 PCB congeners, 19 exhibit asymmetric substitution of chlorine atoms

about their long axis, as well as 3 or 4 chlorine atoms in the *ortho* position, causing restricted rotation about the molecule's C−C single bond, and stable atropisomerism under environmental conditions [109]. Rotational energy barrier's for PCBs with 3- and 4-*ortho*-chlorines have been estimated to be *ca.* 180 and 250 kJ/mol, respectively [110], corresponding to half-lives at environmental conditions of $>10^9$ y, confirming negligible racemization. The environmentally relevant PCB atropisomers include PCBs 45, 84, 91, 95 (Figure 1-2-B), 132, 136, 149, 174, 176, 183, and 196. In contrast to PCBs, the chirality of PFOS isomers occurs due to the existence of a chiral centre at the site of branching. Of the 89 theoretical PFOS isomers, 66 have at least one chiral centre [111]. However, in practice only a handful of these isomers were produced in sufficient quantities to permit their facile environmental measurement. These isomers are 1*m*-, 3*m*-, 4*m*-, and 5*m*-PFOS, where "1*m*-" refers to the numerical position of the singly-branched CF_3 group, relative to the sulfonate moiety (enantiomers of 1*m*-PFOS are shown in Figure 1-2A).

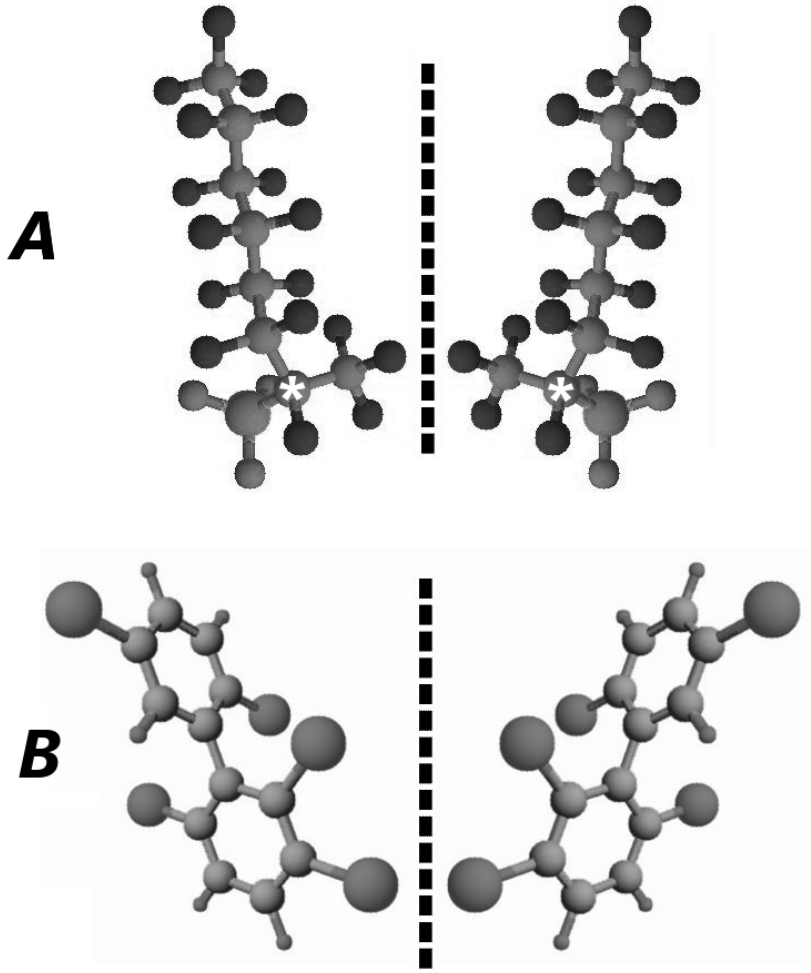

Figure 1-2: *Ball and stick models showing spatial arrangement of the enantiomers of 1m-PFOS (A) and atropisomers of PCB 95 (B). A white asterisk indicates the chiral centre for PFOS. Dashed lines indicate mirrored planes. Relative sizes of PFOS and PCB molecules are not to scale.*

1.4.1 Quantitation of chiral pollutants

A variety of techniques and instrumentation schemes have been used in the separation of chiral environmental pollutants, including gas chromatography, liquid chromatography, and capillary electrophoresis, and have been reviewed elsewhere [112]. Most techniques require the use of a chiral stationary phase which interacts preferentially with one enantiomer over the other. Among the

most common chiral stationary phases used in trace environmental analysis are those based on cyclodextrin molecules, cyclic oligosaccharides that can be chemically modified to be suited to a wide variety of chiral analytes. Over two decades ago, Konig et al. demonstrated the separation of α-HCH, among dozens of other chiral compounds, using modified cyclodextrins, and suggested that this separation may be used to study environmental biodegradation processes [113]. Since then, separation methods using commercially available columns have been published for numerous chiral contaminants. Wong and Garrison successfully separated all 19 stable PCB atropisomers by gas chromatography [114]. Oehme et al. used two capillary columns in series to develop a single method that simultaneously separates the enantiomers of several chiral organochlorine pesticides, including all chiral chlordanes, *o,p'*-DDT, oxy-chlordane, and heptachlor exo-epoxide [115]. More recently, Heeb et al. reported the separation of eight stereoisomers of hexabromocyclododecane, including three pairs of environmentally relevant enantiomers, using a permethylated cyclodextrin HPLC column [116].

The measurement of chiral compounds requires a metric which permits comparison of the relative concentrations of these enantiomers between samples and among studies. Initially, studies relied upon the ratio of the two enantiomers, named the *enantiomer ratio* (ER). By convention, the ER is defined as the ratio of the respective concentrations (or more practically, peak areas) of the (+)-enantiomer divided by the (−)-enantiomer, based on each enantiomer's direction

of rotation of plane polarized light. Harner et al. [117] improved upon this by introducing the enantiomer fraction (EF), depicted by the following equation:

$$EF = \frac{A}{A+B} \qquad \text{Equation 1-2}$$

where *A* and *B* represent the concentrations of the (+) and (−) enantiomers, respectively, when the elution order of the enantiomers is known, or respectively as E1 and E2, the first and second eluted enantiomers under defined chromatographic conditions when the elution order is unknown. The EF is preferred to the ER, since it produces values of pure enantiomers bound by zero and one (rather than zero and infinity), permitting more facile comparison of values and graphical depiction [117]. The EF is the prevailing metric for reporting enantiomer signatures in current literature, and is used throughout this body of work.

1.4.2 Enantiospecific biological interactions

Since biological systems are highly asymmetric environments, the interactions of organisms with the enantiomers of chiral xenobiotic compounds are usually different. This principle has had important and wide-ranging implications, including marked effects on the relative toxicities of enantiomers to pests, non-target organisms, and humans. For example, the 1*R*-stereoisomer of the pyrethroid cycloprothrin is several times more toxic to insect larvae than the racemate [118]. Likewise, chronic toxicity of the pharmaceutical propranolol to fathead minnows is greater for the (*S*)-enantiomer compared to its antipode [119]. Enantiospecific toxic effects have been observed for POPs as well. Both the

cytotoxicity and growth stimulation to rat hepatocytes are more prevalent for (+)-α-HCH versus (−)-α-HCH. In addition, inhibition of Ca^{2+} sequestration by rat cerebellum microsomes – an indicator of neurotoxicity – is more prevalent for the racemate of PCB 84 compared with either of the pure enantiomers [120].

Beyond toxic effects, the analysis of enantiomer signatures has proven to be useful for revealing processes in the environment that would otherwise be difficult to detect using achiral techniques, particularly for *in situ* observations. The presence of nonracemic enantiomer signatures has been used as evidence for the biotransformation of environmental contaminants via microbial degradation as well as metabolism of these pollutants by a wide variety of organisms, from invertebrates to mammals. Nonracemic signatures for several chiral PCB congeners have been detected in the sediment of PCB-impacted water bodies, including the Hudson River in New York and Lake Hartwell in South Carolina [121]. These Lake Hartwell sediments were further studied in a microcosm study which confirmed, by monitoring concentration decreases in spiked PCBs and the formation of metabolites, that nonracemic signatures were due to microbial reductive dechlorination [122]. Nonracemic EFs in sediment have also been found for other contaminants, such as α-HCH [123], *trans*-chlordane [124], and hexabromocyclododecanes [125]. Microbial degradation is likely responsible for the nonracemic EFs detected in other environmental compartments as well, such as soil [126] and seawater [127].

Nonracemic signatures of chiral contaminants are frequently found in biota, since organisms metabolize, uptake, and eliminate these compounds

enantioselectively, although determining the relative importance of these processes can be challenging. Several laboratory studies, where organisms were exposed to the compound of interest and concentrations, EFs, and metabolite formation were monitored, have provided evidence of enantioselective biotransformation. Warner and Wong observed nonracemic signatures of PCBs and *trans*-chlordane in exposed mysids, along with the metabolite oxychlordane, providing the first conclusive evidence of enantioselective biotransformation by an invertebrate [128]. Other laboratory experiments have confirmed nonracemic signatures of organochlorine contaminants in other species, including exposed rainbow trout [129] and rats [130, 131]. EFs have been determined in multiple species across several different food webs, including in the arctic [125, 132-134]. Results of these and other studies confirm that the ability of an organism to enantioselectively biotransform a pollutant varies significantly from species to species, suggesting that the presence of biotransformation-related enzymes also varies among species. However, analysis of predator-prey relationships alongside enantiomer analysis is useful in determining the biotransformation capacity of individual species, including the ability to calculate biotransformation rates quantitatively [133].

1.4.3 Chirality as a tool for source elucidation

Abiotic environmental processes that relate to the fate and transport of a chemical in the environment – partitioning processes such as volatilization and deposition, and degradation processes such as hydrolysis and photolysis – affect

each enantiomer equally. Thus, the enantiomer distributions, which have been previously altered by biochemical weathering, in water, sediment, or other media, will be preserved when these abiotic processes act upon the chemical. Enantiomer distributions can therefore be used as sensitive tracers or "fingerprints" to track sources of a contaminant in the environment. Beginning in 1997, a handful of key studies introduced this concept. Finizio et al. measured distributions of several chiral pesticides in soil and overlying air in agricultural land in British Columbia [135]. Enantiomer ratios in air, both racemic and nonracemic, closely matched those of soil for all chiral pesticides studied. Furthermore, ERs for α-HCH in air, which were significantly nonracemic in soil, exhibited a clear decreasing trend towards racemic signatures with increasing sampling height above the soil [135]. The use of ERs as tracers of air-surface exchange was also applied by Ridal et al. who estimated the contribution of volatilization of α-HCH from Lake Ontario water to the regional atmosphere [136]. Bidleman and Falconer later derived a mathematical relationship for determining the respective contributions of two sources to a receptor sample, based simply on the enantiomer ratios of the two sources [137], which was later updated to replace ER with EF [117]:

$$F_A = \frac{EF_{mix} - EF_B}{EF_A - EF_B} \qquad \text{Equation 1-3}$$

where F_A is the fraction of total contaminant from source A, EF_A and EF_B are the enantiomer fractions of source A and B, respectively, and EF_{MIX} is the enantiomer fraction of the receptor compartment or sample.

Enantiomer distributions have also been tracked temporally, ultimately being correlated with important changes and events in contaminant source history. Notably, Bidleman et al. measured EFs of *cis*- and *trans*-chlordane in Arctic Canadian and Scandinavian air and compared them with those of archived air samples from the early 1970s, finding a shift from racemic signatures in archived samples to nonracemic signatures in modern samples. Along with an analogous trend in dated lake sediment core, these results are consistent with a diminished influence of fresh chlordane sources over time, and a greater influence of emissions of older contaminants from soil [124]. Likewise, Buser et al. observed a rapid change from racemic to nonracemic signatures for the current-use pesticide metolachlor in Swiss lakes between 1998 and 1999, corresponding to a "chiral switch" – the introduction of enantiomerically enriched product and corresponding phase-out of the racemate [138]. In a recent study of atmospheric HCHs in the Canadian Archipelago, Jantunen et al. observed a shift in the EF of atmospheric α-HCH towards nonracemic signatures, corresponding to the summer ice break-up and subsequent increase in open water available for volatilization [139].

In addition to organochlorine pesticides, several other chiral contaminants have been targeted in source apportionment studies. Robson and Harrad measured nonracemic EFs for several PCB congeners in UK soil while measuring racemic signatures in overlying air, suggesting that fresh racemic sources, such as volatilization from in-use transformers, dominated contributions of PCBs to air [140]. This study was significant, in that it contrasted with the previously held

assumption that the primary atmospheric source of PCBs was volatilization from historically deposited contamination in soils. Finally, Fono and Sedlak [141] demonstrated that source apportionment can be applied to nonvolatile pharmaceuticals as well, measuring EFs of the beta-blocker propranolol in treated and untreated wastewater and surface water. They found that water bodies impacted by treated wastewater had nonracemic EFs that were reflective of the weathered drug found in wastewater treatment plant effluent, while water bodies impacted by untreated sewage had EFs for propranolol closer to racemic values.

1.5 Thesis Outline

The following chapters of this thesis are comprised of four original studies that focus on the use of enantiomers for determining contaminant sources in the environment.

In Chapter 2, the enantiomer distribution of several PCB atropisomers in the atmosphere and throughout the water column of the heavily impacted Hudson River estuary is discussed. Comparisons of these distributions are used to distinguish the PCB-impacts of the historically contaminated Upper Hudson River and fresh releases from the metropolitan New York-New Jersey urban area.

Chapter 3 focuses on the quantitation of enantiomer data, by comparing the traditional “valley-drop” integration technique with a deconvolution peak-fitting approach for the accurate determination of enantiomer fractions, using real and simulated chromatographic data. Bias and reproducibility associated with

these quantitation methods are compared and the effects of these errors are applied to calculations that utilize EF, employing real-world data.

In Chapter 4, concentrations and enantiomer distributions of PCBs surrounding a hazardous waste treatment facility are investigated over several seasons. Differences in the enantiomer signatures between air and soil are used to determine the relative impact of historical versus recent emissions from the plant.

In Chapter 5, the enantiomer distribution of a PFOS isomer, along with concentrations and isomer distributions, are measured in several species of fish and invertebrates from Lake Ontario. These data are used to infer the contribution of precursor compounds to the PFOS body burdens of these organisms.

Finally, Chapter 6 presents the specific and broad conclusions of this body of work, as well as a discussion of future directions for research in this area.

1.6 References

1. WHO Stockholm Convention on Persistent Organic Pollutants: Status of Ratifications. http://chm.pops.int/Countries/StatusofRatification/tabid/252/language/en-US/Default.aspx *Accessed: April 23, 2011.*

2. Robson, M.; Melymuk, L.; Csiszar, S. A.; Giang, A.; Diamond, M. L.; Helm, P. A., Continuing sources of PCBs: The significance of building sealants. *Environment International* **2010,** *36*, (6), 506-513.

3. Bidleman, T. F.; Leone, A. D., Soil-air exchange of organochlorine pesticides in the Southern United States. *Environmental Pollution* **2004,** *128*, (1-2), 49-57.

4. Bidleman, T. F.; Leone, A. D.; Wong, F.; van Vliet, L.; Szeto, S.; Ripley, B. D., Emission of legacy chlorinated pesticides from agricultural and orchard soils in British Columbia, Canada. *Environmental Toxicology and Chemistry* **2006,** *25*, (6), 1448-1457.

5. Harner, T.; Mackay, D.; Jones, K. C., Model of the long-term exchange of PCBs between soil and the atmosphere in the southern UK. *Environmental Science & Technology* **1995,** *29*, (5), 1200-1209.

6. Jeremiason, J. D.; Hornbuckle, K. C.; Eisenreich, S. J., PCBs in Lake-Superior, 1978-1992 - decreases in water concentrations reflect loss by volatilization. *Environmental Science & Technology* **1994,** *28*, (5), 903-914.

7. Wania, F.; Haugen, J.-E.; Lei, Y. D.; Mackay, D., Temperature dependence of atmospheric concentrations of semivolatile organic compounds. *Environmental Science & Technology* **1998,** *32*, (8), 1013-1021.

8. Carlson, D. L.; Hites, R. A., Temperature dependence of atmospheric PCB concentrations. *Environmental Science & Technology* **2004,** *39*, (3), 740-747.

9. Willett, K. L.; Ulrich, E. M.; Hites, R. A., Differential toxicity and environmental fates of hexachlorocyclohexane isomers. *Environmental Science & Technology* **1998,** *32*, (15), 2197-2207.

10. Haugen, J. E.; Wania, F.; Ritter, N.; Schlabach, M., Hexachlorocyclohexanes in air in southern Norway. Temporal variation, source

allocation, and temperature dependence. *Environmental Science & Technology* **1998,** *32*, (2), 217-224.

11. Qiu, X.; Zhu, T.; Yao, B.; Hu, J.; Hu, S., Contribution of dicofol to the current DDT pollution in China. *Environmental Science & Technology* **2005,** *39*, (12), 4385-4390.

12. De Silva, A. O.; Mabury, S. A., Isolating isomers of perfluorocarboxylates in polar bears (Ursus maritimus) from two geographical locations. *Environmental Science & Technology* **2004,** *38*, (24), 6538-6545.

13. Tavares, T. M.; Beretta, M.; Costa, M. C., Ratio of DDT/DDE in the All Saints Bay, Brazil and its use in environmental management. *Chemosphere* **1999,** *38*, (6), 1445-1452.

14. Mas, S.; de Juan, A.; Tauler, R.; Olivieri, A. C.; Escandar, G. M., Application of chemometric methods to environmental analysis of organic pollutants: A review. *Talanta* **2009,** *80*, (3), 1052-1067.

15. Hopke, P. K., Recent developments in receptor modeling. *Journal of Chemometrics* **2003,** *17*, (5), 255-265.

16. Harrison, R. M.; Smith, D. J. T.; Luhana, L., Source apportionment of atmospheric polycyclic aromatic hydrocarbons collected from an urban location in Birmingham, U.K. *Environmental Science & Technology* **1996,** *30*, (3), 825-832.

17. Paatero, P.; Tapper, U., Positive matrix factorization: A non-negative factor model with optimal utilization of error estimates of data values. *Environmetrics* **1994,** *5*, (2), 111-126.

18. Gordon, G. E., Receptor models. *Environmental Science & Technology* **1988,** *22*, (10), 1132-1142.

19. Zeng, Y.; Hopke, P. K., A study of the sources of acid precipitation in Ontario, Canada. *Atmospheric Environment (1967)* **1989,** *23*, (7), 1499-1509.

20. Du, S.; Belton, T. J.; Rodenburg, L. A., Source apportionment of polychlorinated biphenyls in the tidal Delaware River. *Environmental Science & Technology* **2008,** *42*, (11), 4044-4051.

21. Li, A.; Jang, J. K.; Scheff, P. A., Application of EPA CMB8.2 model for source apportionment of sediment PAHs in Lake Calumet, Chicago. *Environmental Science & Technology* **2003,** *37*, (13), 2958-2965.

22. Hoh, E.; Hites, R. A., Sources of toxaphene and other organochlorine pesticides in North America as determined by air measurements and potential source contribution function analyses. *Environmental Science & Technology* **2004,** *38*, (15), 4187-4194.

23. Hsu, Y.-K.; Holsen, T. M.; Hopke, P. K., Comparison of hybrid receptor models to locate PCB sources in Chicago. *Atmospheric Environment* **2003,** *37*, (4), 545-562.

24. Yanik, P. J.; O'Donnell, T. H.; Macko, S. A.; Qian, Y.; Kennicutt, M. C., Source apportionment of polychlorinated biphenyls using compound specific isotope analysis. *Organic Geochemistry* **2003,** *34*, (2), 239-251.

25. Stark, A.; Abrajano, T.; Hellou, J.; Metcalf-Smith, J. L., Molecular and isotopic characterization of polycyclic aromatic hydrocarbon distribution and

sources at the international segment of the St. Lawrence River. *Organic Geochemistry* **2003,** *34*, (2), 225-237.

26. Schmidt, T. C.; Zwank, L.; Elsner, M.; Berg, M.; Meckenstock, R. U.; Haderlein, S. B., Compound-specific stable isotope analysis of organic contaminants in natural environments: a critical review of the state of the art, prospects, and future challenges. *Analytical and Bioanalytical Chemistry* **2004,** *378*, (2), 283-300.

27. Ballschmiter, K.; Zell, M., Analysis of polychlorinated-biphenyls (PCBs) by glass-capillary gas-chromatography - composition of technical aroclor-PCB and clophen-PCB mixtures. *Fresenius Zeitschrift Fur Analytische Chemie* **1980,** *302*, (1), 20-31.

28. Breivik, K.; Sweetman, A.; Pacyna, J. M.; Jones, K. C., Towards a global historical emission inventory for selected PCB congeners -- a mass balance approach: 1. Global production and consumption. *The Science of The Total Environment* **2002,** *290*, (1-3), 181-198.

29. Health Canada. Review of Existing Literature on Quantifying and Valuing Human Health Risks Associated with Low Level Exposure to PCBs.; 2007.

30. Hawker, D. W.; Connell, D. W., Octanol water partition coefficients of polychlorinated biphenyl congeners. *Environmental Science & Technology* **1988,** *22*, (4), 382-387.

31. Borga, K.; Gabrielsen, G. W.; Skaare, J. U., Biomagnification of organochlorines along a Barents Sea food chain. *Environmental Pollution* **2001,** *113*, (2), 187-198.

32. Fisk, A. T.; Norstrom, R. J.; Cymbalisty, C. D.; Muir, D. C. G., Dietary accumulation and depuration of hydrophobic organochlorines: Bioaccumulation parameters and their relationship with the octanol/water partition coefficient. *Environmental Toxicology and Chemistry* **1998,** *17*, (5), 951-961.

33. Wania, F.; Mackay, D., Global fractionation and cold condensation of low volatility organochlorine compounds in polar regions. *Ambio* **1993,** *22*, (1), 10-18.

34. Blais, J. M.; Schindler, D. W.; Muir, D. C. G.; Kimpe, L. E.; Donald, D. B.; Rosenberg, B., Accumulation of persistent organochlorine compounds in mountains of western Canada. *Nature* **1998,** *395*, (6702), 585-588.

35. Safe, S. H., Polychlorinated Biphenyls (PCBs): Environmental impact, biochemical and toxic responses, and implications for risk assessment. *Critical Reviews in Toxicology* **1994,** *24*, (2), 87-149.

36. Hardell, L.; VanBavel, B.; Lindstrom, G.; Fredrikson, M.; Hagberg, H.; Liljegren, G.; Nordstrom, M.; Johansson, B., Higher concentrations of specific polychlorinated biphenyl congeners in adipose tissue from non-Hodgkin's lymphoma patients compared with controls without a malignant disease. *International Journal of Oncology* **1996,** *9*, (4), 603-608.

37. Rothman, N.; Cantor, K. P.; Blair, A.; Bush, D.; Brook, J. W.; Helzlsouer, K.; Zahm, S. H.; Needham, L. L.; Pearson, G. R.; Hoover, R. N.; Comstock, G.

W.; Strickland, P. T., A nested case-control study of non-Hodgkin lymphoma and serum organochlorine residues. *Lancet* **1997,** *350*, (9073), 240-244.

38. Bertazzi, P. A.; Riboldi, L.; Pesatori, A.; Radice, L.; Zocchetti, C., Cancer mortality of capacitor manufacturing workers. *American Journal of Industrial Medicine* **1987,** *11*, (2), 165-176.

39. Morgan, R. W.; Ward, J. M.; Hartman, P. E., Aroclor 1254-induced intestinal metaplasia and adneocarcinoma in the glandular stomach of F344 rats. *Cancer Research* **1981,** *41*, (12), 5052-5059.

40. Mayes, B. A.; McConnell, E. E.; Neal, B. H.; Brunner, M. J.; Hamilton, S. B.; Sullivan, T. M.; Peters, A. C.; Ryan, M. J.; Toft, J. D.; Singer, A. W.; Brown, J. F.; Menton, R. G.; Moore, J. A., Comparative carcinogenicity in Sprague-Dawley rats of the polychlorinated biphenyl mixtures Aroclors 1016, 1242, 1254, and 1260. *Toxicological Sciences* **1998,** *41*, (1), 62-76.

41. Environmental Protection Agency. Integrated Risk Information System; Carcinogencity Assessment: Polychlorinated Biphenyls (PCBs). 1996.

42. Jacobson, J. L.; Jacobson, S. W., Intellectual impairment in children exposed to polychlorinated biphenyls in utero. *New England Journal of Medicine* **1996,** *335*, (11), 783-789.

43. Grandjean, P.; Weihe, P.; Burse, V. W.; Needham, L. L.; Storr-Hansen, E.; Heinzow, B.; Debes, F.; Murata, K.; Simonsen, H.; Ellefsen, P.; Budtz-Jorgensen, E.; Keiding, N.; White, R. F., Neurobehavioral deficits associated with PCB in 7-year-old children prenatally exposed to seafood neurotoxicants. *Neurotoxicology and Teratology* **2001,** *23*, (4), 305-317.

44. Walkowiak, J.; Wiener, J. A.; Fastabend, A.; Heinzow, B.; Kramer, U.; Schmidt, E.; Steingruber, H. J.; Wundram, S.; Winneke, G., Environmental exposure to polychlorinated biphenyls and quality of the home environment: effects on psychodevelopment in early childhood. *Lancet* **2001,** *358*, (9293), 1602-1607.

45. Mendola, P.; Buck, G. M.; Sever, L. E.; Zielezny, M.; Vena, J. E., Consumption of PCB-contaminated freshwater fish and shortened menstrual cycle length. *American Journal of Epidemiology* **1997,** *146*, (11), 955-960.

46. Weisglas-Kuperus, N.; Patandin, S.; Berbers, G. A. M.; Sas, T. C. J.; Mulder, P. G. H.; Sauer, P. J. J.; Hooijkaas, H., Immunologic effects of background exposure to polychlorinated biphenyls and dioxins in Dutch preschool children. *Environmental Health Perspectives* **2000,** *108*, (12), 1203-1207.

47. Bustnes, J. O.; Erikstad, K. E.; Skaare, J. U.; Bakken, V.; Mehlum, F., Ecological effects of organochlorine pollutants in the Arctic: A study of the Glaucous Gull. *Ecological Applications* **2003,** *13*, (2), 504-515.

48. Brouwer, A.; Reijnders, P. J. H.; Koeman, J. H., Polychlorinated biphenyl (PCB)-contaminated fish induces vitamin-a and thyroid-hormone deficiency in the common seal (Phoca vitulina). *Aquatic Toxicology* **1989,** *15*, (1), 99-105.

49. Restum, J. C.; Bursian, S. J.; Giesy, J. P.; Render, J. A.; Helferich, W. C.; Shipp, E. B.; Verbrugge, D. A.; Aulerich, R. J., Multigenerational study of the effects of consumption of PCB-contaminated carp from Saginaw Bay, Lake Huron, on mink. 1. Effects on mink reproduction, kit growth and survival, and

selected biological parameters. *Journal of Toxicology and Environmental Health-Part a-Current Issues* **1998,** *54*, (5), 343-375.

50. Paul, A. G.; Jones, K. C.; Sweetman, A. J., A first global production, emission, and environmental inventory for perfluorooctane sulfonate. *Environmental Science & Technology* **2009,** *43*, (2), 386-392.

51. Vyas, S. M.; Kania-Korwel, I.; Lehmler, H. J., Differences in the isomer composition of perfluoroctanesulfonyl (PFOS) derivatives. *Journal of Environmental Science and Health Part a-Toxic/Hazardous Substances & Environmental Engineering* **2007,** *42*, (3), 249-255.

52. Martin, J. W.; Mabury, S. A.; Solomon, K. R.; Muir, D. C. G., Bioconcentration and tissue distribution of perfluorinated acids in rainbow trout *Oncorhynchus mykiss*. *Environmental Toxicology and Chemistry* **2003,** *22*, (1), 196-204.

53. Kannan, K.; Newsted, J.; Halbrook, R. S.; Giesy, J. P., Perfluorooctanesulfonate and related fluorinated hydrocarbons in mink and river otters from the United States. *Environmental Science & Technology* **2002,** *36*, (12), 2566-2571.

54. Kannan, K.; Tao, L.; Sinclair, E.; Pastva, S. D.; Jude, D. J.; Giesy, J. P., Perfluorinated compounds in aquatic organisms at various trophic levels in a Great Lakes food chain. *Archives of Environmental Contamination and Toxicology* **2005,** *48*, (4), 559-566.

55. Olsen, G. W.; Huang, H. Y.; Helzlsouer, K. J.; Hansen, K. J.; Butenhoff, J. L.; Mandel, J. H., Historical comparison of perfluorooctanesulfonate,

perfluorooctanoate, and other fluorochemicals in human blood. *Environmental Health Perspectives* **2005,** *113*, (5), 539-545.

56. Kannan, K.; Corsolini, S.; Falandysz, J.; Fillmann, G.; Kumar, K. S.; Loganathan, B. G.; Mohd, M. A.; Olivero, J.; Van Wouwe, N.; Yang, J. H.; Aldous, K. M., Perfluorooctanesulfonate and related fluorochemicals in human blood from several countries. *Environmental Science & Technology* **2004,** *38*, (17), 4489-4495.

57. Olsen, G. W.; Burris, J. M.; Ehresman, D. J.; Froehlich, J. W.; Seacat, A. M.; Butenhoff, J. L.; Zobel, L. R., Half-life of serum elimination of perfluorooctanesulfonate, perfluorohexanesulfonate, and perfluorooctanoate in retired fluorochemical production workers. *Environmental Health Perspectives* **2007,** *115*, (9), 1298-1305.

58. Seacat, A. M.; Thomford, P. J.; Hansen, K. J.; Olsen, G. W.; Case, M. T.; Butenhoff, J. L., Subchronic toxicity studies on perfluorooctanesulfonate potassium salt in cynomolgus monkeys. *Toxicological Sciences* **2002,** *68*, (1), 249-264.

59. Berthiaume, J.; Wallace, K. B., Perfluorooctanoate, perflourooctane sulfonate, and N-ethyl perfluorooctanesulfonamido ethanol; peroxisome proliferation and mitochondrial biogenesis. *Toxicology Letters* **2002,** *129*, (1-2), 23-32.

60. Hu, W.; Jones, P. D.; Upham, B. L.; Trosko, J. E.; Lau, C.; Giesy, J. P., inhibition of gap junctional intercellular communication by perfluorinated

compounds in rat liver and dolphin kidney epithelial cell lines in vitro and sprague-dawley rats in vivo. *Toxicol. Sci.* **2002,** *68*, (2), 429-436.

61. Lau, C.; Thibodeaux, J. R.; Hanson, R. G.; Rogers, J. M.; Grey, B. E.; Stanton, M. E.; Butenhoff, J. L.; Stevenson, L. A., Exposure to perfluorooctane sulfonate during pregnancy in rat and mouse. II: Postnatal evaluation. *Toxicological Sciences* **2003,** *74*, (2), 382-392.

62. Molina, E. D.; Balander, R.; Fitzgerald, S. D.; Giesy, J. P.; Kannan, K.; Mitchell, R.; Bursian, S. J., Effects of air cell injection of perfluorooctane sulfonate before incubation on development of the white leghorn chicken (Gallus domesticus) embryo. *Environmental Toxicology and Chemistry* **2006,** *25*, (1), 227-232.

63. Newsted, J. L.; Coady, K. K.; Beach, S. A.; Butenhoff, J. L.; Gallagher, S.; Giesy, J. P., Effects of perfluorooctane sulfonate on mallard and northern bobwhite quail exposed chronically via the diet. *Environmental Toxicology and Pharmacology* **2007,** *23*, (1), 1-9.

64. Ankley, G. T.; Kuehl, D. W.; Kahl, M. D.; Jensen, K. M.; Butterworth, B. C.; Nichols, J. W., Partial life-cycle toxicity and bioconcentration modeling of perfluorooctanesulfonate in the northern leopard frog (Rana pipiens). *Environmental Toxicology and Chemistry* **2004,** *23*, (11), 2745-2755.

65. Gebbink, W. A.; Hebert, C. E.; Letcher, R. J., Perfluorinated carboxylates and sulfonates and precursor compounds in herring gull eggs from colonies spanning the Laurentian Great Lakes of North America. *Environmental Science & Technology* **2009,** *43*, (19), 7443-7449.

66. Giesy, J. P.; Kannan, K., Global distribution of perfluorooctane sulfonate in wildlife. *Environmental Science & Technology* **2001,** *35*, (7), 1339-1342.

67. Martin, J. W.; Asher, B. J.; Beesoon, S.; Benskin, J. P.; Ross, M. S., PFOS or PreFOS? Are perfluorooctane sulfonate precursors (PreFOS) important determinants of human and environmental perfluorooctane sulfonate (PFOS) exposure? *Journal of Environmental Monitoring* **2010,** *12*, (11), 1979-2004.

68. Rhoads, K. R.; Janssen, E. M. L.; Luthy, R. G.; Criddle, C. S., Aerobic biotransformation and fate of N-ethyl perfluorooctane sulfonamidoethanol (N-EtFOSE) in activated sludge. *Environmental Science & Technology* **2008,** *42*, (8), 2873-2878.

69. Xu, L.; Krenitsky, D. M.; Seacat, A. M.; Butenhoff, J. L.; Anders, M. W., Biotransformation of N-ethyl-N-(2-hydroxyethyl)perfluorooctane sulfonamide by rat liver microsomes, cytosol, and slices and by expressed rat and human cytochromes P450. *Chemical Research in Toxicology* **2004,** *17*, (6), 767-775.

70. Xie, W.; Wu, Q.; Kania-Korwel, I.; Tharappel, J. C.; Telu, S.; Coleman, M. C.; Glauert, H. P.; Kannan, K.; Mariappan, S. V. S.; Spitz, D. R.; Weydert, J.; Lehmler, H. J., Subacute exposure to N-ethyl perfluorooctanesulfonamidoethanol results in the formation of perfluorooctanesulfonate and alters superoxide dismutase activity in female rats. *Archives of Toxicology* **2009,** *83*, (10), 909-924.

71. Vestergren, R.; Cousins, I. T.; Trudel, D.; Wormuth, M.; Scheringer, M., Estimating the contribution of precursor compounds in consumer exposure to PFOS and PFOA. *Chemosphere* **2008,** *73*, (10), 1617-1624.

72. Simcik, M. F.; Dorweiler, K. J., Ratio of perfluorochemical concentrations as a tracer of atmospheric deposition to surface waters. *Environmental Science & Technology* **2005,** *39*, (22), 8678-8683.

73. Yamashita, N.; Kannan, K.; Taniyasu, S.; Horii, Y.; Okazawa, T.; Petrick, G.; Gamo, T., Analysis of perfluorinated acids at parts-per-quadrillion levels in seawater using liquid chromatography-tandem mass spectrometry. *Environmental Science & Technology* **2004,** *38*, (21), 5522-5528.

74. Ahrens, L.; Barber, J. L.; Xie, Z. Y.; Ebinghaus, R., Longitudinal and latitudinal distribution of perfluoroalkyl compounds in the surface water of the Atlantic Ocean. *Environmental Science & Technology* **2009,** *43*, (9), 3122-3127.

75. Lei, Y. D.; Wania, F.; Mathers, D.; Mabury, S. A., Determination of vapor pressures, octanol-air, and water-air partition coefficients for polyfluorinated sulfonamide, sulfonamidoethanols, and telomer alcohols. *Journal of Chemical & Engineering Data* **2004,** *49*, (4), 1013-1022.

76. Kim, S. K.; Kannan, K., Perfluorinated acids in air, rain, snow, surface runoff, and lakes: Relative importance of pathways to contamination of urban lakes. *Environmental Science & Technology* **2007,** *41*, (24), 8328-8334.

77. Barber, J. L.; Berger, U.; Chaemfa, C.; Huber, S.; Jahnke, A.; Temme, C.; Jones, K. C., Analysis of per- and polyfluorinated alkyl substances in air samples from Northwest Europe. *Journal of Environmental Monitoring* **2007,** *9*, (6), 530-541.

78. Shoeib, M.; Harner, T.; Vlahos, P., Perfluorinated chemicals in the Arctic atmosphere. *Environmental Science & Technology* **2006,** *40*, (24), 7577-7583.

79. Shoeib, M.; Harner, T.; Ikonomou, M.; Kannan, K., Indoor and outdoor air concentrations and phase partitioning of perfluoroalkyl sulfonamides and polybrominated diphenyl ethers. *Environmental Science & Technology* **2004,** *38*, (5), 1313-1320.

80. Dreyer, A.; Ebinghaus, R., Polyfluorinated compounds in ambient air from ship- and land-based measurements in northern Germany. *Atmospheric Environment* **2009,** *43*, (8), 1527-1535.

81. Stock, N. L.; Furdui, V. I.; Muir, D. C. G.; Mabury, S. A., Perfluoroalkyl contaminants in the Canadian Arctic: Evidence of atmospheric transport and local contamination. *Environmental Science & Technology* **2007,** *41*, (10), 3529-3536.

82. Houde, M.; Martin, J. W.; Letcher, R. J.; Solomon, K. R.; Muir, D. C. G., Biological monitoring of polyfluoroalkyl substances: A review. *Environmental Science & Technology* **2006,** *40*, (11), 3463-3473.

83. Smithwick, M.; Mabury, S. A.; Solomon, K. R.; Sonne, C.; Martin, J. W.; Born, E. W.; Dietz, R.; Derocher, A. E.; Letcher, R. J.; Evans, T. J.; Gabrielsen, G. W.; Nagy, J.; Stirling, I.; Taylor, M. K.; Muir, D. C. G., Circumpolar study of perfluoroalkyl contaminants in polar bears (Ursus maritimus). *Environmental Science & Technology* **2005,** *39*, (15), 5517-5523.

84. Bossi, R.; Riget, F. F.; Dietz, R.; Sonne, C.; Fauser, P.; Dam, M.; Vorkamp, K., Preliminary screening of perfluorooctane sulfonate (PFOS) and other fluorochemicals in fish, birds and marine mammals from Greenland and the Faroe Islands. *Environmental Pollution* **2005,** *136*, (2), 323-329.

85. Taniyasu, S.; Kannan, K.; Horii, Y.; Hanari, N.; Yamashita, N., A survey of perfluorooctane sulfonate and related perfluorinated organic compounds in water, fish, birds, and humans from Japan. *Environmental Science & Technology* **2003,** *37*, (12), 2634-2639.

86. Shaw, S.; Berger, M. L.; Brenner, D.; Tao, L.; Wu, Q.; Kannan, K., Specific accumulation of perfluorochemicals in harbor seals (Phoca vitulina concolor) from the northwest Atlantic. *Chemosphere* **2009,** *74*, (8), 1037-1043.

87. Martin, J. W.; Whittle, D. M.; Muir, D. C. G.; Mabury, S. A., Perfluoroalkyl contaminants in a food web from lake Ontario. *Environmental Science & Technology* **2004,** *38*, (20), 5379-5385.

88. Kannan, K.; Corsolini, S.; Falandysz, J.; Oehme, G.; Focardi, S.; Giesy, J. P., Perfluorooctanesulfonate and related fluorinated hydrocarbons in marine mammals, fishes, and birds from coasts of the Baltic and the Mediterranean Seas. *Environmental Science & Technology* **2002,** *36*, (15), 3210-3216.

89. Butt, C. M.; Muir, D. C. G.; Stirling, I.; Kwan, M.; Mabury, S. A., Rapid response of arctic ringed seals to changes in perfluoroalkyl production. *Environmental Science & Technology* **2006,** *41*, (1), 42-49.

90. Hart, K.; Gill, V. A.; Kannan, K., Temporal trends (1992-2007) of perfluorinated chemicals in Northern Sea otters (*Enhydra lutris kenyoni*) from South-Central Alaska. *Archives of Environmental Contamination and Toxicology* **2009,** *56*, (3), 607-614.

91. Holmstrom, K. E.; Johansson, A.-K.; Bignert, A.; Lindberg, P.; Berger, U., Temporal trends of perfluorinated surfactants in Swedish peregrine falcon eggs (*Falco peregrinus*), 1974-2007. *Environmental Science & Technology* **2010**.

92. Bossi, R.; Riget, F. F.; Dietz, R., Temporal and spatial trends of perfluorinated compounds in ringed seal (*Phoca hispida*) from Greenland. *Environmental Science & Technology* **2005,** *39*, (19), 7416-7422.

93. Dietz, R.; Bossi, R.; Riget, F. F.; Sonne, C.; Born, E. W., Increasing perfluoroalkyl contaminants in east Greenland polar bears (*Ursus maritimus)*: A new toxic threat to the Arctic bears. *Environmental Science & Technology* **2008,** *42*, (7), 2701-2707.

94. Ahrens, L.; Siebert, U.; Ebinghaus, R., Temporal trends of polyfluoroalkyl compounds in harbor seals (*Phoca vitulina*) from the German Bight, 1999-2008. *Chemosphere* **2009,** *76*, (2), 151-158.

95. Furdui, V. I.; Helm, P. A.; Crozier, P. W.; Lucaciu, C.; Reiner, E. J.; Marvin, C. H.; Whittle, D. M.; Mabury, S. A.; Tomy, G. T., Temporal trends of perfluoroalkyl compounds with isomer analysis in lake trout from Lake Ontario (1979-2004). *Environmental Science & Technology* **2008,** *42*, (13), 4739-4744.

96. Schiavone, A.; Corsolini, S.; Kannan, K.; Tao, L.; Trivelpiece, W.; Torres Jr, D.; Focardi, S., Perfluorinated contaminants in fur seal pups and penguin eggs from South Shetland, Antarctica. *Science of The Total Environment* **2009,** *407*, (12), 3899-3904.

97. Wang, Y.; Yeung, L. W. Y.; Taniyasu, S.; Yamashita, N.; Lam, J. C. W.; Lam, P. K. S., Perfluorooctane sulfonate and other fluorochemicals in waterbird

eggs from South China. *Environmental Science & Technology* **2008,** *42*, (21), 8146-8151.

98. Martin, J. W.; Smithwick, M. M.; Braune, B. M.; Hoekstra, P. F.; Muir, D. C. G.; Mabury, S. A., Identification of long-chain perfluorinated acids in biota from the Canadian Arctic. *Environmental Science & Technology* **2003,** *38*, (2), 373-380.

99. So, M. K.; Taniyasu, S.; Yamashita, N.; Giesy, J. P.; Zheng, J.; Fang, Z.; Im, S. H.; Lam, P. K. S., Perfluorinated compounds in coastal waters of Hong Kong, South China, and Korea. *Environmental Science & Technology* **2004,** *38*, (15), 4056-4063.

100. Moon, H. B.; Kannan, K.; Yun, S.; An, Y. R.; Choi, S. G.; Park, J. Y.; Kim, Z. G.; Moon, D. Y.; Choi, H. G., Perfluorinated compounds in minke whales (*Balaenoptera acutorostrata*) and long-beaked common dolphins (*Delphinus capensis*) from Korean coastal waters. *Marine Pollution Bulletin* **2010,** *60*, (7), 1130-1135.

101. So, M. K.; Miyake, Y.; Yeung, W. Y.; Ho, Y. M.; Taniyasu, S.; Rostkowski, P.; Yamashita, N.; Zhou, B. S.; Shi, X. J.; Wang, J. X.; Giesy, J. P.; Yu, H.; Lam, P. K. S., Perfluorinated compounds in the Pearl River and Yangtze River of China. *Chemosphere* **2007,** *68*, (11), 2085-2095.

102. Hart, K.; Kannan, K.; Isobe, T.; Takahashi, S.; Yamada, T. K.; Miyazaki, N.; Tanabe, S., Time trends and transplacental transfer of perfluorinated compounds in melon-headed whales stranded along the Japanese coast in 1982,

2001/2002, and 2006. *Environmental Science & Technology* **2008,** *42*, (19), 7132-7137.

103. Houde, M.; Wells, R. S.; Fair, P. A.; Bossart, G. D.; Hohn, A. A.; Rowles, T. K.; Sweeney, J. C.; Solomon, K. R.; Muir, D. C. G., Polyfluoroalkyl compounds in free-ranging bottlenose dolphins (*Tursiops truncatus*) from the Gulf of Mexico and the Atlantic Ocean. *Environmental Science & Technology* **2005,** *39*, (17), 6591-6598.

104. Ahrens, L.; Felizeter, S.; Ebinghaus, R., Spatial distribution of polyfluoroalkyl compounds in seawater of the German Bight. *Chemosphere* **2009,** *76*, (2), 179-184.

105. Kannan, K.; Choi, J. W.; Iseki, N.; Senthilkumar, K.; Kim, D. H.; Masunaga, S.; Giesy, J. P., Concentrations of perfluorinated acids in livers of birds from Japan and Korea. *Chemosphere* **2002,** *49*, (3), 225-231.

106. Smithwick, M.; Muir, D. C. G.; Mabury, S. A.; Solomon, K. R.; Martin, J. W.; Sonne, C.; Born, E. W.; Letcher, R. J.; Dietz, R., Perfluoroalkyl contaminants in liver tissue from East Greenland polar bears (*Ursus maritimus*). *Environmental Toxicology and Chemistry* **2005,** *24*, (4), 981-986.

107. Avetisov, V. A.; Goldanskii, V. I.; Kuzmin, V. V., Handedness, origin of life and evolution. *Physics Today* **1991,** *44*, (7), 33-41.

108. Williams, A., Opportunities for chiral agrochemicals. *Pesticide Science* **1996,** *46*, (1), 3-9.

109. Kaiser, K. L. E., Optical activity of polychlorinated biphenyls. *Environmental Pollution* **1974,** *7*, (2), 93-101.

110. Harju, M. T.; Haglund, P., Determination of the rotational energy barriers of atropisomeric polychlorinated biphenyls. *Fresenius' Journal of Analytical Chemistry* **1999,** *364*, (3), 219-223.

111. Rayne, S.; Forest, K.; Friesen, K. J., Congener-specific numbering systems for the environmentally relevant C4 through C8 perfluorinated homologue groups of alkyl sulfonates, carboxylates, telomer alcohols, olefins, and acids, and their derivatives. *Journal of Environmental Science and Health, Part A: Toxic/Hazardous Substances and Environmental Engineering* **2008,** *43*, (12), 1391 - 1401.

112. Huhnerfuss, H.; Shah, M. R., Enantioselective chromatography-A powerful tool for the discrimination of biotic and abiotic transformation processes of chiral environmental pollutants. *Journal of Chromatography A* **2009,** *1216*, (3), 481-502.

113. Konig, W. A.; Krebber, R.; Mischnick, P., Cyclodextrins as chiral stationary phases in capillary gas-chromatography 5-octakis(3-ortho-butyryl-2,6-di-ortho-pentyl)-gamma-cyclodextrin. *Hrc-Journal of High Resolution Chromatography* **1989,** *12*, (11), 732-738.

114. Wong, C. S.; Garrison, A. W., Enantiomer separation of polychlorinated biphenyl atropisomers and polychlorinated biphenyl retention behavior on modified cyclodextrin capillary gas chromatography columns. *Journal Chromatography A.* **2000,** *866*, (2), 213-220.

115. Oehme, M.; Kallenborn, R.; Wiberg, K.; Rappe, C., Simultaneous enantioselective separation of chlordanes, a nonachlor compound, and o,p'-DDT

in environmental-samples using tandem capillary columns. *Hrc-Journal of High Resolution Chromatography* **1994,** *17*, (8), 583-588.

116. Heeb, N. V.; Schweizer, W. B.; Kohler, M.; Gerecke, A. C., Structure elucidation of hexabromocyclododecanes - a class of compounds with a complex stereochemistry. *Chemosphere* **2005,** *61*, (1), 65-73.

117. Harner, T.; Wiberg, K.; Norstrom, R. J., Enantiomer fractions are preferred to enantiomer raios for describing chiral signatures in environmental analysis. *Environmental Science & Technology.* **2000,** *34*, 218-220.

118. Jiang, B.; Wang, H.; Fu, Q. M.; Li, Z. Y., The chiral pyrethroid cycloprothrin: Stereoisomer synthesis and separation and stereoselective insecticidal activity. *Chirality* **2008,** *20*, (2), 96-102.

119. Stanley, J. K.; Ramirez, A. J.; Mottaleb, M.; Chambliss, C. K.; Brooks, B. W., Enantiospecific toxicity of the beta-blocker propranolol to Daphnia magna and Pimephales promelas. *Environmental Toxicology and Chemistry* **2006,** *25*, (7), 1780-1786.

120. Lehmler, H. J.; Robertson, L. W.; Garrison, A. W.; Kodavanti, P. R. S., Effects of PCB 84 enantiomers on [H-3]-phorbol ester binding in rat cerebellar granule cells and Ca-45(2+)-uptake in rat cerebellum. *Toxicology Letters* **2005,** *156*, (3), 391-400.

121. Wong, C. S.; Garrison, A. W.; Foreman, W. T., Enantiomeric composition of chiral polychlorinated biphenyl atropisomers in aquatic bed sediment. *Environmental Science & Technology.* **2001,** *35*, (1), 33-39.

122. Pakdeesusuk, U.; Jones, W. J.; Lee, C. M.; Garrison, A. W.; O'Niell, W. L.; Freedman, D. L.; Coates, J. T.; Wong, C. S., Changes in enantiomeric fractions during microbial reductive dechlorination of PCB132, PCB149, and Aroclor 1254 in Lake Hartwell sediment microcosms. *Environmental Science & Technology*. **2003,** *37*, (6), 1100-1107.

123. Moisey, J.; Fisk, A. T.; Hobson, K. A.; Norstrom, R. J., Hexachlorocyclohexane (HCH) isomers and chiral signatures of alpha-HCH in the arctic marine food web of the Northwater Polynya. *Environmental Science & Technology* **2001,** *35*, (10), 1920-1927.

124. Bidleman, T. F.; Wong, F.; Backe, C.; Sodergren, A.; Brorstrom-Lunden, E.; Helm, P. A.; Stern, G. A., Chiral signatures of chlordanes indicate changing sources to the atmosphere over the past 30 years. *Atmospheric Environment* **2004,** *38*, (35), 5963-5970.

125. Wu, J.-P.; Guan, Y.-T.; Zhang, Y.; Luo, X.-J.; Zhi, H.; Chen, S.-J.; Mai, B.-X., Trophodynamics of hexabromocyclododecanes and several other non-PBDE brominated flame retardants in a freshwater food web. *Environmental Science & Technology* **2010,** *44*, (14), 5490-5495.

126. Koblickova, M.; Ducek, L.; Jarkovsky, J.; Hofman, J.; Bucheli, T. D.; Klanova, J., Can physicochemical and microbial soil properties explain enantiorneric shifts of chiral organochlorines? *Environmental Science & Technology* **2008,** *42*, (16), 5978-5984.

127. Faller, J.; Huhnerfuss, H.; Konig, W. A.; Krebber, R.; Ludwig, P., Do marine-bacteria degrade alpha-hexachlorocyclohexane stereoselectively? *Environmental Science & Technology* **1991,** *25*, (4), 676-678.

128. Warner, N. A.; Wong, C. S., The freshwater invertebrate Mysis relicta can eliminate chiral organochlorine compounds enantioselectively. *Environmental Science & Technology.* **2006,** *40*, (13), 4158-4164.

129. Wong, C. S.; Lau, F.; Clark, M.; Mabury, S. A.; Muir, D. C. G., Rainbow Trout (*Oncorhynchus mykiss*) can eliminate chiral Organochlorine Compounds Enantioselectively. *Environmental Science & Technology.* **2002,** *36*, 1257-1262.

130. Ulrich, E. M.; Willett, K. L.; Caperell-Grant, A.; Bigsby, R. M.; Hites, R. A., Understanding enantioselective processes: A laboratory rat model for alpha-hexachlorocyclohexane accumulation. *Environmental Science & Technology* **2001,** *35*, (8), 1604-1609.

131. Norstrom, K.; Eriksson, J.; Haglund, J.; Silvari, V.; Bergman, A., Enantioselective formation of methyl sulfone metabolites of 2,2 ', 3,3 ', 4,6 '-hexachlorobiphenyl in rat. *Environmental Science & Technology* **2006,** *40*, (24), 7649-7655.

132. Warner, N. A.; Norstrom, R. J.; Wong, C. S.; Fisk, A. T., Enantiomeric fractions of chiral polychlorinated biphenyls provide insights on biotransformation capacity of arctic biota. *Environmental Science & Technology.* **2005,** *24*, (11), 2763-2767.

133. Wong, C. S.; Mabury, S. A.; Whittle, D. M.; Backus, S. M.; Teixeira, C.; DeVault, D. S.; Bronte, C. R.; Muir, D. C. G., Organochlorine compounds in

Lake Superior: Chiral polychlorinated biphenyls and biotransformation in the aquatic food web. *Environmental Science & Technology.* **2004,** *38*, (1), 84-92.

134. Hoekstra, P. F.; O'Hara, T. M.; Karlsson, H.; Solomon, K. R.; Muir, D. C. G., Enantiomer-specific biomagnification of alpha-hexachlorocyclohexane and selected chiral chlordane-related compounds within an arctic marine food web. *Environmental Toxicology and Chemistry* **2003,** *22*, (10), 2482-2491.

135. Finizio, A.; Bidleman, T. F.; Szeto, S. Y., Emission of chiral pesticides from an agricultural soil in the Fraser Valley, British Columbia. *Chemosphere* **1998,** *36*, (2), 345-355.

136. Ridal, J. J.; Bidleman, T. F.; Kerman, B. R.; Fox, M. E.; Strachan, W. M. J., Enantiomers of alpha-hexachlorocyclohexane as tracers of air-water gas exchange in Lake Ontario. *Environmental Science & Technology.* **1997,** *31*, (7), 1940-1945.

137. Bidleman, T. F.; Falconer, R. L., Enantiomer ratios for apportioning two sources of chiral compounds. *Environmental Science & Technology.* **1999,** *33*, (13), 2299-2301.

138. Buser, H. R.; Poiger, T.; Muller, M. D., Changed enantiomer composition of metolachlor in surface water following the introduction of the enantiomerically enriched product to the market. *Environmental Science & Technology* **2000,** *34*, (13), 2690-2696.

139. Jantunen, L. M.; Helm, P. A.; Kylin, H.; Bidleman, T. F., Hexachlorocyclohexanes (HCHs) In the Canadian Archipelago. 2. Air-water gas

exchange of α- and g-HCH. *Environmental Science & Technology* **2008,** *42*, (2), 465-470.

140. Robson, M.; Harrad, S., Chiral PCB signatures in air and soil: Implications for atmospheric source apportionment. *Environmental Science & Technology.* **2004,** *38*, (6), 1662-1666.

141. Fono, L. J.; Sedlak, D. L., Use of the chiral pharmaceutical propranolol to identify sewage discharges into surface waters. *Environmental Science & Technology.* **2005,** *39*, (23), 9244-9252.

Chapter 2: Chiral Source Apportionment of Polychlorinated Biphenyls to the Hudson River Estuary Atmosphere and Food Web

A version of this chapter has been previously published as Asher, B. J.; Wong, C. S.; Rodenburg, L. A., Chiral source apportionment of polychlorinated biphenyls to the Hudson River estuary atmosphere and food web. Environmental Science & Technology 2007, 41(17), 6163-6169.

2.1 Introduction

The New York-New Jersey (NY/NJ) Harbor Estuary has been heavily impacted by numerous current and historical inputs of polychlorinated biphenyls (PCBs). Historically, the major source of PCBs to the region was the release of large quantities of PCBs into the Upper Hudson River from General Electric capacitor plants between ca. 1947 to 1977 [1]. Several major inputs of PCBs to the estuary have been identified, including contaminated sediment from the Upper Hudson [2-4], storm water runoff and wastewater from the surrounding densely populated NY/NJ urban area [3, 5], and atmospheric deposition of airborne PCBs from urban and industrial releases in the NY/NJ region [6, 7]. Understanding the relative importance of fresh vs. historical releases of PCBs, and Upper Hudson versus local sources to atmospheric and biotic PCB concentrations can have tremendous impact on the future direction of remediation activities in the region. If contamination of the local aquatic food web primarily occurs due to atmospheric sources, then reduction in atmospheric emissions would be effective in reducing the impact on aquatic organisms. Conversely, if transport of contaminated Upper Hudson sediment controls food web concentrations, then mitigation of these contaminated sites would be the most appropriate control measure.

While mass balances have shown that approximately half of PCB loadings to estuarine water are from Upper Hudson River inputs [8, 9], the degree to which the various PCB sources contribute to contamination of the estuary's aquatic ecosystem is still unknown. Some studies have suggested that the role of local

urban and industrial atmospheric sources to the local food web may be significant, despite contributing only a small amount to overall water column loadings [7, 10]. Brunciak et al. found a correlation in congener patterns between the atmosphere and the aquatic dissolved phase, highlighting the importance of PCB air-water exchange in the estuary [7]. Yan used a dynamic model to infer that concentrations of higher chlorinated (>5 Cl) PCBs in phytoplankton were controlled by air-water exchange [10], thus implying that desorption from sediments is slower than phytoplankton uptake from atmospherically-derived PCBs. Rapid phytoplankton growth can deplete concentrations of aqueous-phase hydrophobic pollutants via bioconcentration, resulting in increased absorptive flux from the atmosphere [11, 12]. However, it is not clear to what extent air-water exchange controls PCB uptake in the estuary, and a more definitive method of determining sources is needed.

Recently, the use of chiral signatures has been applied to the identification and characterization of pollutant sources [13-17]. If the sources of an optically-active chemical have different enantiomer signatures, then the chemical's enantiomer composition at the receptor would reflect the respective contributions of each source. Such differences in enantiomer compositions may arise from biological processes, such as stereoselective reductive dechlorination of PCBs by sediment microbes [18]. However, physical and chemical processes, such as volatilization and deposition do not alter enantiomer distributions [19]. As a result, a comparison of enantiomer compositions in different phases can indicate whether the contaminant load in one phase is primarily due to fresh racemic

sources, or old biologically weathered ones, as has been previously demonstrated [13-17]. For example, chlordane chiral signatures in worldwide atmospheric samples shifted from racemic to nonracemic over a 30 year span, indicating the increasing importance of nonracemic emission from weathered soils in recent years [13]. The contribution of α-hexachlorocyclohexane volatilization to the atmosphere over the Arctic Ocean [14] and Lake Ontario [15] waters was similarly deduced. Chiral signatures for the pharmaceutical propranolol were used to distinguish between discharges of racemic untreated wastewater compared to nonracemic treated effluent to surface waters [16]. This technique has also been applied to PCBs, as racemic atmospheric signatures in the U.K. West Midlands were attributed to fresh sources, rather than previously deposited nonracemic weathered sources such as soil [17]. However, to date there has been no attempt to use enantiomer analysis to delineate PCB sources to an aquatic ecosystem.

The objective of this study was to use PCB chiral signatures in air, water, sediment, total suspended matter (TSM), and phytoplankton to determine the relative importance of recent and historical PCB releases to the local atmosphere and its aquatic food web. This approach is likely to be effective in the Hudson, because nonracemic signatures of several PCB congeners in Hudson River sediments have been observed [20]. Phytoplankton was analysed in this study due to its important position at the base of the food web. Phytoplankton appear to lack the capacity to degrade PCBs, enantioselectively or otherwise [21], and accumulate PCBs by passive diffusion from the dissolved phase [22]. Thus, chiral

signatures found in these organisms are expected to match closely those of the water. To our knowledge, this is the first study to investigate chiral PCB signatures in the estuary, and to use chiral techniques to determine sources of PCBs to an aquatic food web.

2.2 Materials and Methods

2.2.1 Sampling

Air, water, phytoplankton, and sediment were sampled (Figure 2-1) during five intensive cruises from 1999 to 2001 at two sites: the nearshore Hudson River estuary (HRE, 40.30°N, 74.05°W) and the Coastal Atlantic Ocean (CAO, 40.30°N, 73.58°W) aboard the research vessel *Walford*. Additional air samples were collected on land at Jersey City (40.71°N, 74.05°W) and Sandy Hook (40.46°N, 74.00°W). Morning (08:30-12:30) and afternoon (13:00-17:00) samples were taken during October 20 and December 3 of 1999; April 19-21, August 21-23 and October 25-27 of 2000; and April 24 of 2001. Additional sampling details, including meteorological data, are presented in Table A-2-1, A2-2, and elsewhere [23]. Briefly, modified high-volume air samplers (Tisch Environmental, Cleves, OH) sampled air over 4 hour intervals at 0.5 $m^3 min^{-1}$. Gas phase was collected on precleaned polyurethane foam (PUF), and particulate phase was captured on precombusted quartz fiber filters (QFFs, Whatman). Water was collected using Infiltrex 100 sampling units (Axys Environmental Systems, Sidney, BC, Canada) at ca. 300 mL min^{-1}, yielding final sample volumes of 18-60 L. Water was passed

through precombusted 0.7 μm glass fiber filters (Whatman) for suspended particulate matter (TSM) collection, while dissolved phase material was captured with XAD-2 resin (Amberlite). Phytoplankton were sampled with a 64 μm plankton net, and filtered onto glass fiber filters prior to extraction. Surficial sediment samples (1 kg) were collected using Ponar grab sampling.

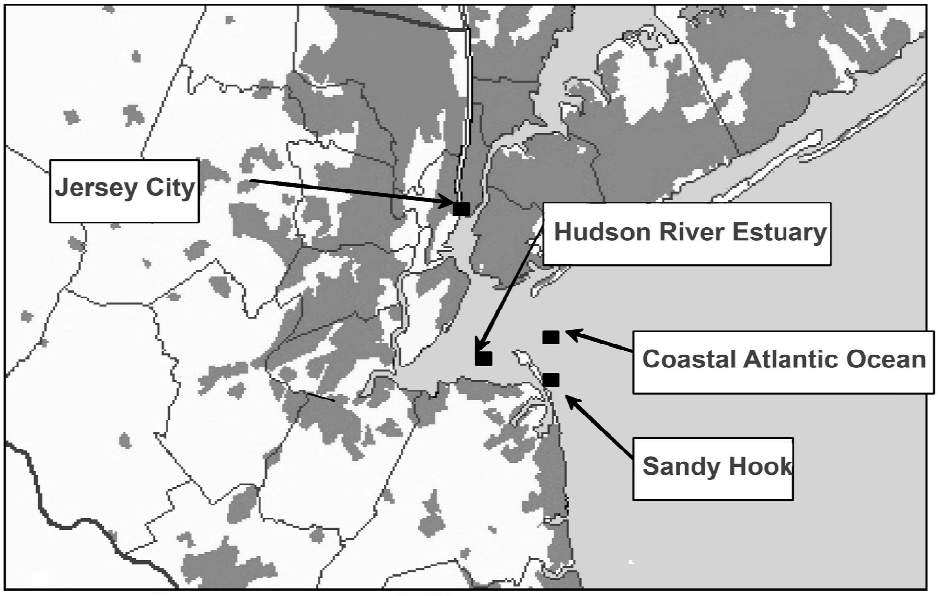

Adapted map courtesy of The National Atlas, USGS

Figure 2-1: *Map of coastal New Jersey showing the Hudson River estuary and the locations of the four sampling sites. Shaded areas indicate regions with dense urban populations.*

2.2.2 Extraction

Details of sample preparation and extraction have been previously published [7, 24] . Briefly, PUF plugs were precleaned by successive Soxhlet extraction in acetone and petroleum ether, and dried under vacuum. Quartz fiber filters were precombusted at 450°C for 6 hours. After sampling, PUFs and QFFs

were spiked with surrogate standards (PCB 23, 65, and 166) and Soxhlet extracted in petroleum ether and dichloromethane, respectively. Sediment was dried with anhydrous sodium sulfate, spiked with surrogate standards, and Soxhlet extracted in dichloromethane. XAD-2 resin was precleaned by successive Soxhlet extraction in methanol, acetone, hexane, acetone, and methanol, followed by rinsing with nanopure water. Both XAD and TSM were Soxhlet extracted in 1:1 acetone:hexane and then liquid-liquid extracted in 60 mL nanopure water with 1 g sodium chloride. Aqueous fractions were back extracted three times with 50 mL hexane. All extracts were concentrated by rotary and N_2 evaporation and fractionated using a 3% water-deactivated alumina column.

2.2.3 Analysis

Achiral analysis was performed after extraction as previously described [23] using an Agilent 6890 gas chromatograph (GC) with a DB-5 capillary column (60 m × 0.25 mm i.d. × 0.25 μm d_f, Agilent, Santa Clara, CA) and a ^{63}Ni electron capture detector (ECD). Enantiomer analysis was performed on these archived extracts, stored at ~4°C in glass vials with Teflon-lined caps. Long-term sample storage is not expected to affect enantiomeric composition [25]. Enantiomers of chiral PCB congeners 91, 95, 136, and 149 were quantified using a Waters Quattro Micro tandem quadrupole GC/MS/MS with a Chirasil-Dex capillary column (25 m × 0.25 mm i.d. × 0.25 μm d_f, Varian, Walnut Creek, CA) under previously described GC temperature conditions [25]. Briefly, oven temperatures were set at 60°C with a 2 minute hold, 10°C/min to 150°C, and 1°C/min to 250°C, with a 20 minute hold. Helium carrier gas was set at 1mL/min

constant flow, and the injector temperature was set at 250°C. Multiple reaction monitoring mode was employed, with $[M]^+$ and $[M-2Cl]^+$ as precursor and product ions, respectively. These four congeners were monitored as they were present in sufficient amounts [23] in the samples for enantiomer quantification. Sample chiral signatures for each congener were determined by calculating the enantiomeric fraction (EF; Equation 1-2) [26], defined as the (+)-enantiomer concentration divided by the sum concentration of both enantiomers for PCBs 136 and 149, and as the first-eluting enantiomer concentration divided by the sum concentration of both enantiomers for PCBs 91 and 95 for which elution order is unknown [27].

2.2.4 QA/QC

Surrogate standards were used to correct PCB congener concentrations for extraction recoveries: PCB 23 for congeners eluting before PCB 45 on DB-5, PCB 65 for those eluting from PCB 45 to PCB 110+70, and PCB 166 for all subsequently eluting congeners. Average percent recoveries (±SD) determined by GC-ECD for PCBs 23, 65, and 166 were: PUF, 92±7%, 94±12%, and 91±11%, respectively; QFF, 87±9%, 84±8%, and 99±8%, respectively; XAD, 97±10%, 105±9%, and 103±11%, respectively; TSM, 98±9%, 95±16%, and 102±15%, respectively; phytoplankton, 95±5%, 96±9%, and 100±15%, respectively [23].

For EF determination, additional criteria were employed for quality assurance/quality control. First, standard solutions collectively containing all 209 PCB congeners [28] were analysed by GC/MS/MS prior to sample analysis, to ensure that no interferences with the target chiral PCB congeners were present

[25]. Interferences were defined as the coelution of a target congener's enantiomers with another homologous congener, with the exception of congeners that are not environmentally relevant (i.e., non-Aroclor congeners) [25, 29]. Secondly, measured signals for each peak were to be above the limit of quantification. Thirdly, chlorine isotope ratios ($[M]^+$ to $[M-2]^+$) were to be within ±10% of standards. Peak area quantification for enantiomer analysis was determined using PeakFit v4.06 (Systat Software, San Jose, CA), with fitting procedures described in detail in Chapter 3, and elsewhere [30].

2.2.5 Analytical Performance

Enantiomer quantification was done by GC/MS/MS due to its potential for lower detection limits and its relative lack of isobaric interferences that could significantly alter the measured EF, compared with single-MS techniques [31]. As a result, our conservative criterion, used in previous studies [21, 32], of ±0.032 for classifying a measured EF as nonracemic was not used here. Instead, EFs were considered to be non-racemic if they were statistically different from mean EFs of racemic standards: 0.498±0.003 (±SD), 0.496±0.002, 0.499±0.003, and 0.497±0.004 for PCBs 91, 95, 136, and 149, respectively. The EF precisions of standards ranged between 0.4 and 0.7% RSD for all four target chiral congeners. Detection limits for PCBs 91, 95, 136, and 149 were 1.0, 1.3, 1,3, and 1.2 pg on column, respectively, based on a signal-to-noise ratio of 3.

2.2.6 Statistics

All EFs are presented as mean±SD unless otherwise indicated. Statistical significances of differences in EFs among sample groups and standards were

determined using ANOVA and Tukey Honestly-Significant-Difference post-hoc tests. Concentrations among the four sampling seasons were compared using paired t-tests. Unless otherwise noted, a confidence level of 95% was used for all statistical tests and linear regressions.

2.3 Results and Discussion

2.3.1 Concentrations and fluxes.

The achiral evaluation of PCB concentrations and air-water fluxes in this study is presented in detail elsewhere [23]. Briefly, 90 congeners were quantified. Mean gas phase ΣPCB concentrations were 1420 pg/m^3 and 1670 pg/m^3 in August and October 2000, respectively. Higher temperatures during these months were the most likely reason why vapour phase ΣPCB were significantly different than the mean of ca. 600 pg/m^3 observed in October 1999, December 1999, April 2000 and April 2001. Other potential reasons for elevated air concentrations include a low mixing height and a stable air mass, as investigated by MacLeod et al. in a study of semivolatile contaminant variability in air over 24 hour periods [33]. Mean dissolved phase ΣPCB concentrations at the nearshore HRE were constant throughout the year and were significantly greater (1100±240 pg/L) than at offshore CAO (420±65 pg/L). Particulate phase concentrations averaged 1600±1200 pg/L, varied throughout the year, and were significantly correlated to total suspended matter and particulate organic carbon concentrations. A net volatilization of lower chlorinated (≤5 Cl) PCBs throughout the year was

calculated using the two-film model [34-36] in the HRE (+170 ng m^{-2} d^{-1}) and CAO (+37 ng m^{-2} d^{-1}). Fluxes for higher chlorinated PCBs (≥6 Cl) were not determined, but are likely a minor fraction of overall flux because of slower mass transfer coefficients and lower dissolved phase concentrations. Observed congener patterns (not shown) for all phases showed a high proportion of lower chlorinated (tri through penta) congeners, and was consistent among air, water, TSM, and phytoplankton.

2.3.2 Enantiomer analysis and chiral signatures.

Atropisomeric PCBs 95 and 149 were the most detected chiral congeners at 90% and 70% frequencies, respectively. The other targeted chiral congeners, PCBs 91 and 136, were infrequently detected (23% and 29%, respectively). This discussion will therefore focus on the former two congeners. Although isobaric PCB 93 coelutes with the first-eluting enantiomer of PCB 95 on Chirasil-Dex [25], it is a non-Aroclor congener [29], not present in these samples [23] and is therefore unlikely to be an interference. Furthermore, all non-racemic EFs for PCB 95 were < 0.5. If PCB 93 was present, it would have biased EFs in the opposite direction (i.e., > 0.5).

2.3.3 Atmospheric sources.

Atmospheric gas-phase EFs for PCBs 91, 95, 136, and 149 were all racemic: 0.492±0.011, 0.496±0.012, 0.497±0.008, and 0.503±0.014, respectively. No significant differences in any atmospheric EFs were observed among the four sites. Nor were there any temporal EF differences over the four sampling dates.

This is likely caused by an overwhelming year-round urban racemic source, as described below.

These signatures indicate that atmospheric sources of penta- and hexa-chlorinated PCBs to the airshed were racemic, and were likely to be unweathered contamination originating from nearby urban and industrial sources. Previous work found higher atmospheric concentrations of PCBs [34] and PAHs [37] at locations in close proximity to areas of dense urbanization in this region. Similar results have been found for other urban locations, including PCBs in the UK West Midlands [38], Baltimore Harbor, and the northern Chesapeake Bay [39]. The atmospheric sample collection sites are all within 30 to 40 km of New York City, Newark, and Jersey City. Thus, they should reflect the chiral signatures of these urban centres. The signatures of urban air have not yet been assessed, but are likely to be racemic given observations of exclusively racemic PCBs 95, 136, and 149 in urban U.K. air [17, 38]. The other possible source of PCBs to the regional atmosphere is volatilization from estuarine waters (ca. 30 kg/yr) [40] occurring year-round [23, 34]. However, this source is likely dwarfed by localized urban sources of at least 300 kg/yr [40], as evidenced by racemic atmospheric signatures for PCB 95 that were significantly different from the nonracemic signatures of this congener in the water column (Figure 2-2a). This was true regardless of the higher volatilization in the summer months [23] which did not change atmospheric chiral signatures.

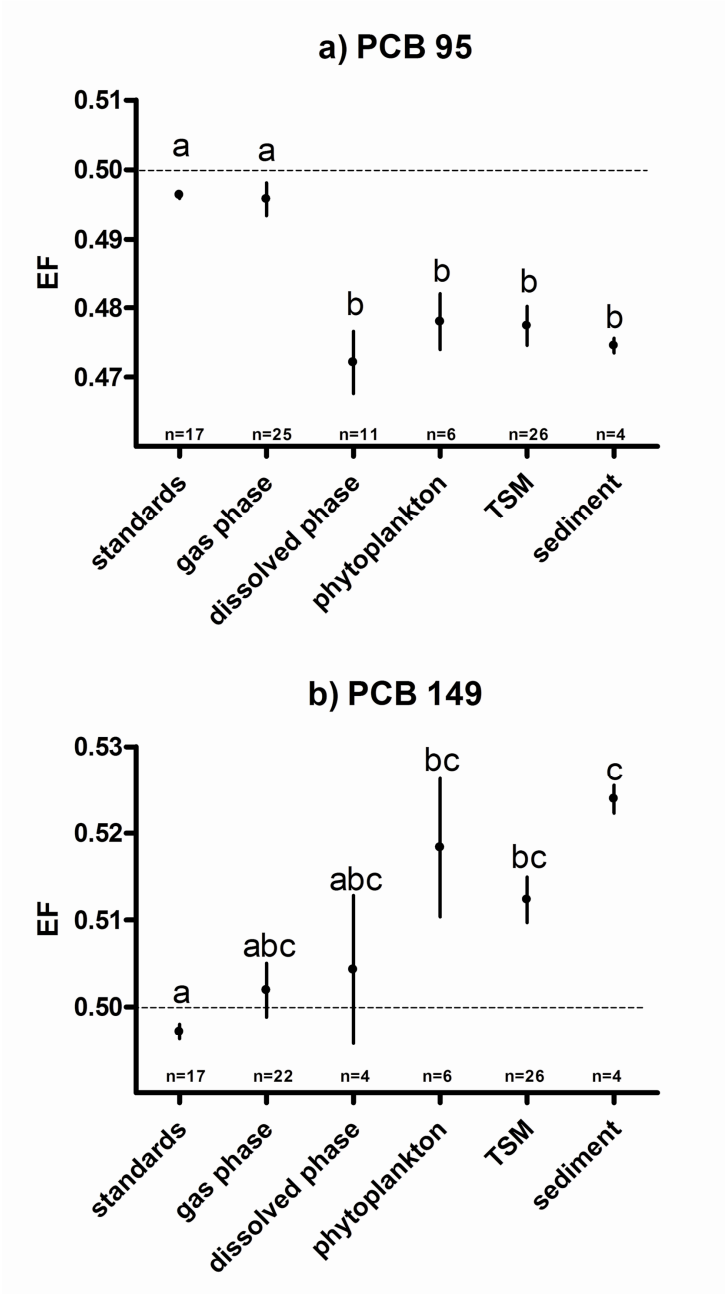

Figure 2-2: *Enantiomeric fractions (EFs) for PCBs 95 (a) and 149 (b) in racemic standards and five environmental compartments in the estuary. Points indicate mean value, while error bars indicate standard error. EF distributions sharing a letter designation (a, b, c) are not statistically different. Dotted line represents theoretical racemic EF (EF = 0.5).*

Our conclusions about atmospheric sources of PCBs in the estuary are similar to results reported by other chiral source apportionment studies at different locations worldwide. Robson and Harrad observed racemic signatures for PCBs 95, 136, and 149 in U.K. air, but nonracemic amounts in topsoil at adjacent sites [17]. Thus, atmospheric PCBs arose predominantly from primary sources [40], rather than volatilization of weathered PCBs from soil. Similarly, Gouin et al. observed racemic signatures of chlordane in air in the urban areas of Toronto and Chicago, and non-racemic atmospheric signatures in rural and remote regions [41]. Ridal et al. observed generally racemic signatures for α-hexachlorocyclohexane in air above nonracemic Lake Ontario and Niagara River waters [15]. In that study, however, chiral signatures in air varied seasonally, and reflected the nonracemic character of the water more when temperatures, and consequently volatilization, were at their highest. In contrast, the dominant source of legacy organochlorine pesticides to the atmosphere today is weathered sources, such as agricultural emissions, evidenced by significantly nonracemic signatures observed for both soil and the overlying air [19, 42], as well as over long-range transport [43]. Our results clearly show that while the potential for nonracemic airborne PCB signatures exists due to the significantly weathered output from the estuarine waters, the actual atmospheric EF is overwhelmed by a strong output of racemic local urban sources.

2.3.4 Water column sources.

In contrast to air, PCB 95 was significantly nonracemic in water, TSM, phytoplankton, and sediments (Figure 2-2a), with mean EFs of 0.472±0.015, 0.477±0.014, 0.478±0.010 and 0.475±0.002 respectively. Water column EFs were nearly all from the nearshore HRE, as few samples from CAO were taken, and were mostly nondetects in GC/MS/MS analysis (e.g., only 3 TSM EFs). The near-identical EFs for phytoplankton and TSM are not surprising, as most of the TSM was phytoplankton based on visual inspections during sampling. Measured ΣPCB concentrations in phytoplankton and TSM collected at the same time and location were highly correlated ($p<0.01$) [10].

The most likely source of nonracemic PCB 95 in the estuary is weathered sediments from the Hudson River, where extensive microbial reductive dechlorination has occurred [44], likely stereoselectively [20]. This is consistent with the nonracemic signatures for this congener previously found in Upper Hudson River sediment. The direction and approximate magnitude of PCB enantiomer enrichment observed here was similar to that at four sediment locations in the Upper Hudson [20], with a mean EF of 0.452±0.014 converted from enantiomeric ratios [26].

There were no significant differences among PCB 95 EFs in water, phytoplankton, TSM, and sediment (Figure 2-2a). This observation implies a close association of contaminant exchange among these four components of the water column, distinct from atmospheric sources. More specifically, it suggests that water concentrations of PCB 95 are influenced more by sediment sources

than by atmospheric sources. Inputs of weathered PCB 95 from the Hudson River to estuarine waters are likely to be much greater than racemic atmospheric absorption fluxes.

A similar but less obvious trend was found for PCB 149 (Figure 2-2b). Although nonracemic signatures were observed for phytoplankton, TSM, and sediment, only the sediment was significantly different from air. While PCB 149 in water exhibited a wide range of EFs (Figure 2-2b), these were not significantly different from EFs in air or racemic standards. The lack of statistical significance is likely because EFs for PCB 149 in Upper Hudson sediments were closer to racemic values (0.518±0.018) [20] than those for PCB 95. The differences between EFs in the two considered sources (Upper Hudson sediment and atmospheric deposition) were small, so source apportionment assessments are difficult to make. In addition, Hudson River sediments contain dechlorinated Aroclor 1242 [44], so the proportion of hexa congeners, including PCB 149, is low compared to lighter congeners. As a result, lighter congeners have higher Hudson River inputs to the estuary compared to those of PCB 149. The smaller weathered fluvial non-racemic PCB 149 flux to the estuary is therefore more similar to the racemic PCB 149 gas absorption flux, likely to be low as previously discussed [23]. For these reasons, the influence of Upper Hudson contamination on PCB 149 phytoplankton uptake compared to atmospheric sources is lower than for PCB 95.

2.3.5 Phytoplankton Sources.

The rate at which phytoplankton accumulate contaminants can vary greatly and consequently can play a significant role in the contaminant distribution of the compartments around them. During periods of significant growth, particularly during the summer months, phytoplankton can uptake contaminants from surrounding waters faster than equilibrium conditions would dictate [22]. Furthermore, high degrees of collective uptake by these organisms can result in depletion of contaminants from the dissolved phase, resulting in a loss of air-water equilibrium, and more absorption of gas phase contaminants into the water [11, 12]. Hence, phytoplankton should be subject to increased uptake of atmosphere-originating contaminants. While this may be the case in the estuary for light PCB congeners (≤ 4 Cl), it was not the case for PCB 95 and to a lesser extent PCB 149. For these congeners and possibly other congeners in the penta and hexa homologs, PCBs from the Upper Hudson dominated dissolved phase concentrations in the estuary, via desorption or resuspended sediment transported downstream, and dwarfed the effect of air-water exchange on phytoplankton.

2.3.6 Trends in EFs.

The similarity in EFs throughout the estuarine water column to those of Upper Hudson sediment [20] suggests that the river, and not the atmosphere, was the predominant source of PCB 95 (and likely other homologous congeners) to the estuary and its food web. This hypothesis is supported by correlations of EFs with Hudson River flow. The U.S. Geological Survey monitoring station

hydrograph at Waterford, NY was used to estimate average streamflow in the Upper Hudson. Monthly volumetric discharge for April 2000, August 2000, October 2000, and April 2001 averaged 594, 244, 157, and 641 m^3/s, respectively [45], representing high flow over spring runoff and lower flow in summer and autumn. The EFs for individual samples were correlated with five-day average river discharges at Waterford 30 days prior to each sample's sampling date, based on the calculated residence time between Waterford and the HRE site. For PCB 95, river discharge significantly correlated with EF for TSM and dissolved phase at 95% and 90% confidence, respectively (Figures 2-3a and 2-3b). In addition, a small, non-significant correlation between river flow and EFs for PCB 149 in TSM samples was observed (Figure 2-3c). A similar correlation was not calculated for dissolved phase PCB 149 given insufficient data. Generally, the high flow rates observed in the spring, when contributions from the Upper Hudson to the estuary were high, corresponded with more nonracemic EFs in the water column. This effect is also evident between PCB 95 TSM EF as a function of ΣPCB concentrations at 90% confidence (Figure 2-3d). During high flow conditions, contributions from the Upper Hudson are at their highest, resulting in both higher estuarine concentrations and more non-racemic EFs. Similar results were observed for scenarios with one-day to thirty-one-day average discharges, suggesting that these results are robust.

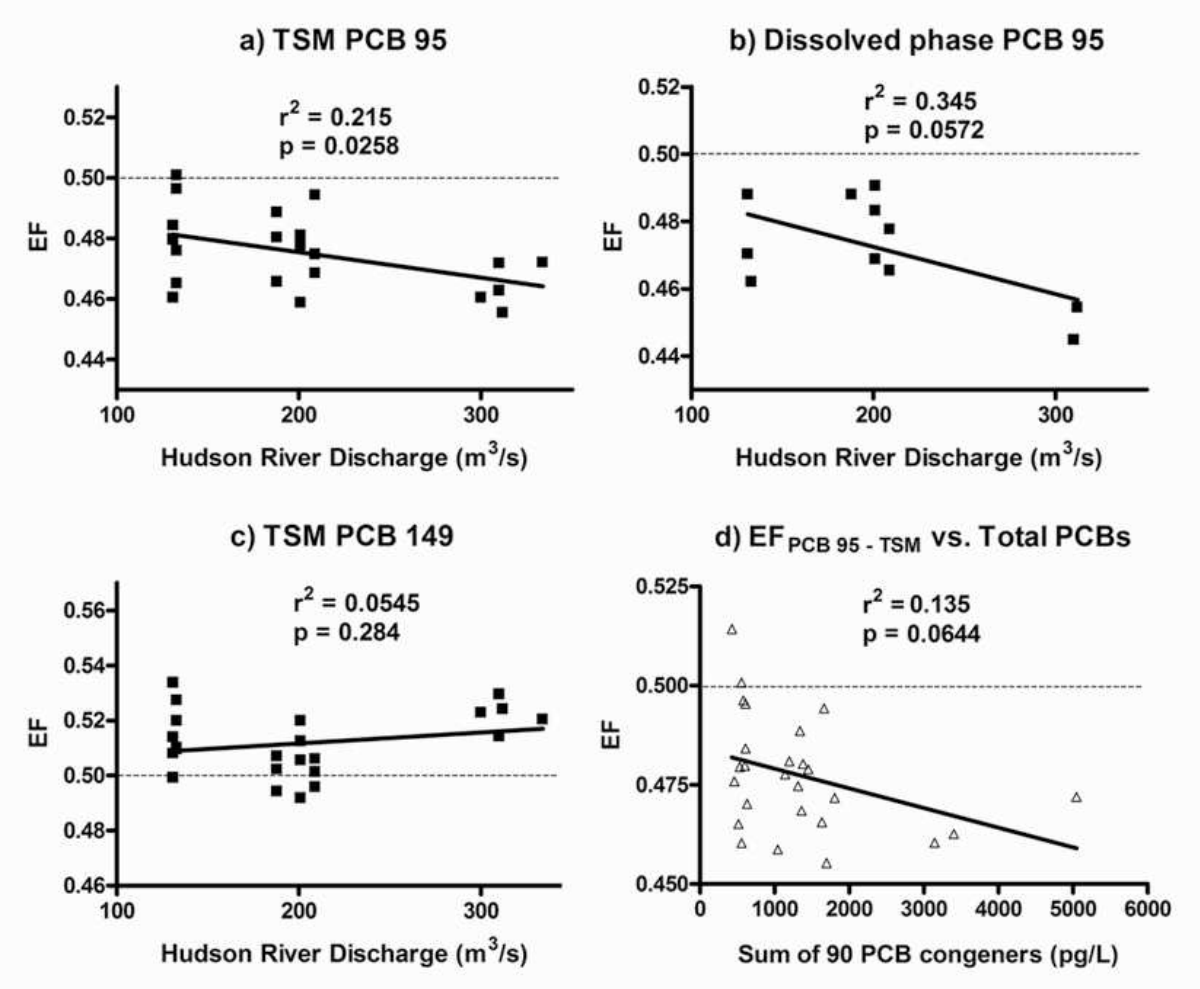

Figure 2-3: *Relation of Upper Hudson River volumetric discharge at Waterford station to enantiomeric fractions (EFs) of PCB 95 for dissolved phase (a) and TSM (b) and of PCB 149 for TSM (c) in the estuary, and EFs of PCB 95 in TSM as a function of total PCB concentration (sum of 90 congeners) (d). Dotted line represents theoretical racemic EF (EF = 0.5).*

These trends in EF data are consistent with a previous study performed on this data set [46]. Gigliotti used Positive Matrix Factorization to determine three factors influencing PCB concentrations in the estuary. Two of the three factors represented the dissolved and particulate phases of the Upper Hudson, and

contributions from these two factors were highest when discharge in the Upper Hudson River was also high. Transport of contaminated sediments to the estuary is significant, with an estimated 300,000 metric tons/yr of new deposits in 1998 and 1999, and were highest following the spring freshet [47], consistent with our observations. The correlations between Hudson discharge and PCB 95 EFs in both the dissolved phase and TSM are consistent with studies suggesting PCB desorption from resuspended Upper Hudson sediments [4, 48] . Following resuspension, desorption into the dissolved phase happens quickly, over the course of several days [4]. Thus, estuarine water becomes nonracemic, and weathered PCB 95 is bioconcentrated by estuarine phytoplankton.

2.4 Conclusion: Implications for the local aquatic food web.

For both PCB 95 and 149, chiral signatures for phytoplankton closely matched those of sediment in the estuary. The relative importance of sediment and air in determining phytoplankton concentrations can be quantified using the following chiral two-source apportionment relationship [26, 49]:

$$f_A = (EF_{MIX} - EF_B)/(EF_A - EF_B) \qquad \text{Equation 2-1}$$

where f_A is the fraction of total contaminant from source A, EF_A and EF_B are the enantiomeric fractions of source A and B, respectively, and EF_{MIX} is the enantiomeric fraction of the affected compartment, in this case phytoplankton. For PCB 95, 86% of the phytoplankton PCB load originated from contaminated sediment. Likewise, for PCB 149, a high proportion (73%) was sediment-

derived, although the value for this congener should be regarded as inconclusive due to the larger error associated with these EF measurements resulting in the lack of significant difference in EFs between air and phytoplankton. Nevertheless, it is clear that atmospheric sources do not significantly control phytoplankton uptake of PCBs 95 and 149, and by extension penta- and hexa-PCBs. Consequently, air-water exchange may have little effect on the estuarine aquatic food web for these homologs, although its effect on other homologs may be significant. Therefore, future efforts to reduce PCB contamination and mobilization in the Upper Hudson should be effective in reducing contamination in the estuarine aquatic food web, as well as human exposure via ingestion of local fish.

2.5 References

1. U.S. Environmental Protection Agency, "Hudson River PCBs Site New York. Record of Decision" 2002.

2. Connolly, J. P.; Zahakos, H. A.; Benaman, J.; Ziegler, C. K.; Rhea, J. R.; Russell, K., A Model of PCB Fate in the Upper Hudson River. *Environmental Science & Technology* **2000,** *34*, (19), 4076-4087.

3. Bopp, R. F.; Simpson, H. J.; Olsen, C. R.; Kostyk, N., Polychlorinated-biphenyls in sediments of the tidal Hudson River, New-York. *Environmental Science & Technology* **1981,** *15*, (2), 210-216.

4. Schneider, A. R.; Porter, E. T.; Baker, J. E., Polychlorinated biphenyl release from resuspended hudson river sediment. *Environmental Science & Technology* **2007,** *41*, (4), 1097-1103.

5. Durell, G. S.; Lizotte, R. D., PCB levels at 26 New York City and New Jersey WPCPs that discharge to the New York/New Jersey Harbor Estuary. *Environmental Science & Technology* **1998,** *32*, (8), 1022-1031.

6. Totten, L. A.; Gigliotti, C. L.; VanRy, D. A.; Offenberg, J. H.; Nelson, E. D.; Dachs, J.; Reinfelder, J. R.; Eisenreich, S. J., Atmospheric concentrations and deposition of polychorinated biphenyls to the Hudson River Estuary. *Environmental Science & Technology* **2004,** *38*, (9), 2568-2573.

7. Brunciak, P. A.; Dachs, J.; Gigliotti, C. L.; Nelson, E. D.; Eisenreich, S. J., Atmospheric polychlorinated biphenyl concentrations and apparent degradation in coastal New Jersey. *Atmospheric Environment* **2001,** *35*, (19), 3325-3339.

8. Totten, L.A. Present-day sources and sinks for polychlorinated biphenyls (PCBs) in the Lower Hudson River Estuary; Rutgers, The State University of New Jersey: New Brunswick, NJ, October 2004, 2004.

9. Farley, K. J.; Thomann, R. V.; Cooney, T. F. I.; Damiani, D. R.; Wands, J.R. An integrated model of organic chemical fate and bioaccumulation in the Hudson River Estuary; The Hudson River Foundation: March 1999.

10. Yan, S. Air-water exchange controls phytoplankton concentrations of polychlorinated biphenyls in the Hudson River Estuary. Master's Thesis, Rutgers University, New Brunswick, NJ, 2003.

11. Dachs, J.; Eisenreich, S. J.; Baker, J. E.; Ko, F. C.; Jeremiason, J. D., Coupling of phytoplankton uptake and air-water exchange of persistent organic pollutants. *Environmental Science & Technology* **1999,** *33*, (20), 3653-3660.

12. Jeremiason, J. D.; Eisenreich, S. J.; Paterson, M. J.; Beaty, K. G.; Hecky, R.; Elser, J. J., Biogeochemical cycling of PCBs in lakes of variable trophic status: A paired-lake experiment. *Limnol. Oceanogr.* **1999,** *44*, (3), 889-902.

13. Bidleman, T. F.; Wong, F.; Backe, C.; Sodergren, A.; Brorström-Lunden, E.; Helm, P. A.; Stern, G. A., Chiral signatures of chlordanes indicate changing sources to the atmosphere over the past 30 years. *Atmospheric Environment* **2004,** *38*, (35), 5963-5970.

14. Harner, T.; Kylin, H.; Bidleman, T. F.; Strachan, W. M. J., Removal of alpha- and gamma-hexachlorocyclohexane and enantiomers of alpha-hexachlorocyclohexane in the eastern Arctic Ocean. *Environmental Science & Technology* **1999,** *33*, (8), 1157-1164.

15. Ridal, J. J.; Bidleman, T. F.; Kerman, B. R.; Fox, M. E.; Strachan, W. M. J., Enantiomers of alpha-hexachlorocyclohexane as tracers of air-water gas exchange in Lake Ontario. *Environmental Science & Technology* **1997,** *31*, (7), 1940-1945.

16. Fono, L. J.; Sedlak, D. L., Use of the chiral pharmaceutical propranolol to identify sewage discharges into surface waters. *Environmental Science & Technology* **2005,** *39*, (23), 9244-9252.

17. Robson, M.; Harrad, S., Chiral PCB signatures in air and soil: Implications for atmospheric source apportionment. *Environmental Science & Technology* **2004,** *38*, (6), 1662-1666.

18. Pakdeesusuk, U.; Jones, W. J.; Lee, C. M.; Garrison, A. W.; O'Niell, W. L.; Freedman, D. L.; Coates, J. T.; Wong, C. S., Changes in enantiomeric fractions during microbial reductive dechlorination of PCB132, PCB149, and Aroclor 1254 in Lake Hartwell sediment microcosms. *Environmental Science & Technology* **2003,** *37*, (6), 1100-1107.

19. Bidleman, T. F.; Jantunen, L. M.; Harner, T.; Wiberg, K.; Wideman, J. L.; Brice, K.; Su, K.; Falconer, R. L.; Aigner, E. J.; Leone, A. D.; Ridal, J. J.; Kerman, B.; Finizio, A.; Alegria, H.; Parkhurst, W. J.; Szeto, S. Y., Chiral pesticides as tracers of air-surface exchange. *Environmental Pollution* **1998,** *102*, (1), 43-49.

20. Wong, C. S.; Garrison, A. W.; Foreman, W. T., Enantiomeric composition of chiral polychlorinated biphenyl atropisomers in aquatic bed sediment. *Environmental Science & Technology* **2001,** *35*, (1), 33-39.

21. Wong, C. S.; Mabury, S. A.; Whittle, D. M.; Backus, S. M.; Teixeira, C.; DeVault, D. S.; Bronte, C. R.; Muir, D. C. G., Organochlorine compounds in Lake Superior: Chiral polychlorinated biphenyls and biotransformation in the aquatic food web. *Environmental Science & Technology* **2004,** *38*, (1), 84-92.

22. Skoglund, R. S.; Stange, K.; Swackhamer, D. L., A kinetics model for predicting the accumulation of PCBs in phytoplankton. *Environmental Science & Technology* **1996,** *30*, (7), 2113-2120.

23. Yan, S.; Rodenburg, L. A.; Dachs, J.; Eisenreich, S. J., Seasonal air-water exchange fluxes of polychlorinated biphenyls in the Hudson River Estuary. *Environmental Pollution* **2008,** *152*, (2), 443-451.

24. Gigliotti, C. L.; Dachs, J.; Nelson, E. D.; Brunciak, P. A.; Eisenreich, S. J., Polycyclic aromatic hydrocarbons in the New Jersey coastal atmosphere. *Environmental Science & Technology* **2000,** *34*, (17), 3547-3554.

25. Wong, C. S.; Garrison, A. W., Enantiomer separation of polychlorinated biphenyl atropisomers and polychlorinated biphenyl retention behavior on modified cyclodextrin capillary gas chromatography columns. *Journal of Chromatography A* **2000,** *866*, (2), 213-220.

26. Harner, T.; Wiberg, K.; Norstrom, R. J., Enantiomer fractions are prefered to enantiomer raios for describing chiral signatures in environmental analysis. *Environmental Science & Technology* **2000,** *34*, 218-220.

27. Wong, C. S.; Hoestra, P. F.; Karlsson, H.; Backus, S. M.; Mabury, S. A.; Muir, D. C. G., Enantiomer fractions of chiral organochlorine pesticides and polychlorinated biphenyls in standard and certified reference materials. *Chemosphere* **2002,** *49*, (10), 1339-1347.

28. Frame, G. M., A collaborative study of 209 PCB congeners and 6 Aroclors on 20 different HRGC columns .1. Retention and coelution database. *Fresen. J. Analytical Chemistry* **1997,** *357*, (6), 701-713.

29. Frame, G. M.; Cochran, J. W.; Bowadt, S. S., Complete PCB congener distributions for 17 aroclor mixtures determined by 3 HRGC systems optimized for comprehensive, quantitative, congener-specific analysis. *J. High-Resol. Chromatogr.* **1996,** *19*, (12), 657-668.

30. Ulrich, E. M.; Hites, R. A., Enantiomeric ratios of chlordane-related compounds in air near the Great Lakes. *Environmental Science & Technology* **1998,** *32*, (13), 1870-1874.

31. Bucheli, T. D.; Brandli, R. C., Two-dimensional gas chromatography coupled to triple quadrupole mass spectrometry for the unambiguous determination of atropisomeric polychlorinated biphenyls in environmental samples. *Journal of Chromatography A* **2006,** *1110*, (1-2), 156-164.

32. Morrissey, J. M.; Bleackley, D. S.; Warner, N. A.; Wong, C. S., Enantiomer fractions of polychlorinated biphenyls in three selected Standard Reference Materials. *Chemosphere* **2007,** *66*, 326-331.

33. MacLeod, M.; Scheringer, M.; Podey, H.; Jones, K. C.; Hungerbuhler, K., The Origin and Significance of Short-Term Variability of Semivolatile Contaminants in Air. *Environmental Science & Technology* **2007,** *41*, (9), 3249-3253.

34. Totten, L. A.; Brunciak, P. A.; Gigliotti, C. L.; Dachs, J.; Glenn, T. R.; Nelson, E. D.; Eisenreich, S. J., Dynamic air-water exchange of polychlorinated biphenyls in the New York - New Jersey Harbor Estuary. *Environmental Science & Technology* **2001,** *35*, (19), 3834-3840.

35. Nelson, E. D.; McConnell, L. L.; Baker, J. E., Diffusive exchange of gaseous polycyclic aromatic hydrocarbons and polychlorinated biphenyls across the air-water interlace of the Chesapeake Bay. *Environmental Science & Technology* **1998,** *32*, (7), 912-919.

36. Gigliotti, C. L.; Brunciak, P. A.; Dachs, J.; Glenn, T. R.; Nelson, E. D.; Totten, L. A.; Eisenreich, S. J., Air-water exchange of polycyclic aromatic hydrocarbons in the New York-New Jersey, USA, Harbor Estuary. *Environ. Toxicol. Chem.* **2002,** *21*, (2), 235-244.

37. Gigliotti, C. L.; Totten, L. A.; Offenberg, J. H.; Dachs, J.; Reinfelder, J. R.; Nelson, E. D.; Glenn, T. R.; Eisenreich, S. J., Atmospheric concentrations and deposition of polycyclic aromatic hydrocarbons to the Mid-Atlantic East Coast Region. *Environmental Science & Technology* **2005,** *39*, (15), 5550-5559.

38. Jamshidi, A.; Hunter, S.; Hazrati, S.; Harrad, S., Concentrations and chiral signatures of polychlorinated biphenyls in outdoor and indoor air and soil in a major UK conurbation. *Environmental Science & Technology* **2007,** *41*, 2153-2158.

39. Bamford, H. A.; Ko, F. C.; Baker, J. E., Seasonal and annual air-water exchange of polychlorinated biphenyls across Baltimore Harbor and the northern

Chesapeake Bay. *Environmental Science & Technology* **2002,** *36*, (20), 4245-4252.

40. Totten, L. A.; Stenchikov, G.; Gigliotti, C. L.; Lahoti, N.; Eisenreich, S. J., Measurement and modeling of urban atmospheric PCB concentrations on a small (8 km) spatial scale. *Atmospheric Environment* **2006,** *40*, (40), 7940-7952.

41. Gouin, T.; Jantunen, L.; Harner, T.; Blanchard, P.; Bidleman, T., Spatial and temporal trends of chiral organochlorine signatures in Great Lakes air using passive air samplers. *Environmental Science & Technology* **2007,** *41*, (11), 3877-3883.

42. Finizio, A.; Bidleman, T. F.; Szeto, S. Y., Emission of chiral pesticides from an agricultural soil in the Fraser Valley, British Columbia. *Chemosphere* **1998,** *36*, (2), 345-355.

43. Bidleman, T. F.; Jantunen, L. M. M.; Helm, P. A.; Brorstrom-Lunden, E.; Juntto, S., Chlordane enantiomers and temporal trends of chlordane isomers in arctic air. *Environmental Science & Technology* **2002,** *36*, (4), 539-544.

44. Bedard, D. Q. I., J.;, Microbial reductive dechlorination of polychlorinated biphenyls. In *Microbial Transformation and Degradation of Toxic Organic Contaminants*, Young, L. C., C.;, Ed. Wiley-Liss: New York, 1995; pp 127-216.

45. U.S. Geological Survey, http://waterdata.usgs.gov/nwis. Accessed February 3, 2007.

46. Gigliotti, C. L. Environmental origin, chemical transport, and fate of hazardous pollutants in atmospheric and aquatic systems in the Mid-Atlantic region. Ph.D. Thesis, Rutgers University, New Brunswick, NJ, 2003.

47. Woodruff, J. D.; Geyer, W. R.; Sommerfield, C. K.; Driscoll, N. W., Seasonal variation of sediment deposition in the Hudson River estuary. *Marine Geology* **2001,** *179*, 105-119.

48. Butcher, J. B.; Garvey, E. A., PCB loading from sediment in the Hudson River: Congener signature analysis of pathways. *Environmental Science & Technology* **2004,** *38*, (12), 3232-3238.

49. Bidleman, T. F.; Falconer, R. L., Enantiomer ratios for apportioning two sources of chiral compounds. *Environmental Science & Technology* **1999,** *33*, (13), 2299-2301.

Chapter 3: Comparison of Peak Integration Methods for the Determination of Enantiomeric Fraction in Environmental Samples

A version of this chapter has been previously published as Asher, B. J.; D'Agostino, L. A.; Way, J. D.; Wong, C. S.; Harynuk, J. J., Comparison of peak integration methods for the determination of enantiomeric fraction in environmental samples. Chemosphere 2009, 75, (8), 1042-1048.

3.1 Introduction

The measurement of individual enantiomers of environmental contaminants is a current area of significant interest. Numerous compounds of environmental concern are chiral, including organochlorine pesticides such as α-hexachlorocyclohexane, 19 of the 209 polychlorinated biphenyl (PCB) congeners, hexabromocyclododecanes, and many pharmaceuticals such as propranolol and fluoxetine. Enantioselective analysis of a chiral compound can provide valuable information about its environmental fate, including the occurrence and extent of biotransformation [1, 2] and the proportions of contaminant originating from multiple sources [3-5]. This also has potential implications for ecological risk assessments given the differential toxicities of the enantiomers of many chiral environmental contaminants [6-8]. The preferred metric for quantifying these relative concentrations is the enantiomeric fraction (EF) [9], defined as:

$$EF = \frac{A}{A+B} \qquad \text{Equation 3-1}$$

where A and B represent concentrations of the (+) and (−) enantiomers, respectively, or of the first- and second-eluted enantiomers under defined enantioselective chromatographic conditions if the elution order is unknown. Pure enantiomers have EFs of 0 or 1, while racemates have an EF of 0.5 [9]. EFs are commonly used in environmental calculations when performing source apportionment [9] and when calculating minimum biotransformation rate constants [10]. These calculations are sensitive to slight errors in EF.

Consequently, the accuracy in determining enantiomer peak areas is especially important.

While the complete chromatographic separation of enantiomers is desirable; in practice, the quantification of environmental chiral contaminants is often performed when the two enantiomers are only partially resolved. Complete separation of enantiomers is often impractical for routine analyses, such as those quantifying several pairs of enantiomers at once [11, 12]. The most commonly used technique for integrating partially resolved chromatographic peaks of environmental analytes is the *valley drop method* (VDM). In this process, which can be performed using standard chromatographic software, a perpendicular line is dropped from the valley between the two peaks to the baseline (Figure 3-1). This method will always result in biased peak areas [13], except when the peaks are equal in size (EF = 0.5) and symmetrical [14]. When these conditions are not met, a significant portion of the area of one enantiomer's peak will inevitably fall under the peak of its antipode in disproportionate amounts (Figure 3-1). Enantioselective chromatography, which often suffers from slower mass transfer kinetics and more frequent non-linear isotherms [15, 16], can result in more severe peak tailing, causing even larger biases when using the VDM.

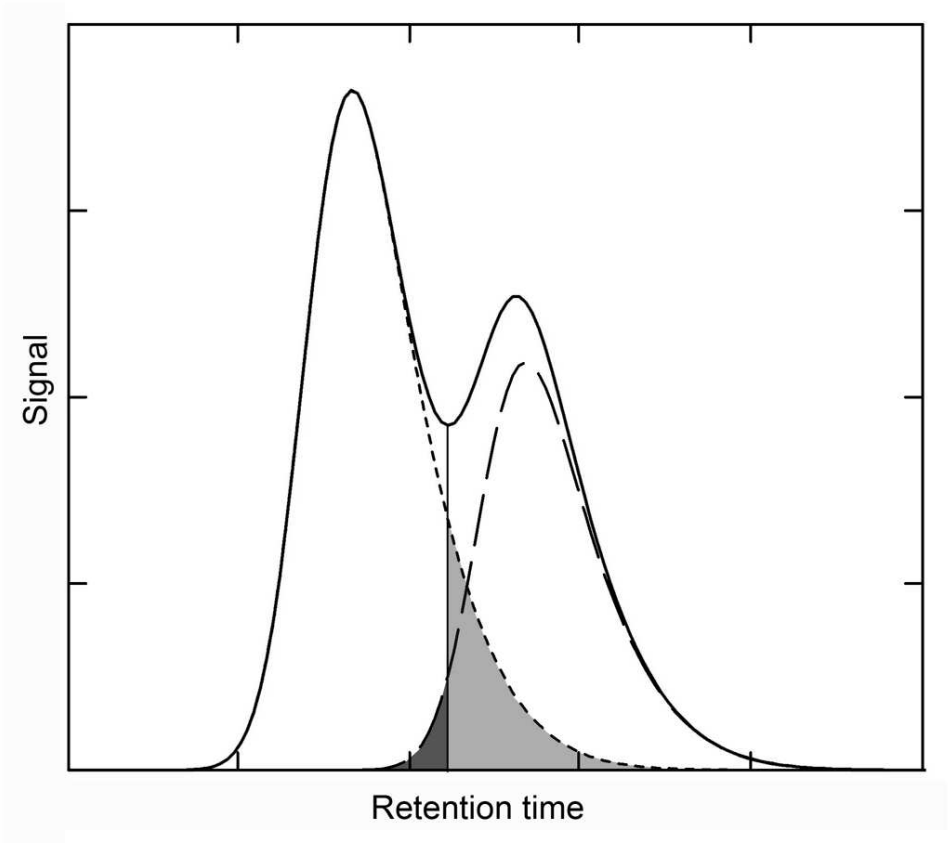

Figure 3-1: *Integration of partially resolved enantiomers by the valley drop method. Dashed lines indicate the peak traces of individual enantiomers. Shaded regions indicate the peak area of each enantiomer that is erroneously attributed to its antipode, resulting in a calculated EF that is too small. The example shown has a true EF=0.6, Rs=1.0, and As=1.5.*

Biases associated with the VDM have been previously studied by Meyer [17], who showed that errors in area can be as high as 40% when working with pairs of peaks having appreciably different sizes (area ratios of 10 to 1) and significant tailing (asymmetry of 2). Bicking studied four different integration techniques, including the VDM and a "Gaussian skim" method, where true peak areas are estimated by adding a skimming line that approximates a Gaussian function under each peak, and adding the area between the skim line and the baseline to the parent peak [18]. In that study, the Gaussian skim method

produced errors that, in most cases, were similar to, or even worse than the VDM. A less commonly used but potentially more accurate integration technique is the *deconvolution method* (DM). Here, a least squares method is used to fit the chromatographic data to the sum of two independent Gaussian-based mathematical functions via commercially available software. Since each peak is fit to its own function, the algorithms account for peak overlap (including tailing when appropriate models are used). This results in peak areas that are not subject to the biases of the VDM. Peak deconvolution has been used successfully in the determination of environmental contaminants, including polybrominated diphenyl ether congeners [19], pesticides [20], and their enantiomerization energy barriers [21], and an automated deconvolution method has been developed [22]. This analysis has also been applied to comprehensive two-dimensional gas chromatographic (GC×GC) data [23].

Although the variability in error associated with traditional integration techniques has been established, details associated with peak integration have been absent from the experimental sections of chiral environmental literature, with a few exceptions [5, 24, 25]. The potential improvement in the accuracy of enantioselective environmental analyses by using an advanced integration technique, such as the DM, has not yet been assessed. Our objective is to compare the errors in EF determination between the VDM and the DM, utilizing commercially available software for both techniques. Both instrument-generated (hereafter referred to as "real") and simulated chromatograms were analysed to assess the accuracy and precision of each integration method, and to investigate

the effects of true EF, signal-to-noise ratio, resolution, and peak asymmetry on the performance of each technique. The implications of such errors (having magnitudes observed in this study) on environmental calculations that utilize EF, using published environmental data, is also discussed.

3.2 Materials and Methods

3.2.1 Preparation of enantiomerically enriched standards

PCB 132 (Figure 3-2, inset) was chosen as a model compound for the real chromatograms because its enantiomers can be readily separated and collected by high performance liquid chromatography (HPLC), and can be baseline-resolved by gas chromatography (GC) [26], providing a means for establishing a true EF. A method for isolation of individual PCB 132 enantiomers has been previously published [27]. Briefly, seven 50-μL aliquots of 15 μg mL^{-1} racemic PCB 132 were injected into an Agilent HPLC 1050 system with a Nucleodex β-PM column (200 mm × 4.6 mm i.d. × 5 μm particle size, Macherey-Nagel, Düren, Germany). A flow rate of 0.5 mL min^{-1} and a 75:25 methanol:water isocratic mobile phase was used. The eluent fractions containing individual enantiomers were collected, combined, transferred to hexane via liquid-liquid extraction, and evaporated to approximately 1 mL under nitrogen. Solutions with an approximate EF = 0.3, 0.4, 0.6, and 0.7 were generated by combining the enantiomerically pure solutions in appropriate proportions.

3.2.2 Chromatographic conditions for instrument-generated data

Analysis was performed with a HP 5890/5971 GC/MS using electron impact ionization in selective ion monitoring mode for *m/z* of 358, 360, and 362. A Chirasil-Dex column (30 m × 0.25 mm i.d. × 0.25 μm d_f, Varian, Walnut Creek, CA) was used for the separation. Seven chromatographic resolutions (R_s; calculated as the difference in retention times of the peaks divided by the mean of the peak widths measured at the base of each peak) were achieved using the following column conditions: injector and MS transfer line temperatures of 280 and 250 °C, respectively, He carrier gas at 1 mL min^{-1} constant flow, initial oven temperature of 60°C with a 2 minute hold, 15°C min^{-1} to the final temperature, and hold until 2 minutes after the second-eluted enantiomer. Final temperatures employed were 175, 180, 185, 190, 195, 205, and 215 °C for R_s of 1.57, 1.35, 1.16, 0.98 0.84, 0.62, and 0.48, respectively. Elution times ranged from 21 to 63 minutes. Asymmetric (tailing) peaks were generated by attaching a 1/16" Swagelok tube fitting between the injector and column to act as a mixing chamber, resulting in an average peak asymmetry of 2.7. Identical oven conditions were employed to yield average resolutions of 0.85, 0.72, 0.61, 0.51, 0.43, 0.33, and 0.20, respectively. Example chromatograms of the separation of PCB 132 atropisomers for both symmetric and asymmetric conditions are presented in Figure 3-2. Results for all real chromatographic data are based on the mean of 3 separate analyses of each mixture, and had signal-to-noise ratios with a range of approximately 40 to 80 (based on the largest peak), depending on the elution time and the extent of peak broadening for each temperature program.

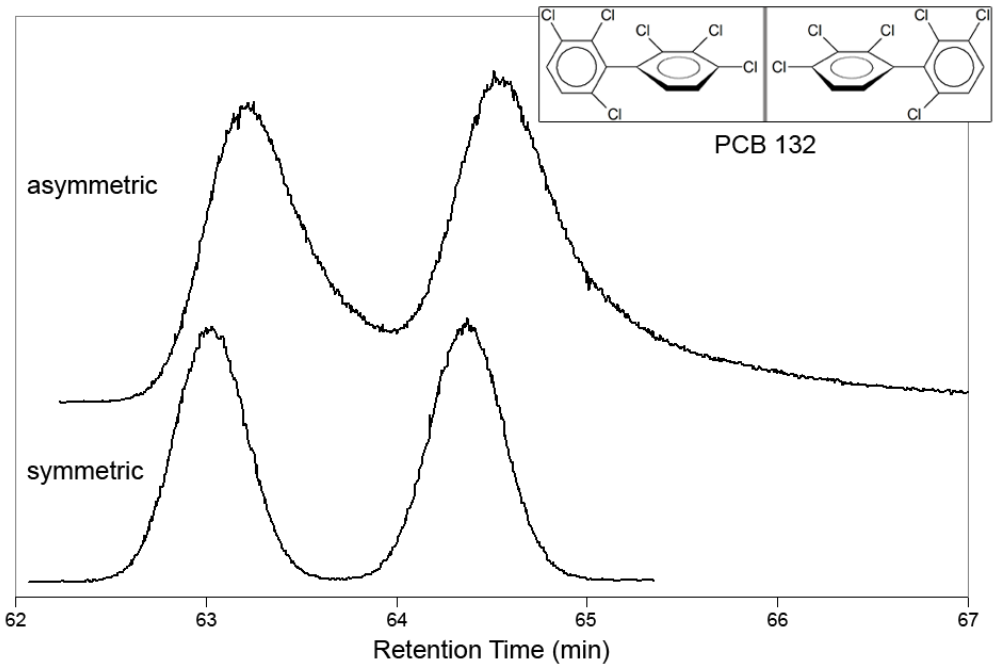

Figure 3-2: *Sample chromatograms of racemic PCB 132 standard under symmetric (As=1.0) and asymmetric (As=2.7) separation conditions. Inset: Chemical structures of PCB 132 atropisomers.*

3.2.3 Generation of simulated data

The simulation of chromatographic data was employed for integration comparisons, as simulations allow for precise control over individual peak parameters that cannot be achieved using real chromatograms. This simulated data approach has been used previously to look at peak integration methods [17] as well as other aspects of quantitation [28, 29]. A 4-parameter generalized exponentially modified Gaussian (GEMG) function was chosen to simulate chromatographic peak shapes. This function is produced by convolving a Gaussian function with a hybrid function of a half-Gaussian multiplied by an exponentially modified Gaussian , shown here [30]:

$$y = \frac{a_0 \exp\left(-\frac{1}{2}\frac{(x-a_1)^2}{a_3^{\,2}+a_2^{\,2}}\right)\left[1+\operatorname{erf}\left(\frac{a_3(x-a_1)}{\sqrt{2}a_2\sqrt{a_3^{\,2}+a_2^{\,2}}}\right)\right]}{\sqrt{2\pi}\sqrt{a_3^{\,2}+a_2^{\,2}}} \quad \text{Equation 3-2}$$

where x and y represent the retention time and response, respectively, and a_0, a_1, a_2, and a_3 represent the peak area, centre, width, and distortion parameters, respectively. It effectively describes chromatographic peaks, including those exhibiting significant asymmetry, and is described in detail elsewhere [31, 32]. Chromatograms were generated by summing two GEMG functions, simulating an enantioselective separation. Using Mathcad 14.0 software (Parametric Technology, Needham, MA, USA), the functions were solved at intervals of 1/94 s to simulate a data acquisition rate of 1.57 Hz, equal to that of our real chromatograms.

Instrumental noise was simulated by adding normally distributed random numbers with a chosen mean and standard deviation (σ_N) to the data. The mean acted as a signal offset, ensuring no negative intensity values were recorded. The standard deviation was used to control S/N. EF was controlled by adjusting the areas of each peak, according to Equation 3-1. Retention times of the simulated peaks were varied to adjust R_s. Peak asymmetries (A_s) were calculated as the width of the tailing half of the peak divided by the width of the leading half of the peak at 10% of the maximum peak height. Asymmetries were modified by controlling the distortion parameter of the GEMG function, and were kept invariant among the peak pairs. Peak resolution, asymmetry, S/N, and EF were

varied with all possible combinations of parameters listed in Table 3-1. Ten replicate chromatograms for each set of parameters were generated, creating a total of 590 chromatograms.

Table 3-1: *Chromatographic parameters used for the generation of simulated data.*

A_s	S/N for Largest Peak	EF	Resolution
1	20	0.2, 0.4, 0.5, 0.6, 0.8	0.5
		0.5, 0.6, 0.8	0.7
	3, 10, 20	0.5	0.7
1.5	10	0.4, 0.45, 0.5, 0.55, 0.6	0.9, 0.7, 0.5
	20	0.2, 0.4, 0.5, 0.6, 0.8	1.5, 1.3, 1.1, 0.9, 0.7, 0.5
	75	0.4, 0.5, 0.6	0.5

3.2.4 Data handling and peak integration

All chromatograms were integrated using both the VDM and the DM. Integrations of the former were performed with the MSD Chemstation Integrator (version E.01.00.237; Agilent Technologies, Mississauga, Canada). Division of the peak pair was performed manually by placing the boundary between peaks at the centre of the valley. Simulated chromatograms, generated as text files by Mathcad, were converted to .CDF format using GC and GCMS File Translator Pro 5.0 (ChemSW, Fairfield, CA, USA) software. Prior to integration using the DM, real chromatograms were converted to ASCII (.TXT) format using GC and

GCMS File Translator Pro, based on the sum total response of the three ions monitored.

Integrations using the DM were performed using PeakFit v4.06 (Systat Software, San Jose, CA) software. Peakfit's nonparametric digital filter option, which simplifies the data set, was not employed. The "Autofit Peaks I: Residuals" mode, which determines initial peak location and parameters by minimizing evaluated residuals, was selected for peak detection and fitting [30]. The 4-parameter GEMG model was chosen as the mathematical model for fitting both real and simulated chromatograms [5, 24, 33]. Because the simulated data was generated using the same function, errors in EF associated with the DM fit of simulated data should be solely due to the addition of random noise, thereby providing a baseline for error when comparing to the VDM. This point was verified by the fact that fits of simulated chromatograms without added noise using Peakfit, produced zero error in EF and an r^2 of unity. Real and simulated chromatographic data was sectioned to exclude unnecessary parts of the chromatogram. Peakfit's fast Fourier transform filtering option was employed to determine initial peak placement. Additional peak fitting options of "Vary Widths" and "Vary Shape" were employed, except where otherwise noted. Fitting was iterated until the r^2 yielded a stable maximum value.

Biases in EF were determined according to the following equation:

$$BIAS = EF_{measured} - EF_{true} \qquad \text{Equation 3-3}$$

where $EF_{measured}$ is the enantiomeric fraction as determined by each integration method, according to Equation 3-1. For symmetric peaks, EF_{true} was based on the measured EF of the same mixture fully resolved and analysed on the same day, as determined by manual integration. For asymmetric (mixing chamber) trials, EF_{true} was determined by taking the average of three analyses of each mixture under conditions where the enantiomers were baseline-resolved before the addition of the mixing chamber. Peak shapes for GC trials in the absence of the mixing chamber were near Gaussian, with asymmetries ranging from 1.01 to 1.06. For simulated chromatograms, EF_{true} was determined based on the relative peak areas input into the peak generation algorithm.

3.3 Results and Discussion

3.3.1 Comparison of integration methods with instrument-generated data

The EFs of fully resolved chromatograms showed good agreement between the VDM and DM, with a mean EF difference of 0.005 (Figure 3-3), indicating our choice of "true EF" values was acceptable. The DM produced small biases in EF when analyzing symmetric peaks, with averages less than 0.01 for all EFs and resolutions (Figure 3-3a). No trends in bias with changes in EF or increasing resolution were apparent. Enantiomer separations even at very poor resolutions (R_s=0.48) showed reasonably low systematic error. At this resolution, mean biases for nominal EFs 0.3, 0.4, 0.5, 0.6, 0.7 were 0.01, 0.004, −0.005, 0.007, and 0.003, respectively. The success of the DM in this case is significant, as no valley between the peaks was present at this resolution; thereby precluding

the use of the VDM. Application of the DM may allow enantiomer analysis of chiral compounds that are poorly resolved chromatographically, provided that some minimal peak resolution is obtained and peak asymmetry is not extreme. In addition, the DM (with the GEMG-4 function) produced acceptable fits of the chromatographic data, with an $r^2 > 0.997$ for all chromatograms, and randomly distributed residuals (Figure 3-4).

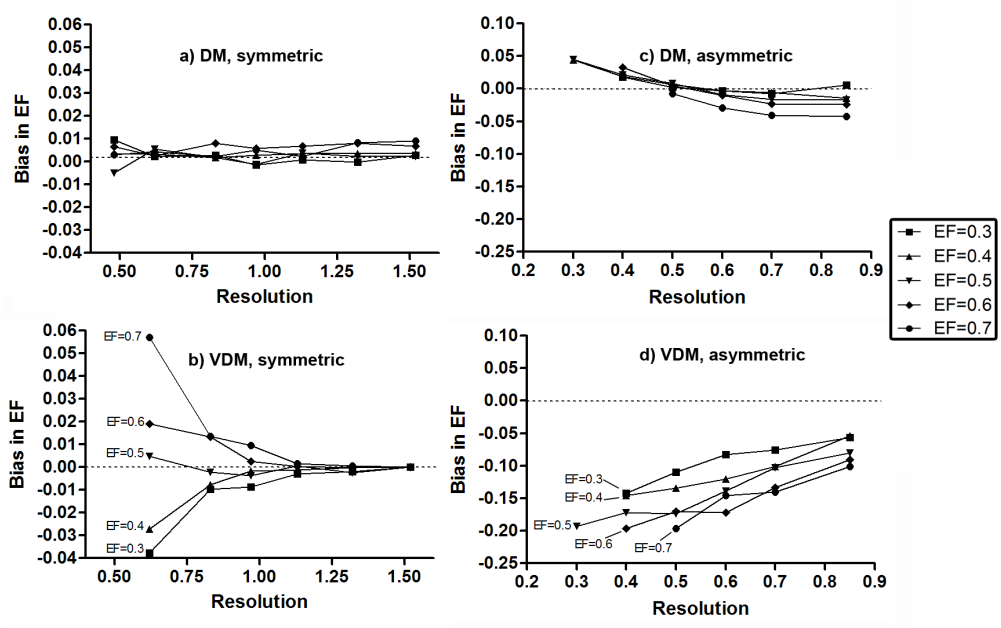

Figure 3-3: *Mean biases in EF as a function of resolution for symmetric (As=1) and asymmetric (As=2.7) peaks using DM and VDM methodologies for real chromatograms of PCB 132 atropisomer separations.*

In contrast, the biases produced by the VDM for symmetric peaks were significantly increased in magnitude as resolution decreased (Figure 3-3b). Racemic standards (EF=0.5) expectedly produced small average biases. However, EFs greater than 0.5 produced positively biased results to a maximum of +0.057, while EFs less than 0.5 produced negatively biased results to a

minimum of −0.038. The source of this bias is the movement of the valley towards the smaller peak. This overall effect is consistent with previous analyses of symmetric peak pairs [17], and results in a tendency for samples of nonracemic composition to be reported as more extreme values.

The modified mixing chamber was intended to approximate asymmetric conditions which are encountered under poor chromatographic conditions. This asymmetry produced an increase in biases with both integration methods. Integration with the DM yielded negatively biased results (−0.035 at the most extreme) which tended towards zero and a slightly positive value with decreasing resolution (Figure 3-3c). The DM could not produce meaningful EFs at the worst chromatographic conditions, failing at R_s 0.20 and 0.33, and at 0.43 for EF of 0.7, as the model treated the peak pair as a single peak. The GEMG fit of the highly asymmetric data was poor compared to that of symmetric peaks, with large nonrandom residuals (Figure 3-4b) similar to those previously reported [32]. The poor fits may be due to the fact that the asymmetry was generated by a mixing chamber that ideally produces an exponential dilution effect on peak shape. The GEMG function is ideally applied to chromatographic peaks that are asymmetric due to typically observed non-linear sorption and slow stationary phase-mobile phase mass transfer effects that are difficult to generate artificially. Indeed, other peak models, such as the empirically transformed Gaussian function [34], may provide better fits in this particular case. However, a comparison of chromatographic peak models is beyond the scope of this study.

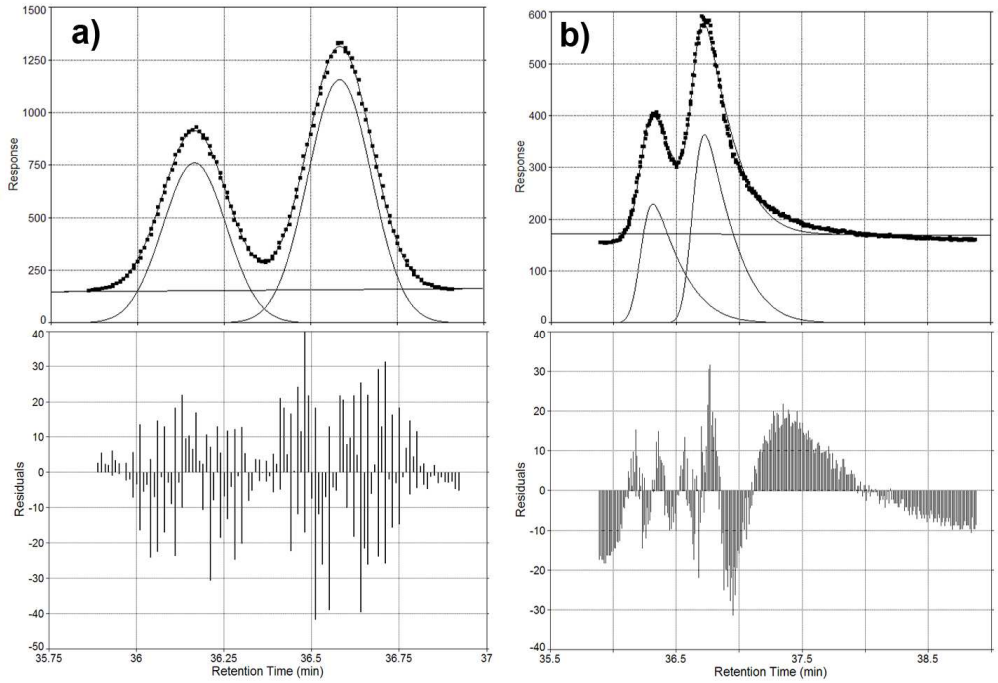

Figure 3-4: *Chromatograms showing fits and residuals of the GEMG function for symmetrical (a) and asymmetrical (b) chromatograms of PCB 132 atropisomer separations. Examples shown have a true EF of 0.4.*

While the DM performance with asymmetric peaks was acceptable, at least at the higher resolutions, the VDM performance was exceptionally poor. All VDM integrations resulted in severely negative biases, with averages ranging from 0.054 to 0.197 (Figure 3-3d). The magnitude of this bias increased with decreasing resolution. When using the VDM, this asymmetry can result in gross misinterpretations of enantiomer data. For example, racemic PCB 132, with an EF_{true} of 0.50, produced calculated EFs ranging from 0.42 to 0.30. These EFs would lead the analyst to conclude erroneously that a racemic EF is non-racemic.

3.3.2 Comparison of integration methods with simulated data

Biases when using the DM were relatively low, with averages ranging from −0.013 to +0.008 for peaks with an asymmetry of 1.5 and S/N of 20 for the largest peak (Figure 3-5). This range in bias is in good agreement with those obtained with the real symmetrical chromatograms. As with the real chromatographic data, no trend was observable in EF bias with either resolution or EF. In contrast, the VDM produced biases that were significantly higher, ranging from −0.058 to +0.052 (Figure 3-5a). Biases were positive for EFs below 0.5 and negative for EFs above 0.5, and increased in magnitude with decreasing resolution.

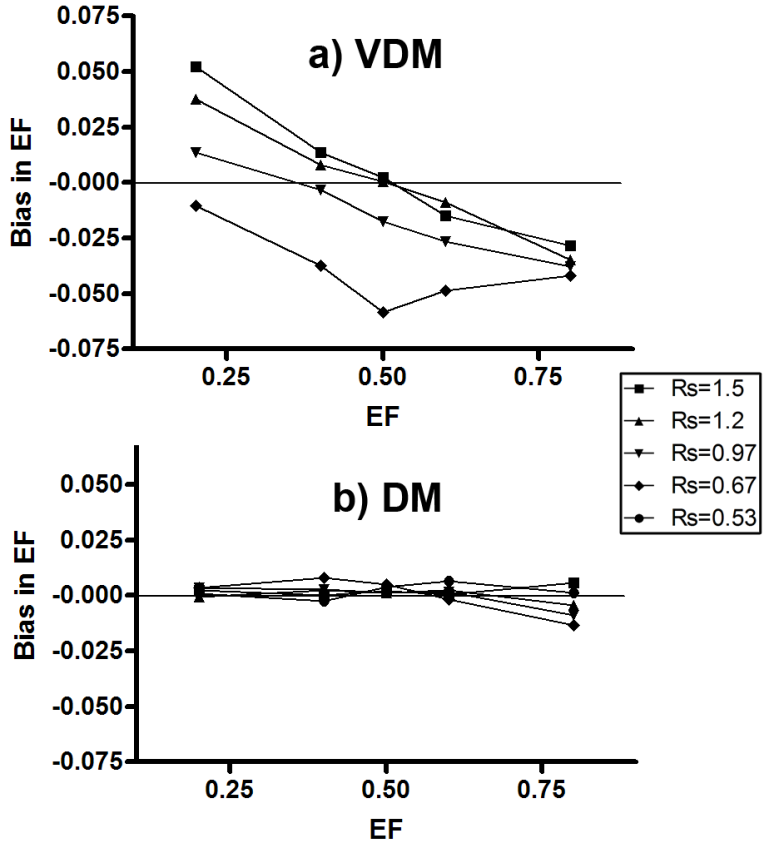

Figure 3-5: *Mean biases in EF as a function of EF for various peak resolutions using the VDM and the DM, based on simulated data. S/N=20 for largest peak, As=1.5.*

The S/N had no effect on average biases for either the VDM or DM. The S/N did, however, affect the precision of EF measurements with both the VDM and DM, as shown for 10 replicates at a R_s of 0.68 and A_s of 1.5 (Figure 3-6). As expected, precision worsened with decreasing S/N, an effect more pronounced for the DM (Figure 3-6). In the worst case tested, σ_N was greater than 0.07 for an EF of 0.4 and S/N of 10 (limit of quantification) when using the DM. This effect highlights the dangers inherent in attempting to model noisy data, and suggests that with a

skilled analyst, the VDM is capable of better precision at low resolution and S/N compared with the DM. It is hypothesized that should the data rate be increased above 1.57 Hz (i.e. by using a more modern fast-scanning quadrupole) that the performance of the DM would be improved due to the increased number of available data points to perform the fitting. It is unlikely that there would be as great an improvement in performance for the VDM. Additionally, the occasional poor precision of the DM can be improved if simplifications are made to the fitting model. By disabling the "vary widths" and "vary shape" options in the Peakfit software, the number of parameters in the GEMG function is reduced. Under those conditions, σ_{EF} (the standard deviation of the EF) improved dramatically for a set of symmetric peaks at R_s 0.7. The initial values for σ_{EF} improved from 0.008, 0.010, and 0.05 to 0.003, 0.004, and 0.02 for S/N of 20, 10, and 3 respectively. This technique for improving the DM fit can be applied to most enantiomer separations, particularly those performed by GC, where the peak widths and shapes for a pair of enantiomers are nearly identical. This may, however, introduce more error in EF determination for separations where differing peak shapes and widths are observed for enantiomers, as is the case for many enantiomer separations performed by gradient HPLC.

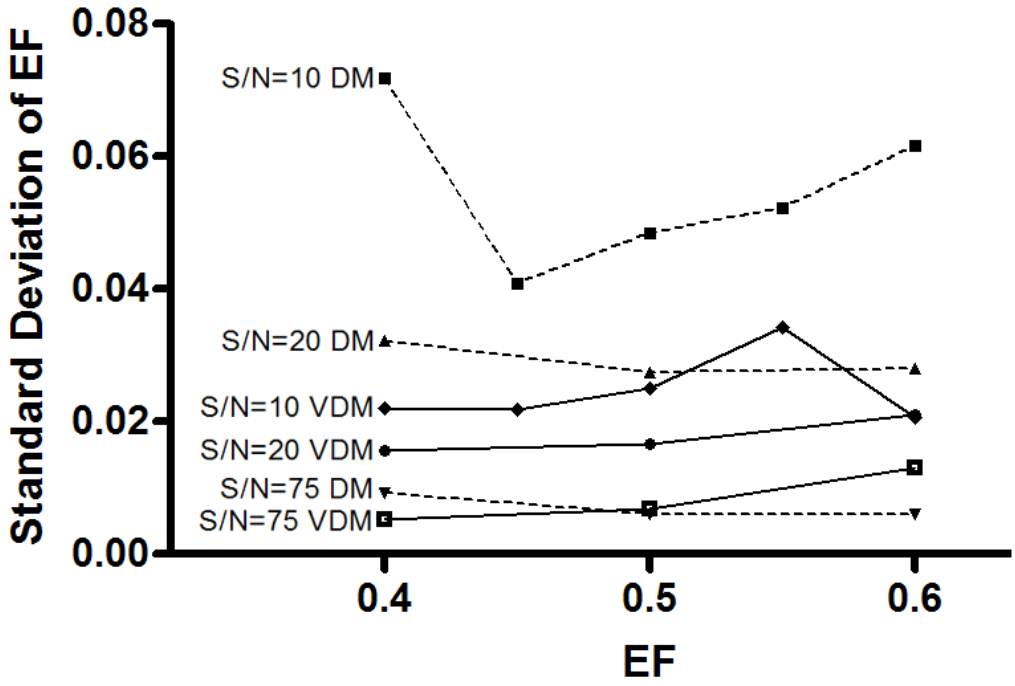

Figure 3-6: *Standard deviation of EF measurements (R_s = 0.68, A_s = 1.5) as a function of EF for the VDM and DM at three different signal-to-noise ratios. All precisions are based on ten replicate measurements.*

3.3.3 Applications of EF and the effects of bias

Biases in EF that are apparently "small" (±0.05) can be reflected and indeed magnified when they are used in environmental calculations. For example, the relative importance of two sources of a chiral chemical to a receptor can be estimated [4, 9]:

$$f_A = (EF_{MIX} - EF_B)/(EF_A - EF_B) \qquad \text{Equation 3-4}$$

where f_A is the fraction of total contaminant from source A; EF_A and EF_B are the enantiomeric fractions observed in sources A and B, respectively; and EF_{MIX} is the enantiomeric fraction of the affected compartment or site. By analyzing a previous study of enantiomer signatures in the atmosphere and water column of the Hudson River estuary [5], the effect of biased EFs can be demonstrated. In that study it was estimated that 86% of PCB 95 in phytoplankton originated from contaminated sediment and 14% was from atmospheric sources. A relatively small error in EF is assumed, as that study employed the DM for peak integration. For simplicity, zero bias is assumed for the atmospheric contribution, as it is close to racemic [5] and unlikely to be biased by the VDM assuming symmetric peaks. A negative bias is applied to the reported phytoplankton and sediment EFs sequentially in 0.01 intervals (Table 3-2). With a bias of −0.05 in the two nonracemic compartments, the proportion of PCB 95 attributable to the atmosphere dropped significantly, from 14% to 4%.

Table 3-2: *The effect of biases on the enantiomeric fractions of phytoplankton, air, and sediment and the resulting source apportionment fractions attributable to air and sediment in the Hudson River Estuary. Original data was produced using the DM integration technique [5].*

	original data	**bias −0.01**	**bias −0.02**	**bias −0.03**	**bias −0.04**	**bias −0.05**
phytoplankton EF	0.478	0.468	0.458	0.448	0.438	0.428
air EF	0.496	0.496	0.496	0.496	0.496	0.496
sediment EF	0.475	0.465	0.455	0.445	0.435	0.425
calculated fraction from air	**0.14**	**0.10**	**0.07**	**0.06**	**0.05**	**0.04**
calculated fraction from sediment	**0.86**	**0.90**	**0.93**	**0.94**	**0.95**	**0.96**

A more extreme example of the magnification of this bias is the calculation of minimum biotransformation rate constants from EFs. Based on initial racemic proportions and the assumption that biodegradation occurs for only one enantiomer, the rate constant for either enantiomer ($k_{b(+)}$ or $k_{b(-)}$) is [10]:

$$EF = \frac{1}{1 + e^{(k_{b(+)} - k_{b(-)})t}} \qquad \text{Equation 3-5}$$

where *EF* is the enantiomeric fraction of the compound in a sample, and *t* is the time. This calculation was recently applied to PCBs in dated sediment cores from the highly contaminated Superfund site in Lake Hartwell, SC [35]. Table 3-3 shows the effect of +0.01, −0.01, +0.05, and −0.05 biases on the calculated minimum biotransformation rates and half lives of PCBs 132 and 149 in two of

these sediment cores. PCB 132 had a half-life of approximately 81 years, based on the original data (which employed the DM for integration). Biases in EF of +0.01 and −0.01 yielded moderately erroneous calculated half lives of 95 and 71 years, respectively. However, a larger bias of +0.05 yielded a calculated half life of 296 years. Further bias to +0.06 resulted in a calculated half-life of 626 years.

Table 3-3: *Effect of bias on the EF and calculated minimum biotransformation rates and half-lives for PCB 132 and 149 in two dated sediment cores from Lake Hartwell, SC. Original data was produced using the DM integration technique [35].*

PCB 132, 1987 sediment depth, G47 core

	original data	**bias -0.01**	**bias +0.01**	**bias -0.05**	**bias +0.05**
EF	0.431	0.421	0.441	0.381	0.481
k	0.00855	0.00981	0.00730	0.0149	0.00234
half-life	81.1	70.7	95.0	46.4	296

PCB 149, 1987 sediment depth, G30 Core

	original data	**bias -0.01**	**bias +0.01**	**bias -0.05**	**bias +0.05**
EF	0.497	0.487	0.507	0.447	0.547
k	0.000571	0.00473	0.00255	0.0193	0.0171
half-life	1210.0	147	272	35.8	40.4

In contrast, PCB 149 exhibited little enantioselective degradation in the original data set, with a half-life of 1210 years. Biases +0.05 and −0.05 resulted in calculated half-lives of 40 and 36 years, respectively, incorrectly implying relatively fast biotransformation of PCB 149. Biases of this magnitude, however, would be unlikely in this situation, as close-to-racemic values have small biases except when the peaks are significantly asymmetrical. Nevertheless, the distorted results of these calculations underscore the need to employ highly accurate methods for EF determination. The VDM may be sufficient in cases where peak

resolution is adequate ($R_s \geq 1$) and peak shape is close to Gaussian. Enantiomer separations with lower resolution and/or significant asymmetry require a more robust integration technique, such as the DM, for accurate EF determination.

3.4. Conclusions

The effect of integration method on the determination of EF was investigated using simulated and instrument-generated data. The deconvolution method was shown to impart relatively small bias to the calculated EF, whereas the valley drop method suffered significant bias in EF determination, especially when applied to enantiomers which are poorly resolved and/or have high asymmetry. As a result of these biases, errors in environmental calculations that use EF can be severe, potentially leading to erroneous conclusions about the fate of chiral contaminants. While complete separation of enantiomers is always the preferred method to avoid quantitation biases, in cases where incomplete separation of enantiomers is unavoidable, a peak deconvolution method is recommended when determining EF. Furthermore, the simplification of peak deconvolution models (elimination of model parameters), when used appropriately, can allow EF determination that is both accurate and precise, even when signal-to-noise ratios suffer. In addition to ensuring that each enantiomer is free from chemical interference (i.e. no "hidden" compounds are present under the peaks of each enantiomer), we suggest that the choice of integration technique be included as part of a comprehensive QA/QC protocol for EF determination in future studies. Because the actual chromatographic parameters achieved are

rarely reported in studies of chiral contaminants, caution should be exercised when interpreting and comparing EFs, especially when applying them to environmental calculations.

3.5 References

1. Wong, C. S.; Mabury, S. A.; Whittle, D. M.; Backus, S. M.; Teixeira, C.; DeVault, D. S.; Bronte, C. R.; Muir, D. C. G., Organochlorine compounds in Lake Superior: Chiral polychlorinated biphenyls and biotransformation in the aquatic food web. *Environmental Science & Technology* **2004,** *38*, (1), 84-92.

2. Warner, N. A.; Norstrom, R. J.; Wong, C. S.; Fisk, A. T., Enantiomeric fractions of chiral polychlorinated biphenyls provide insights on biotransformation capacity of arctic biota. *Environmental Science & Technology* **2005,** *24*, (11), 2763-2767.

3. Ridal, J. J.; Bidleman, T. F.; Kerman, B. R.; Fox, M. E.; Strachan, W. M. J., Enantiomers of alpha-hexachlorocyclohexane as tracers of air-water gas exchange in Lake Ontario. *Environmental Science & Technology* **1997,** *31*, (7), 1940-1945.

4. Bidleman, T. F.; Falconer, R. L., Enantiomer ratios for apportioning two sources of chiral compounds. *Environmental Science & Technology* **1999,** *33*, (13), 2299-2301.

5. Asher, B. J.; Wong, C. S.; Rodenburg, L. A., Chiral source apportionment of polychlorinated biphenyls to the Hudson River estuary atmosphere and food web. *Environmental Science & Technology* **2007,** *41*, (17), 6163-6169.

6. Hühnerfuss, H.; Pfaffenberger, B.; Gehrcke, B.; Karbe, L.; Konig, W. A.; Landgraff, O., Stereochemical effects of PCBs in the marine-environment - seasonal variation of coplanar and atropisomeric PCBs in blue mussels (*Mytilus edulis L.*) of the German Bight. *Marine Pollution Bulletin* **1995,** *30*, (5), 332-340.

7. Jin, Y. X.; Wang, W. Y.; Xu, C.; Fu, Z. W.; Liu, W. P., Induction of hepatic estrogen-responsive gene transcription by permethrin enantiomers in male adult zebrafish. *Aquatic Toxicology* **2008,** *88*, (2), 146-152.

8. Wilson, W. A.; Konwick, B. J.; Garrison, A. W.; Avants, J. K.; Black, M. C., Enantioselective chronic toxicity of fipronil to Ceriodaphnia dubia. *Archives of Environmental Contamination and Toxicology* **2008,** *54*, (1), 36-43.

9. Harner, T.; Wiberg, K.; Norstrom, R. J., Enantiomer fractions are preferred to enantiomer raios for describing chiral signatures in environmental analysis. *Environmental Science & Technology* **2000,** *34*, 218-220.

10. Wong, C. S.; Lau, F.; Clark, M.; Mabury, S. A.; Muir, D. C. G., Rainbow trout (*Oncorhynchus mykiss*) can eliminate chiral organochlorine compounds onantioselectively. *Environmental Science & Technology* **2002,** *36*, 1257-1262.

11. Wong, C. S.; Garrison, A. W., Enantiomer separation of polychlorinated biphenyl atropisomers and polychlorinated biphenyl retention behavior on modified cyclodextrin capillary gas chromatography columns. *Journal of Chromatography A.* **2000,** *866*, (2), 213-220.

12. Janak, K.; Covaci, A.; Voorspoels, S.; Becher, G., Hexabromocyclododecane in marine species from the Western Scheldt Estuary:

Diastereoisomer- and enantiomer-specific accumulation. *Environmental Science & Technology* **2005,** *39*, (7), 1987-1994.

13. Westerberg, A. W., Detection and resolution of overlapped peaks for an on-line computer system for gas chromatographs. *Analytical Chemistry* **1969,** *41*, (13), 1770-1777.

14. Meyer, V. R., Accuracy in the chromatographic determination of extreme enantiomeric ratios: A critical reflection. *Chirality* **1995,** *7*, (8), 567-571.

15. Fornstedt, T.; Zhong, G. M.; Guiochon, G., Peak tailing and mass transfer kinetics in linear chromatography. *Journal of Chromatography A* **1996,** *741*, (1), 1-12.

16. Fornstedt, T.; Zhong, G. M.; Guiochon, G., Peak tailing and slow mass transfer kinetics in nonlinear chromatography. *Journal of Chromatography A* **1996,** *742*, (1-2), 55-68.

17. Meyer, V. R., Errors in the area determination of incompletely resolved chromatographic peaks. *J. Chrom. Sci.* **1995,** *33*, (1), 26-33.

18. Bicking, M. K. L., Integration errors in chromatographic analysis, part I: Peaks of approximately equal size. *LC GC N. Am.* **2006,** *24*, (4), 402-414.

19. Mydlova, J.; Krupcik, J.; Korytar, P.; Sandra, P., On the use of computer assisted resolution of non-separable peaks in a congener specific polybrominated diphenyl ether capillary gas chromatographic analysis. *Journal of Chromatography A* **2007,** *1147*, (1), 95-104.

20. Krupcik, J.; Mydlova, J.; Spanik, I.; Tienpont, B.; Sandra, P., Computerized separation of chromatographically unresolved peaks. *Journal of Chromatography A* **2005,** *1084*, (1-2), 80-89.

21. Krupcik, J.; Oswald, P.; Spanik, I.; Majek, P.; Bajdichova, M.; Sandra, P.; Armstrong, D. W., On the use of a peak deconvolution procedure for the determination of energy barrier to enantiomerization in dynamic chromatography. *Analusis* **2000,** *28*, (9), 859-863.

22. Shackman, J. G.; Watson, C. J.; Kennedy, R. T., High-throughput automated post-processing of separation data. *Journal of Chromatography A* **2004,** *1040*, (2), 273-282.

23. Kong, H. W.; Ye, F.; Lu, X.; Guo, L.; Tian, J.; Xu, G. W., Deconvolution of overlapped peaks based on the exponentially modified Gaussian model in comprehensive two-dimensional gas chromatography. *Journal of Chromatography A* **2005,** *1086*, (1-2), 160-164.

24. Ulrich, E. M.; Hites, R. A., Enantiomeric ratios of chlordane-related compounds in air near the Great Lakes. *Environmental Science & Technology* **1998,** *32*, (13), 1870-1874.

25. Ross, M. S.; Verreault, J.; Letcher, R. J.; Gabrielsen, G. W.; Wong, C. S., Chiral Organochlorine Contaminants in Blood and Eggs of Glaucous Gulls (Larus hyperboreus) from the Norwegian Arctic. *Environmental Science & Technology* **2008**.

26. Haglund, P.; Wiberg, K., Determination of the gas chromatographic elution sequences of the (+)- and (-)-enantiomers of stable atropisomeric PCBs on Chirasil-Dex. *HRC-J. High Res. Chrom.* **1996,** *19*, (7), 373-376.

27. Haglund, P., Isolation and characterisation of polychlorinated biphenyl (PCB) atropisomers. *Chemosphere* **1996,** *32*, (11), 2133-2140.

28. Khummueng, W.; Harynuk, J.; Marriott, P. J., Modulation ratio in comprehensive two-dimensional gas chromatography. *Analytical Chemistry* **2006,** *78*, (13), 4578-4587.

29. Harynuk, J. J.; Kwong, A. H.; Marriott, P. J., Modulation-induced error in comprehensive two-dimensional gas chromatographic separations. *Journal of Chromatography A* **2008,** *1200*, (1), 17-27.

30. SPSS, *Peakfit - Peak Separation and Analysis Software User's Manual*. AISN Software: Chicago, IL, 1997.

31. Nikitas, P.; Pappa-Louisi, A.; Papageorgiou, A., On the equations describing chromatographic peaks and the problem of the deconvolution of overlapped peaks. *Journal of Chromatography A* **2001,** *912*, (1), 13-29.

32. Li, J., Comparison of the capability of peak functions in describing real chromatographic peaks. *Journal of Chromatography A* **2002,** *952*, (1-2), 63-70.

33. Wong, C. S.; Garrison, A. W.; Foreman, W. T., Enantiomeric composition of chiral polychlorinated biphenyl atropisomers in aquatic bed sediment. *Environmental Science & Technology* **2001,** *35*, (1), 33-39.

34. Li, J. W., Development and evaluation of flexible empirical peak functions for processing chromatographic peaks. *Analytical Chemistry* **1997,** *69*, (21), 4452-4462.

35. Wong, C. S.; Pakdeesusuk, U.; Morrissey, J. A.; Lee, C. M.; Coates, J. T.; Garrison, A. W.; Mabury, S. A.; Marvin, C. H.; Muir, D. C. G., Enantiomeric composition of chiral polychlorinated biphenyl atropisomers in dated sediment cores. *Environmental Toxicology and Chemistry* **2007,** *26*, (2), 254-263.

Chapter 4: Characterization of Recent and Historical Emissions of Chiral and Achiral Polychlorinated Biphenyls from a Hazardous Waste Treatment Facility

A version of this chapter has been submitted to Environmental Toxicology and Chemistry as Asher, B. J.; Ross, M.S.; and Wong, C. S.; Tracking chiral polychlorinated biphenyls sources near a hazardous waste incinerator: Fresh emissions or weathered revolatilization? *Submitted September 5th, 2011*.

4.1 Introduction

Canada, as a signatory country to the Stockholm Convention on Persistent Organic Pollutants, has committed to destroying all of its remaining stockpiles of polychlorinated biphenyls (PCBs) by the end of 2028 [1]. This included recent requirements for the removal of all in-use equipment containing high concentrations of PCBs (>500 mg/kg) by the end of 2009 [2]. As of 2005, Canada's national inventory of PCBs reported 112×10^6 and 8.09×10^6 kg of stored and in-use PCB wastes, respectively [3]. The majority of Canada's high concentration PCB wastes are treated at the Swan Hills Treatment Centre (SHTC; formerly the Alberta Special Waste Treatment Centre), a permanent incinerator facility designed to destroy up to 40,000 tonnes of hazardous waste per year [4]. The treatment plant is located near the town of Swan Hills in central Alberta, Canada, 180 km northwest of Edmonton, and is the only point source of PCBs to the region [5]. The SHTC processes PCB wastes via rotary kiln incineration, and regularly reports destruction and removal efficiencies (DRE) greater than the minimum legal requirement of 99.9999% [4].

Despite the high DRE, significant PCB contamination has been shown in the region immediately surrounding the treatment plant [5, 6]. This may, at least in part, be due to a single fugitive emission episode that occurred in 1996 where kilogram quantities of PCBs and polychlorinated dibenzodioxins and furans (PCDD/Fs) were released into the atmosphere after a transformer furnace malfunction [7]. As a result of this fugitive release, a fish and wild game

consumption advisory (30 km radius around the SHTC) has been in effect, as well as a long term human exposure assessment program [8]. A handful of studies have investigated PCB contamination in the region, however only one of those has been published in peer-reviewed journals. Blais et al. investigated PCBs in snow, vegetation, and sediment, around the SHTC, and suggested long term fugitive emissions were the major source of PCBs to the region, rather than the accidental release [5]. However, the relative importance of the plant's historic and recent contamination to the region's PCB load is not fully understood. Nor is it clear if fugitive emissions continue to play a role in contributing to PCB contamination in the local surroundings in the decade since the Blais et al. study.

The distinction between historical and recent releases may be effectively made by studying the enantiomer distribution of a chiral contaminant [9]. Freshly released PCB contaminants are expected to generate a racemic signal, i.e., equal concentrations of both enantiomers. In contrast, biological weathering (e.g. microbial reductive dechlorination) has been shown to alter the enantiomer distribution of a contaminant in an environmental medium such as soil or sediment, leading to a significantly nonracemic composition [10, 11]. Since abiotic processes such as volatilization and deposition affect enantiomers equally, comparison of a chiral compound's distribution in air to its distribution in weathered sources such as soil or sediment can provide evidence of the air-bound pollutant's source. For example, racemic distributions of chiral PCBs in air have been used to reveal fresh racemic sources as the major contributor to atmospheric PCB loadings at urban and rural sites in the U.K. [12] as well as the historically

contaminated Hudson River estuary [13]. Atmospheric sources of organochlorine pesticides such as chlordane [14] and hexachlorocyclohexane [15] have also been quantified using enantiomer distributions.

The objective of this study was to use soil and passive air sampling in the area immediately surrounding the SHTC to determine recent trends in PCB contamination of the region. Passive samplers were chosen as they offer significant advantages over traditional high-volume active samplers for source elucidation. Numerous samplers can be deployed simultaneously to reveal spatial trends, and passive samplers can integrate atmospheric contamination over longer periods relative to active samplers (weeks versus hours), permitting a robust and versatile sampling strategy [16]. Here, individual atropisomers (hereafter, simply referred to as "enantiomers") of chiral PCB congeners were quantified in PUF discs as well as soil to determine whether recent or historic emissions dominate the region's atmospheric PCB load. Sampling was performed over several seasons from 2005 to 2008 to assess temporal trends. In addition, enantiomer distributions in soil were used to reveal evidence of biodegradation of PCBs over the course of the plant's operation in the region, as well as to estimate degradation rates [17]. To our knowledge, this study is the first to use enantiomer analysis to examine emissions from a known single point source in an otherwise remote and thus relatively uncontaminated region.

4.2 Materials and Methods

4.2.1 Sampling

Air and soil were sampled at a total of 25 sites located various distances (0.53 to 12 km) from the SHTC (Figure 4-1) over four sampling seasons. For each site, geographical coordinates (latitude/longitude), distances from the SHTC, sampling seasons, and the compartment sampled (air and/or soil) are presented in Table 4-1. Polyurethane foam (PUF) passive air samplers [16] were deployed in each sampling season. Samplers consisted of a polyurethane (PUF) disc (14.0 cm diameter; 1.27 cm thick; surface area 364 cm^2; mass 4.60 g; volume 196 cm^3; density 0.0235 g cm^{-3}; Pacwill Environmental, Beamsville, ON) housed in a stainless steel domed chamber, similar to those described elsewhere [18]. Air samplers were hung in trees at approximately 2.5 meters from the ground. Sampler PUF discs were precleaned by Soxhlet extraction in pesticide grade acetone (24 h) followed by petroleum ether (2 × 24 h), dried in a vacuum desiccator, and stored in precombusted glass jars with Teflon-lined lids until deployment. The first deployment was for a 5 month period (August 2005 to January 2006) to assess semi-quantitatively the spatial distribution of PCBs around the plant. This sampling period cannot be used to estimate actual air concentrations, since sampler deployments of this length resulted in uptake profiles for mid-sized congeners that approached equilibrium, rather than the linear uptake that is desirable for accurate sampling rate determination [16]. Three additional 8-week deployments were performed with estimated uptake rates taken to be 3.8 m^3/day, as determined previously [19]. A certain amount of

uncertainty is expected to be associated with these uptake rates [20], therefore calculated air concentrations are expected to be an approximation. Enantiomer distributions, however, are unaffected by these estimated uptake rates. A soil corer (AMS Inc., American Falls, ID) was used to sample surface soil with a depth of 0-5 cm, after the removal of the litter layer. At each site, soil was sampled within 10 meters of the PUF deployment.

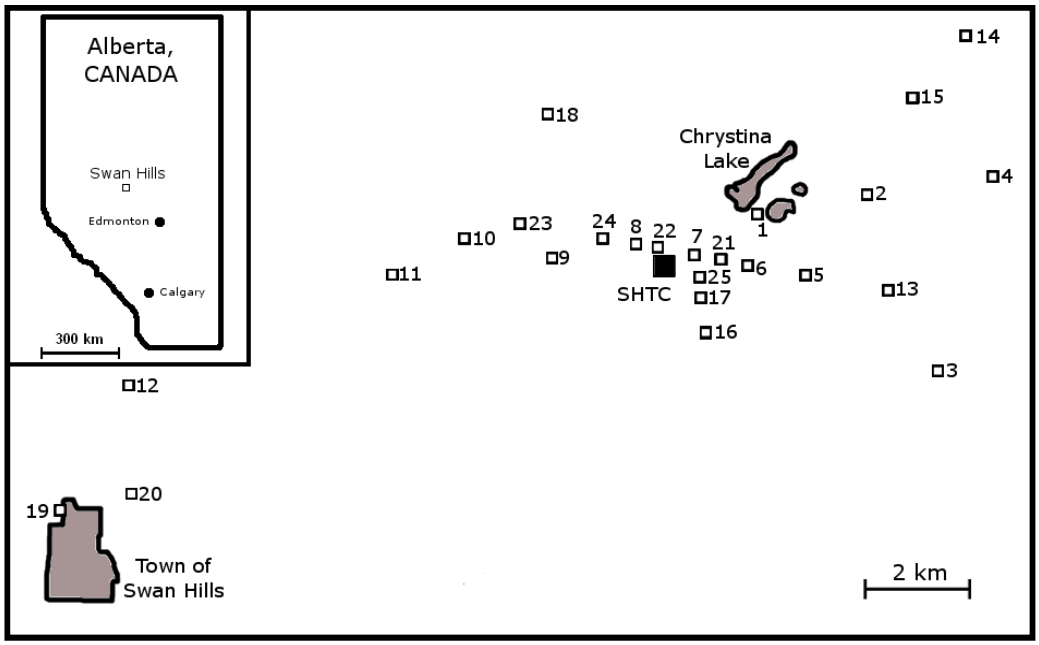

Figure 4-1: *Map of sampling locations around the Swan Hills Treatment Centre (SHTC). Inset: Location of Swan Hills within the province of Alberta, Canada.*

Table 4-1: *Coordinates of sampling sites and seasons for PUF passive air and soil samples. Numbers indicating sampling seasons for PUFs are as follows: 1) August 2005 to February 2006, 2) June to July 2006, 3) May to July 2007, 4) December 2007 to February 2008. Numbers indicating sampling for soil are as follows: 1) August 2005, 2) May 2007, 3) August 2008.*

	Latitude	Longitude	Distance from SHTC (m)	PUF sampling	Soil sampling
1	54.78103	-115.19240	**1905**	1,2,3,4	1,2
2	54.78457	-115.15838	**4106**	1	1
3	54.75268	-115.13621	5906	1	1
4	54.78791	-115.11957	**6618**	1,2	1
5	54.77025	-115.17724	**2781**	1,2,3	1
6	54.77190	-115.19539	**1600**	1,2,3,4	1,2
7	54.77374	-115.21171	**530**	1,2,3,4	1,2,3
8	54.77569	-115.22994	**663**	1,2,3,4	1,2
9	54.77318	-115.25558	2306	1,2	1
10	54.77685	-115.28303	**4075**	1	1
11	54.77016	-115.30527	**5520**	1,2,3	1,2
12	54.75029	-115.38682	11082	1,2	1
13	54.76733	-115.15202	**4436**	1	1
14	54.81338	-115.12788	**7323**	1	1
15	54.80215	-115.14442	5739	1	1
16	54.75947	-115.20833	**1836**	1,2	1
17	54.76608	-115.20968	**1147**	1,2,3,4	1,2
18	54.79933	-115.25723	**3659**	1	1
19	54.72743	-115.40756	**13175**	1,2,3,4	1,2
20	54.73036	-115.38583	11764	2	1
21	54.77285	-115.20371	1054	2	1
22	54.77493	-115.22167	**126**	2,3,4	2,3
23	54.77939	-115.26584	**3009**	2,3,4	2
24	54.77687	-115.24030	1343	2,3,4	2
25	54.76987	-115.21023	**809**	2,3,4	2
SHTC	54.77457	-115.21982	-	-	-

4.2.2 Extraction

Sample and field blank PUF discs were Soxhlet extracted in petroleum ether (16 h), solvent exchanged into hexane, and rotary-evaporated to 1 mL.

Samples were subsequently fractionated by column chromatography using 3% by weight deactivated silica gel (70-230 mesh, Sigma-Aldrich, St. Louis, MO) and 8.5% by weight deactivated aluminum oxide (80-200 mesh, Fisher Scientific, Fairlawn, NJ), with the PCB fraction being eluted with 30 mL hexane. Finally, extracts were concentrated via nitrogen evaporation to approximately 250 μL and spiked with PCB 159 as an internal standard. Soil samples were homogenized with anhydrous sodium sulfate (Fisher Scientific, Fairlawn, NJ) and Soxhlet extracted as above with dichloromethane. Activated copper (99.90% ACS reagent grade, Sigma-Aldrich, St. Louis, MO) was added to soil extracts for sulfur removal.

4.2.3 PCB congener and enantiomer analysis

Total PCBs as well as hexachlorobenzene (HCB) concentrations were quantified with either a Hewlett Packard 5890, or Agilent (Santa Clara, CA) 6890 gas chromatograph, each equipped with a ^{63}Ni electron capture detector. Chromatographic separation was achieved using a DB-XLB column (5% diphenyl dimethyl polysiloxane, 30 m × 0.25 mm i.d. × 0.5 μm d_f, J&W Scientific) with injector and oven conditions as presented elsewhere [21]. For PCB congener analysis, a total of 82 chromatographic peaks were quantified, representing 95 congeners. Enantiomers of PCBs 91, 95, 136, and 149 were quantified using a Thermo Scientific (Waltham, MA) DSQ II single quadrupole GC/MS operated in electron impact mode. These chiral congeners were chosen for analysis as they were present in sufficient concentrations in samples for enantiomer quantitation.

A Chirasil-Dex column (30 m × 0.25 mm i.d. × 0.25 µm d_f, Varian, Walnut Creek, CA) was used for the separation of PCBs 91, 136, and 149. The presence of a non-PCB isobaric interference in soil samples prevented reliable quantification of PCB 95 on the Chirasil-Dex column, so a Cyclosil-B column (30 m × 0.25 mm i.d. × 0.5 µm d_f, Agilent) was used for enantiomer analysis of this congener. For both columns, GC oven and injector temperature conditions were applied as described in Chapter 2 and elsewhere [22]. Pentachlorinated (PCBs 91 and 95) and hexachlorinated congeners (PCBs 136 and 149) were quantified by summing the total of three monitored chlorine isotopes (*m/z* values) 324, 326, 328 and 358, 360, 362, respectively. To quantify enantiomer distributions, the enantiomer fraction (EF) was used [23]. The EF is defined as the (+)-enantiomer concentration divided by the sum concentration of both enantiomers for PCBs 136 and 149, for which the elution orders are known, and the first-eluted enantiomer (E1) concentration divided by the sum concentration of both enantiomers (E1 + E2) for PCBs 91 and 95, where the elution orders are unknown. Detection limits on the DSQ II were 3.0, 2.5, 2.9, and 2.7 pg (on column) for PCBs 91, 95, 136, and 149, respectively.

4.2.4 QA/QC

PCBs 30 and 204 were added to each sample prior to extraction to assess extraction recoveries. Average percent recoveries (±SD) for PCB 30 and 204 were PUF, 84±18% and 109±31%, respectively; and soil, 78±32% and 87±34%, respectively, excluding the August 2005 PUF deployment. Field and laboratory blanks for air and soil samples consisted of precleaned PUF discs and

precombusted sodium sulfate, respectively. Samples and field blanks were transported to and from sampling sites in glass jars with Teflon lined lids, and kept at −20°C until extraction. Analyte concentrations in both field and laboratory blanks were low (e.g. field blanks were 0.06±0.04 ng/g total PCBs; 5% of mean sample concentrations for samples > 2km from SHTC and 0.09% of the mean concentration for all samples, based on a typical 50 g samples size for soil), therefore no blank corrections were made.

To ensure reliability in enantiomer analysis, additional quality assurance measures were employed, similar to those presented elsewhere [13] and are briefly described here. Nine standard mixtures containing all 209 PCB congeners were analysed on each enantioselective column to ensure that no interferences (i.e. coelution of another homologous Aroclor congener) with the four target chiral congeners were present. EF data was rejected if the signal-to-noise ratio of at least one of the compound's two peaks was less than 10, or if the chlorine isotope ratios were not within ±10% of standards. To avoid bias in the quantitation of partially resolved enantiomers, deconvolution of overlapping peaks was performed using Peakfit v4.06 software (Systat Software, San Jose, CA) using previously published fitting procedures [24].

4.2.5 Statistics

All EFs are numerically presented as mean ± standard deviation. Statistical differences between sample groups were determined using a one-way analysis of variance (ANOVA) and the Tukey Honestly-Significant-Difference post hoc test.

Sample groups were considered nonracemic when they were found to be significantly different from racemic standards, PCB 95 (0.496±0.003), PCB 91 (0.498±0.004), PCB 136 (0.499±0.004), and PCB 149 (0.504±0.004). A minimum confidence level of 95% was used for all statistical tests.

4.3 Results and Discussion

4.3.1 PCB spatial distributions and congener patterns

Concentrations of PCBs in air were highest at sampling locations closest to the SHTC, and rapidly decreased as proximity to the treatment centre decreased (Figures 4-2 and 4-3). This spatial distribution of PCB concentrations is consistent with the typical profile of a point source, and is similar to previously measured spatial distributions of PCBs in vegetation at this site [5] as well as other point sources of PCBs [25, 26]. While estimated air concentrations decreased with increasing distance from the treatment centre, ΣPCBs (95 congeners, Figure 4-2) were elevated at Site 19, within the Town of Swan Hills, with an estimated concentration of 110±30 pg/m^3, potentially influenced by PCB sources within the town. A similar spatial distribution was observed during the initial sampling season, based on PCB 95 (Figure 4-3). Estimated ΣPCB air concentrations for samples closest to the SHTC (less than 1 km) averaged 430 pg/m^3, similar to ambient gas-phase concentrations of PCBs measured near major populated centres, such as Jersey City [27] and Chicago [28]. Total PCB concentrations in air at sampling sites >5 km from the SHTC averaged 58±49 pg/m^3, similar to mean background concentrations in air compiled for multiple sites in North America (mean: 79 pg/m^3) [29].

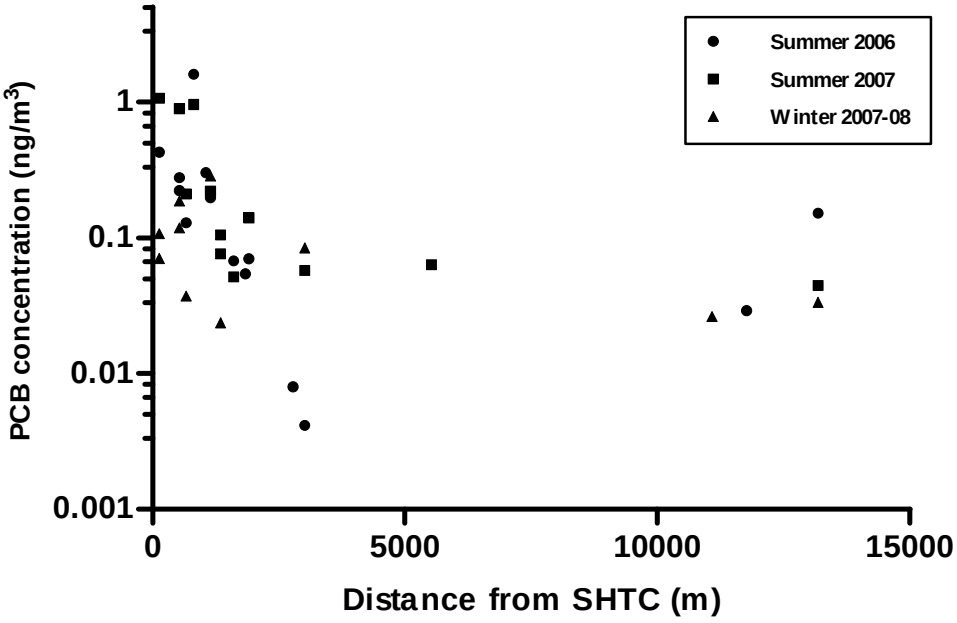

Figure 4-2: *Estimated ΣPCB concentration in air over three sampling seasons as a function of the distance from the Swan Hills Treatment Centre (logarithmic scale on the y-axis).*

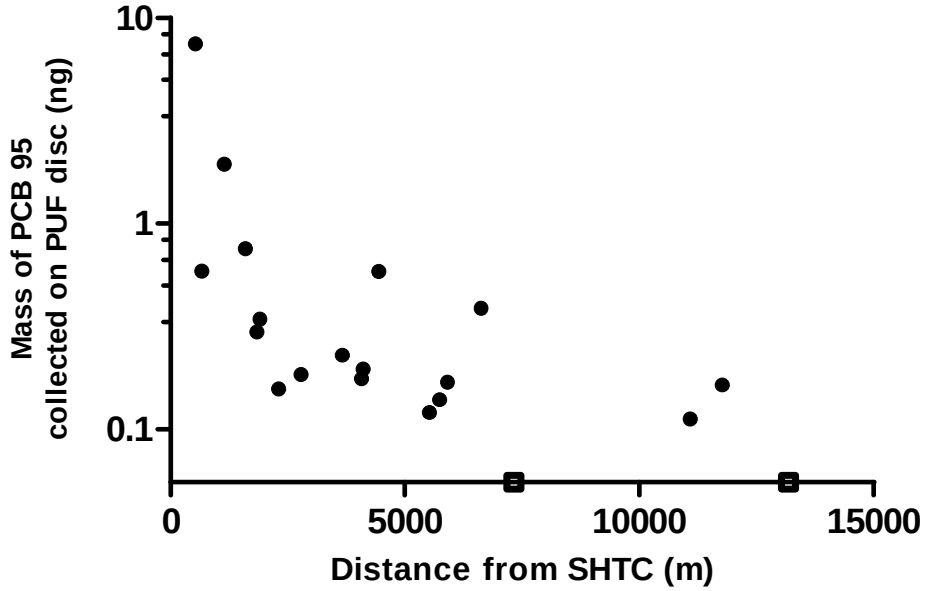

Figure 4-3: *Mass of PCB 95 collected on PUF discs during the fall/winter of 2005 as a function of distance from the Swan Hills Treatment Centre (logarithmic scale on the y-axis). PCB 95 masses are based on enantiomer analysis by GC-MS, as described. Unfilled squares indicate data points that were measured below the limit of detection.*

Similar to air, ΣPCB concentrations in soil were highest at sites closest to the SHTC, 10.8±11.6 ng/g dry weight for sites < 1 km from the treatment plant. Concentrations dropped off exponentially with increasing distance from the plant (Figure 4-4) and reached background levels at sites > 5 km away, with a mean concentration of 0.18±0.14 ng/g d.w, on the lower end of previously determined background soil concentrations in North America (mean 4.3 ng/g d.w.) [29].

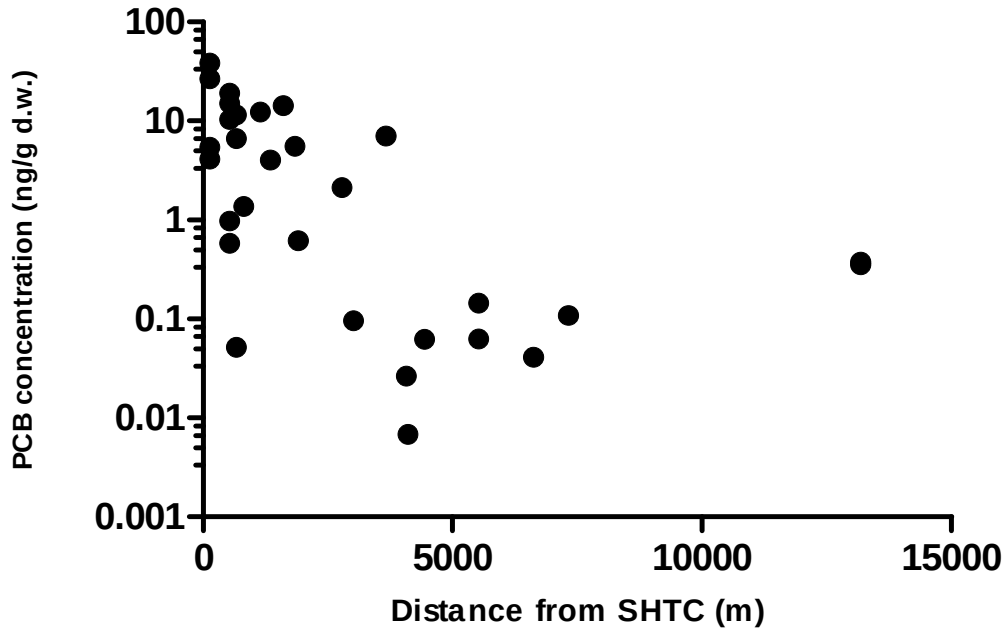

Figure 4-4: *ΣPCB concentration in soil as a function of distance from the Swan Hills Treatment Centre (logarithmic scale on the y-axis).*

Air at sampling sites close to the treatment plant (< 2 km) was dominated by penta- and hexachlorinated congeners. These homologue patterns, as exemplified in Figures 4-5 and 4-6, were generally more variable from site to site than those for soil (e.g. fraction of total PCBs; hexa: 0.27±0.12; penta: 0.26±0.09; tetra: 0.16±0.05 for sites within 2 km from the treatment plant). Congener patterns in soil (Figure 4-6) were dominated by hexachlorinated biphenyls, followed by penta- and hepta-chlorinated congeners in relative abundance. Homologue patterns in soil varied only slightly among sampling locations, as the variance in relative abundance among sites close to the treatment plant (< 2 km) was small (e.g. fraction of total PCBs; hexa: 0.52±0.06; penta: 0.20±0.06; hepta: 0.18±0.04). The greater variability in homologue patterns in air versus soil may

be explained by the fact that the PCB soil load in the region likely reflects a long-term accumulation, effectively averaging wind directions and the variable congener profiles from the multiple Aroclors processed at the SHTC over a period of years, rather than weeks for PUF samples. The congener pattern in soil at site 19, the furthest from the SHTC, had a greater predominance of tri-, tetra-, and heptachlorinated congeners than at other sites, likely reflecting background sources, or possibly localized sources within the town of Swan Hills, rather than emissions from the SHTC. While air and soil had not been studied at this site previously, Blais et al. found hexa- and heptachlorinated congeners to be dominant in vegetation and snow at sites within 3 km and to the east of the treatment plant. They similarly showed a significantly different pattern at sites far from the SHTC compared with those close to the plant, indicating a distinct PCB source [5], likely background contributions via long range atmospheric transport.

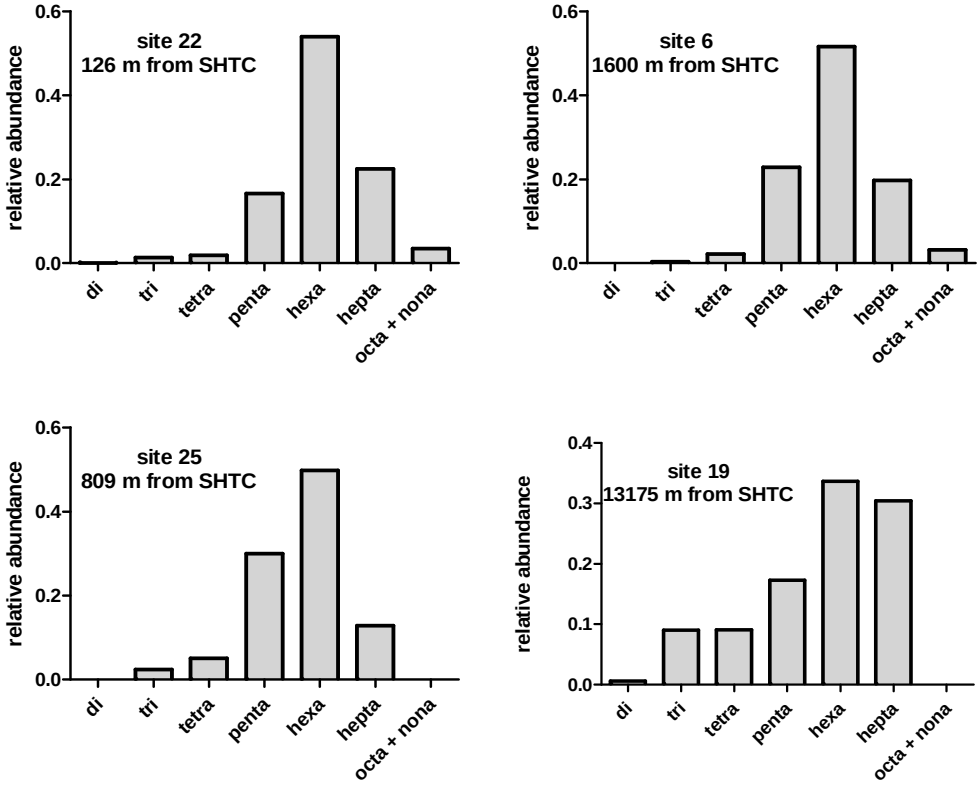

Figure 4-5: *PCB homologue patterns in soil samples for four sites near the Swan Hills Treatment Centre, sampled in May, 2007.*

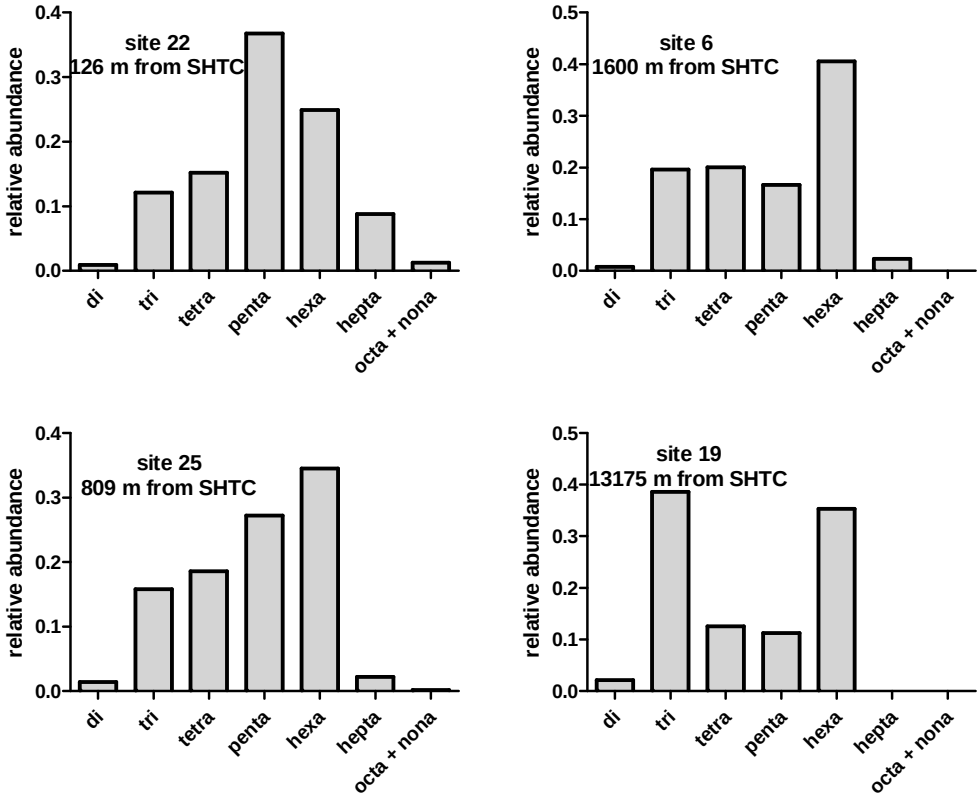

Figure 4-6: *PCB homologue patterns in air samples for four sites near the Swan Hills Treatment Centre, sampled during the summer of 2007.*

4.3.2 Chiral PCBs in soil

Of the four target chiral congeners, only PCB 95 was significantly nonracemic in soil (Figure 4-7) with significant depletion of the E2 enantiomer (EF = 0.434±0.034). The magnitude and direction of the enantiomer depletion observed here are similar to those in previous studies of this congener in soil in the U.K. [12, 30], Czech Republic [31], and Toronto, Canada [32]. Nonracemic

distributions of PCBs have been shown to be indicative of significant biodegradation taking place in the local soil, likely via aerobic microbial activity [33]. EFs of PCB 95 in soil showed significant variation, with a range of 0.363 to 0.489 (near-racemic). This suggests a high degree of local variability in the soil microbial consortia's ability to process persistent organic pollutants enantioselectively. Greater variability has been observed previously for other organochlorine contaminants in soil, even among samples taken a few meters apart [34]. Such variability has been explained by differences in a soil's ability to sustain viable and active microbial communities [35], as trends in EF with soil components such as humic acid and ash have been shown to be closely related [36]. EFs of all target congeners in soil did not correlate with the distance from the treatment plant ($p=0.53$). This is consistent with a lack of correlation of EF with total PCB concentrations (also $p=0.45$), and is indicative of the importance of local soil conditions on microbial populations and their resulting ability to biotransform these compounds.

In contrast to PCB 95, PCB 149 showed only slight (although nonsignificant) enrichment of the (+)-enantiomer (EF = 0.516±0.023), while PCBs 91 and 136 were essentially racemic, with EFs of 0.498±0.014 and 0.497±0.018, respectively. Statistically, all three congeners were not significantly different from racemic standards ($p>0.05$). The comparatively weaker ability of PCBs 149 and 136 to undergo enantioselective degradation as compared with PCB 95 observed in this study is consistent with measurements of these congeners in soil in previous studies [12, 32]. This observation is also consistent with the

fact that resistance to aerobic microbial degradation has been shown to be greater in congeners with a greater degree of chlorination [37]. The racemic distributions observed for PCB 91 in soil diverges from this trend, and illustrates that enantioselective transformation is compound specific, with similar regioselectivity observed previously [38].

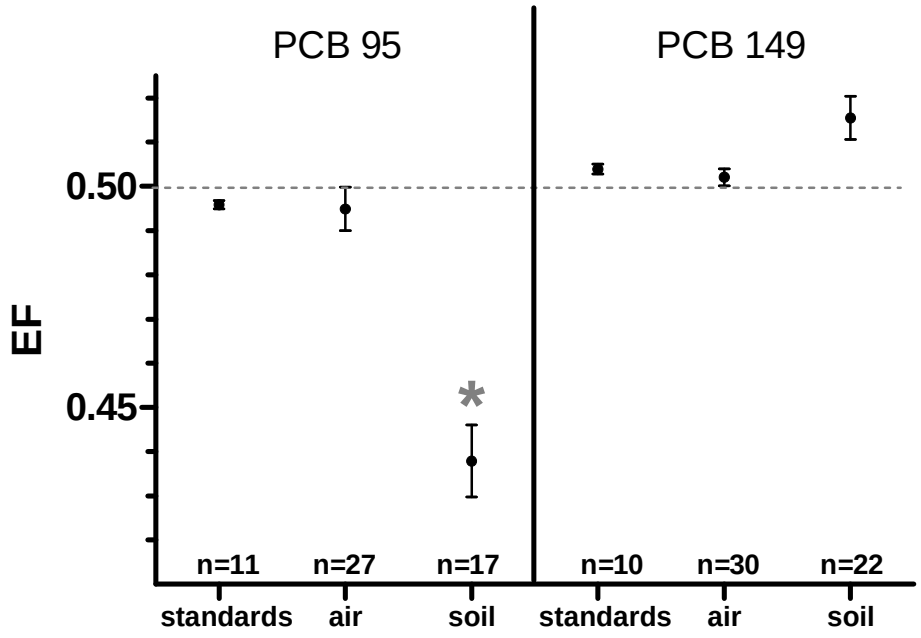

Figure 4-7: *Plot of mean±standard error EF of Swan Hills air, soil and racemic standards for PCB 95 and 149. The dashed line indicates a theoretical racemic composition of EF = 0.5. The asterisk indicates a statistical difference was found at >95% confidence.*

4.3.3 Chiral PCBs in air and source elucidation

While the ΣPCB concentrations vs. distance profile and the distribution of PCBs homologues in PUF samples around the treatment plant clearly indicates that the SHTC is the prevailing source of PCBs to the local atmosphere, this spatial information alone cannot imply that the contamination was recently

emitted. Indeed, the fugitive emission incident from 1996, in the absence of subsequent releases, could generate a similar spatial distribution today, via revolatilization of PCBs from historically contaminated soil. However, the enantiomer fraction data observed here, particularly for the PCB 95 congener, provides compelling evidence that the current load of vapour-phase PCBs is from recent effluence from the treatment plant. This conclusion is supported by the observation that PCB 95, was found in racemic proportions in air (mean for all sampling seasons combined), with no significant difference from racemic standards. In contrast, PCB 95 was found to be significantly nonracemic in soil, and with a mean EF statistically different from that in air samples ($p<0.001$). This suggests that, over the sampling period, volatilization of older, biologically weathered deposits from the local soil was not a significant source of this congener to the atmosphere. Rather, fresh releases of PCB 95 by the treatment plant, and by extension other homologous congeners and possibly other congeners, were dominant. Similarly, PCB 149, while not significantly nonracemic in soil, had an enantiomer distribution in air that more closely matched the EF of racemic standards, rather than soil (Figure 4-7). Racemic distributions in air were also found for PCBs 91 and 136, although a source distinction could not be made for these congeners, as their enantiomer distribution in soil was also racemic.

Interestingly, a literature review of enantiomer distributions for PCBs in air showed them to be nearly exclusively racemic (e.g. [12, 13, 30]). As with this study, this phenomenon has been generally explained by a prevalence of fresh,

racemic sources of PCBs overwhelming any nonracemic distributions from historically contaminated environmental surfaces such as soil. Here we consider some alternate explanations. One possibility is that only a portion of the solvent-extractable PCB load within the entire soil matrix is available for volatilization [12]. If there is an inverse correlation between the proportion of soil-bound PCBs available for volatilization and the likelihood of microbial degradation that would lead to nonracemic EFs, we may in fact be observing racemic EFs being emitted from predominantly nonracemic PCB soil. To test this hypothesis, we removed topsoil from high concentration sites close to the SHTC (sites 7 and 21) and placed it in glass sealed chambers with 2 precleaned PUF discs per chamber (Figure 4-8b). This chamber experiment was designed to simulate a PUF-air-soil interaction in the absence of fresh PCB sources, and was performed with two separate soil-containing chambers and repeated 3 times for periods of 16 to 18 days per replicate. In addition, a chamber without soil was also employed as a control to assess potential contamination from laboratory air, yielding non-detects for target analytes. As expected, nonracemic distributions of PCB 95 in PUF discs in the chambers (Figure 4-8a) were similar to soil. PCB 149 also showed EFs for PUF discs that were closer to soil than racemic standards (Figure 4-8a). These results suggest that, in the absence of fresh sources, volatilization of nonracemic PCBs from soil indeed yields nonracemic distributions in air. This result is further substantiated by the observation of seasonal variation of PCB EFs in air. Significantly nonracemic distributions for PCB 95 were observed in air during the summer 2007 sampling season, statistically different ($p=0.0036$) from

the winter 2007 and summer 2006 air samples which were dominated by racemic distributions (Figure 4-9), and not statistically different from the enantiomer distribution in soil ($p>0.05$). In contrast, no seasonal variation was observed for PCB 149, although this is likely due to PCB 149 in soil having EF values that were far closer to racemic. The seasonal variation in PCB 95 EFs could possibly be explained by reduced PCB-processing activities during that sampling period, allowing greater reflection of the nonracemic distributions from volatilized soil-bound PCBs. However, ΣPCB concentrations in air were not lower during the summer 2007 compared with other sampling seasons.

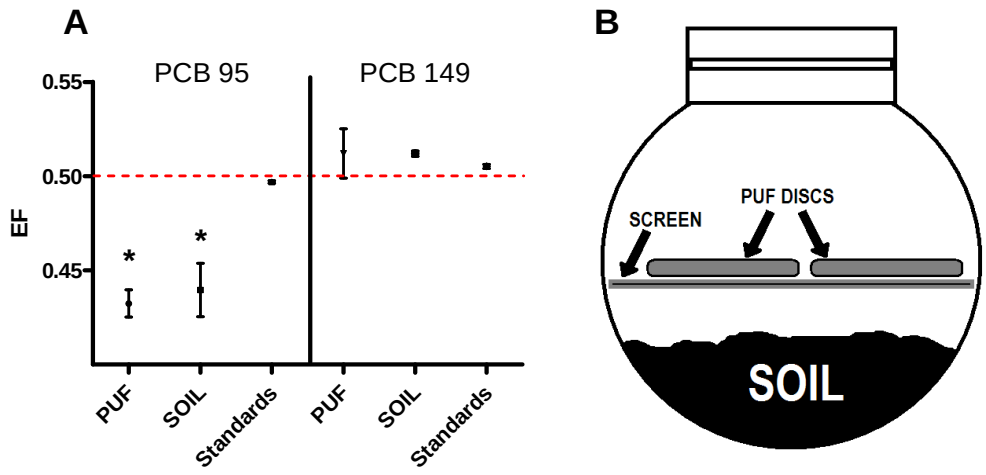

Figure 4-8: *A) Enantiomer distributions of PCBs 95 and 149 in PUF discs and soil after a 16 to 18 day enclosure in a sealed glass chamber. Asterisks indicate a significant difference from racemic standards ($p<0.05$). B) Experimental setup of chamber experiment.*

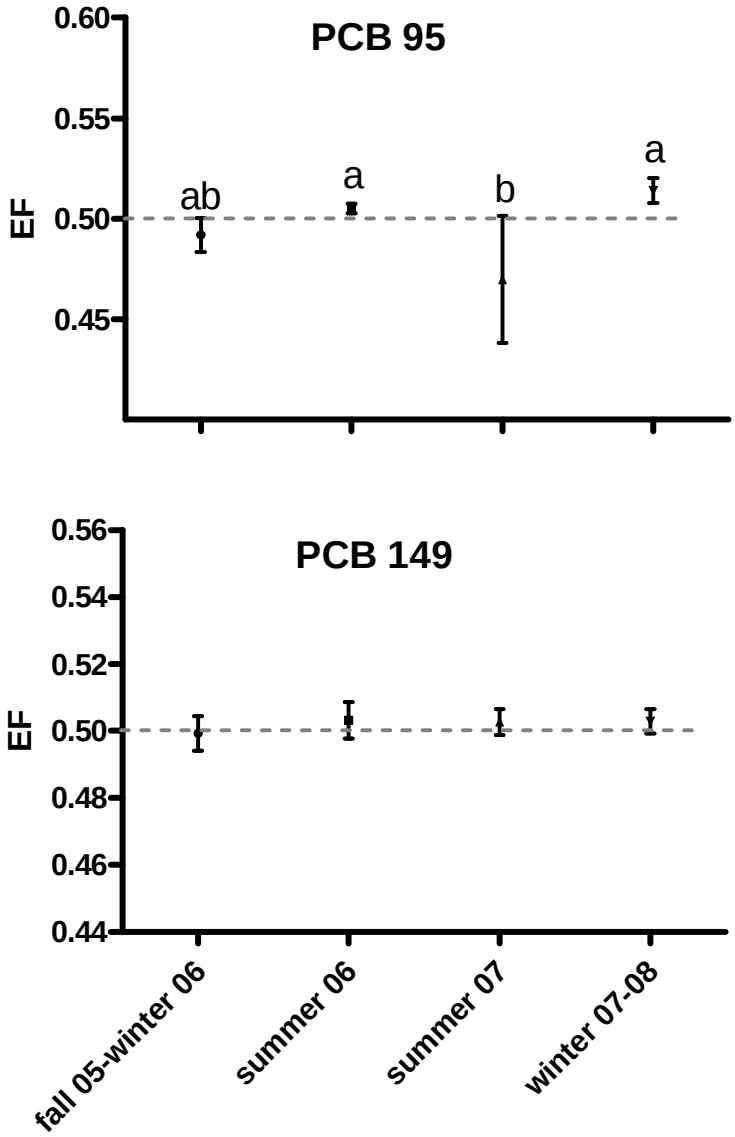

Figure 4-9: *Enantiomer fraction of PCBs 95 and 149 in PUF discs by sampling season. In the upper plot (PCB 95), sample groups marked with the same letter have no statistical difference. All sample groups for PCB 149 are not statistically different. The dashed line indicates a theoretical racemic composition of EF = 0.5.*

Another alternative explanation to the racemic distributions in air is that only a thin upper portion of the forest floor is available for air-surface exchange, and therefore racemic distributions of PCBs in this layer will be reflected in the bulk air even if the bulk soil is nonracemic. Moeckel et al. showed that the continuous deposition of vapour-phase PCBs to boreal forest vegetation and the subsequent fall of tree needles and shedding of waxes is an important source of PCBs to the forest floor and soil [39]. This may lead to uncertainty in our assessment of the PCB contamination responsible for the load of PCBs in local air, as the litter layer may represent a significant source of PCB to the air. However, average age of the litter layer (Oi Horizon) has been estimated to be 2.8 years [40], based on typical decomposition rates [40]. Thus, PCB contamination emitted from the treatment plant in 1996 would be incorporated into the soil layer prior to our soil sampling (10 years later). In addition, the PCB load deposited to soil in 1996 is expected to be mixed beyond the upper layer of soil available for air-surface exchange. This could not be directly observed in this study, as limitations in analytical sensitivity made studying the enantiomer distributions with high depth resolution in soil impractical. However, McLachlan et al. highlighted the importance of vertical mixing of these compounds in soil via transport of sorbed phases by considering bioturbation, cryoturbation, and the transport of particles into macropores [41], rather than simple diffusion through soil-gas and soil-liquid, which was exclusively considered in earlier models [42]. The movement of contaminant through the soil can be estimated by calculating diffusion length:

$$\Delta x = \sqrt{2 D_{eff} \Delta t} \qquad \text{Equation 4-1}$$

where Δx is the mean diffusion length, D_{eff} is the effective diffusivity, and Δt is time. Applying a conservative estimate of effective diffusivity of 2 $cm^2\ yr^{-1}$ (similarly applied in [41], and calculated based on the modeling of carbon transport in soils [43]), the PCB will travel downwardly approximately 2 cm in 5 years. This suggests that PCBs emitted from the SHTC in 1996, a decade prior to soil analysis, have had adequate time to mix beyond the upper soil layer. When considered alongside the enantiomer distribution data, this demonstrates that the single fugitive emission incident in 1996 has little influence on recent local atmospheric PCB concentrations. Again, the observation of nonracemic distributions in air during the summer of 2007 suggests that racemic distributions during the other sampling seasons are due to recent emissions from the SHTC.

It is important to note that the nonracemic distributions in soil may not be exclusively the result of microbial degradation in soil. Recently, the biotransformation of PCB 95 was reported in laboratory exposed poplars, demonstrating that plants have the capability to enantioselectively biotransform PCBs [44]. In light of this, some nonracemic distributions observed in Swan Hills soil may be, in part, due to biotransformation by trees and the subsequent incorporation of nonracemic PCBs into soil. This possibility, however, does not impact our source apportionment conclusions, as racemic distributions in air show a lack of influence of volatilization from environmental surfaces, regardless of the enantiomer distribution in leaf litter.

The relative lack of importance of the 1996 incident on the region's current atmospheric PCB load suggested here is consistent with data from previous studies that have highlighted the importance of continual emissions. Blais et al. showed similar deposition patterns in snow and new-growth spruce needles near the SHTC between March 1997 (the winter following the 1996 incident) and March 1998 [5]. In addition, increasing concentrations of PCBs and PCDD/Fs in wildlife were found in the years prior to the 1996 incident [8]. These two results each point to long term fugitive emissions as the major source of contamination. In contrast, PCB concentrations in a dated sediment core of nearby Chrystina Lake did show higher levels in 1996 and 1997 [5], although this may simply be due to increased quantities of hazardous wastes being processed at the facility, with 10,013 tonnes of PCBs treated in 1996, compared to annual amounts from 1988 to 1995 of 1548, 2057, 1092, 1961, 2380, 1664, 6698, and 2939 tonnes per year, respectively (personal communication - SHTC).

While the accidental release episode of 1996 is not the major contributing factor, more recent emissions during plant processing are likely the cause of the fresh releases responsible for the largely racemic enantiomer distributions observed here in air. These fresh releases can fall under one of two categories: i) stack emissions, which comprise expected releases of unincinerated material due to inherent limitations in the incineration process (as determined by DRE); and ii) fugitive emissions, which are unexpected releases due to leaks and other malfunctions. Fugitive emissions have been suggested as the cause of airborne PCB concentrations at another smaller PCB incineration facility in Canada [26].

Some evidence for this can be obtained by monitoring HCB, commonly used as an indicator of incomplete and low-temperature combustion of organochlorine compounds, and the production of PCDD/Fs [45]. As reported previously in other compartments [5], HCB was found at concentrations in air (12.1±0.7 pg/m^3) similar to other Canadian rural locations [46], and no trend or correlation ($p=0.48$) was observed with either distance from the SHTC or ΣPCB concentrations, suggesting that low temperature combustion is not a significant contributor of PCB emissions. Fresh PCB releases in the region may also be due to release of unincinerated PCBs, even when the treatment plant is operating at the minimum required DRE. At 2×10^6 kg per year processed at the facility and a 99.9999% DRE, 2 kg of PCBs will be released annually via stack emissions, although it is unclear what this mass would translate to with respect to observed air concentrations. Given uncertainty in our air concentration data, it is difficult to generate a reliable estimated air concentration for comparison purposes. It is worth noting, however, that this value of 2 kg per year is approximately half of that released by the fugitive emission episode in 1996 (4.9 kg of total PCBs [7]). As the 1996 episode caused an observed increase in local PCB concentrations in snow, vegetation, and sediment (and air, by inference) [5], the similarity in magnitude between annual estimated stack emissions and the single fugitive emission episode suggests that stack emissions could conceivably account for the concentrations observed in air. Considerably higher DREs would eliminate stack emissions as a possible cause of the fresh releases observed in this study.

4.3.4 Minimum biotransformation rate

In addition to the qualitative assessment of PCB degradation by enantiomer distributions, enantiomer fractions can also be used to estimate degradation rate constants. Such a technique has been used previously to estimate biotransformation rates of PCBs and other organochlorine contaminants in laboratory-exposed rainbow trout [17] and PCB-contaminated sediment from Lake Hartwell, SC [47], using the following equation [17]:

$$EF = \frac{1}{1 + \frac{(-)_0}{(+)_0} e^{(k_{m(+)} - k_{m(-)})t}} \qquad \text{Equation 4-2}$$

where $(+)_0$ and $(-)_0$ are the initial concentrations of the (+) and (−) enantiomers prior to degradation, respectively, $k_{m(+)}$ and $k_{m(-)}$ are the first order rate constants for the biotransformation of the (+) and (−) enantiomers, respectively, and *t* is time. To estimate biotransformation rates in Swan Hills soil from observed EFs, a number of assumptions must be made. First, we appropriately assume that initial concentrations of the (+) and (−) enantiomers are equal, as PCBs are expected to be in racemic proportions following release from an abiotic environment such as a treatment plant. Secondly, we must assume that observed changes in EF are due to degradation of one enantiomer only, while the degradation rate of the other enantiomer is zero. Thirdly, we assume that addition of more racemic PCBs (via emission from the SHTC) to the soil after the defined start time is negligible. As it is likely that both enantiomers are being biotransformed (observed EFs are due to differential degradation rates between the two enantiomers) and some quantity of PCBs has been emitted to soil in recent years, both the second and third

assumptions will likely lead to an underestimation of the true biodegradation rate, hence this calculation determines a *minimum* biotransformation rate constant in soil, k_m, with the following simplified equation:

$$k_m = \left|\frac{\ln(1-EF)/EF}{t}\right| \qquad \text{Equation 4-3}$$

Here, a value for *t* of 17 years was used, which corresponds to the approximate time between the commencement of PCB processing at the SHTC and the sampling of soil in this study, hence an absolute minimum rate. Minimum biotransformation rate constants and half lives for PCBs 95 and 149, the congeners that showed measurable enantioselective degradation, were calculated to be 0.015 y^{-1} ($t_{1/2}$ = 47 y) and 0.038 y^{-1} ($t_{1/2}$ = 180 y), respectively. Alternatively, we may assume that all PCB contamination is due to the 1996 incident (*t* = 9 y), yielding half lives of 25 and 97 years for PCBs 95 and 149, respectively. These biotransformation rates are similar to other estimates of PCB degradation in soil, although the assumptions made here cause the degradation to appear slower. For example, half lives of 6.4 to 30 years for tetra to hepta-chlorinated PCBs were found in boreal forest soil using a mass balance approach [39]. Similarly, using the same enantiomer-biotransformation rate approach, half lives for PCB 95 ranged from 6.6 to 86 years, and PCB 149 ranged from 42 to 1400 years, in Lake Hartwell sediment cores, depending on the core analysed and the calculation scenario. The biotransformation half-lives determined here provide evidence that PCB concentrations in the region are expected to gradually decline, in the absence of fresh inputs from SHTC activities. Apart from human

activities such as incineration, this natural elimination process represents another important contribution to the reduction of Canada's environmental burden of PCBs.

4.4 Conclusions

PCB concentrations and enantiomer distributions were measured in air and soil samples in the region immediately surrounding the SHTC. PCB concentrations in both air and soil were found to be highest for samples collected closest to the SHTC, with concentrations decreasing exponentially with increasing distance from the treatment plant. Enantiomer analysis yielded racemic signals for all target PCB congeners in air and significantly nonracemic distributions for PCB 95 in soil, suggesting that the primary source of this congener, and likely other PCB congeners, is due to recent and continual releases from the SHTC, and not old, biologically weathered sources such as volatilization from soil, originating from historical releases. In addition, significant biodegradation of some PCBs is occurring in local soil, with calculated minimum biotransformation half -lives. Results of this research suggest that reductions in fugitive releases from the treatment plant may be the most effective way of reducing atmospheric PCB concentrations in the region.

4.5 References

1. UNEP, United Nations Environmental Programme. Stockholm Convention on Persistent Organic Pollutants. 2009.

2. Government of Canada, PCB regulations, Canada Gazette Part II, Canadian Environmental Protection Act; 2008.

3. National Inventory of PCBs in Use and PCB Wastes in Storage in Canada: 2005 Annual Report.; Pollution Prevention, Environmental Stewardship Branch: Ottawa, Ontario, 2006.

4. Earth Tech Canada Inc. Swan Hills Treatment Centre Statement of Qualifications.; 2008.

5. Blais, J. M.; Froese, K. L.; Kimpe, L. E.; Muir, D. C. G.; Backus, S.; Comba, M.; Schindler, D. W., Assessment and characterization of polychlorinated biphenyls near a hazardous waste incinerator: analysis of vegetation, snow, and sediments. *Environmental Toxicology and Chemistry* 2003, 22, (1), 126-133.

6. Bovar Waste Management. Environmental Monitoring Results Volume II.; 1997.

7. Bovar Waste Management. Transformer Furnace Incident press release.; November 12, 1996.

8. Alberta Health and Wellness. Long-Term Follow-Up Health Assessment Program 1997-2002; 2004.

9. Bidleman, T. F.; Falconer, R. L., Enantiomer ratios for apportioning two sources of chiral compounds. *Environmental Science & Technology* 1999, 33, (13), 2299-2301.

10. Singer, A. C.; Wong, C. S.; Crowley, D. E., Differential enantioselective transformation of atropisomeric polychlorinated biphenyls by multiple bacterial strains with different inducing compounds. *Applied and Environmental Microbiology* 2002, 68, (11), 5756-5759.

11. Pakdeesusuk, U.; Jones, W. J.; Lee, C. M.; Garrison, A. W.; O'Niell, W. L.; Freedman, D. L.; Coates, J. T.; Wong, C. S., Changes in enantiomeric fractions during microbial reductive dechlorination of PCB132, PCB149, and Aroclor 1254 in Lake Hartwell sediment microcosms. *Environmental Science & Technology* 2003, 37, (6), 1100-1107.

12. Robson, M.; Harrad, S., Chiral PCB signatures in air and soil: Implications for atmospheric source apportionment. *Environmental Science & Technology* 2004, 38, (6), 1662-1666.

13. Asher, B. J.; Wong, C. S.; Rodenburg, L. A., Chiral source apportionment of polychlorinated biphenyls to the Hudson River estuary atmosphere and food web. *Environmental Science & Technology* 2007, 41, (17), 6163-6169.

14. Bidleman, T. F.; Wong, F.; Backe, C.; Sodergren, A.; Brorstrom-Lunden, E.; Helm, P. A.; Stern, G. A., Chiral signatures of chlordanes indicate changing sources to the atmosphere over the past 30 years. *Atmospheric Environment* 2004, 38, (35), 5963-5970.

15. Jantunen, L. M.; Helm, P. A.; Kylin, H.; Bidleman, T. F., Hexachlorocyclohexanes (HCHs) In the Canadian Archipelago. 2. Air-Water Gas Exchange of α- and γ-HCH. *Environmental Science & Technology* 2008, 42, (2), 465-470.

16. Shoeib, M.; Harner, T., Characterization and comparison of three passive air samplers for persistent organic pollutants. *Environmental Science & Technology* 2002, 36, (19), 4142-4151.

17. Wong, C. S.; Lau, F.; Clark, M.; Mabury, S. A.; Muir, D. C. G., Rainbow trout (*Oncorhynchus mykiss*) can eliminate chiral organochlorine compounds enantioselectively. *Environmental Science & Technology* 2002, 36, 1257-1262.

18. Harner, T.; Shoeib, M.; Diamond, M.; Stern, G.; Rosenberg, B., Using passive air samplers to assess urban - Rural trends for persistent organic pollutants. 1. Polychlorinated biphenyls and organochlorine pesticides. *Environmental Science & Technology* 2004, 38, (17), 4474-4483.

19. Pozo, K.; Harner, T.; Lee, S. C.; Wania, F.; Muir, D. C. G.; Jones, K. C., Seasonally resolved concentrations of persistent organic pollutants in the global atmosphere from the first year of the GAPS study. *Environmental Science & Technology* 2009, 43, (3), 796-803.

20. Persoon, C.; Hornbuckle, K. C., Calculation of passive sampling rates from both native PCBs and depuration compounds in indoor and outdoor environments. *Chemosphere* 2009, 74, (7), 917-923.

21. Frame, G. M., A collaborative study of 209 PCB congeners and 6 Aroclors on 20 different HRGC columns 1. Retention and coelution database. Fresen. J. *Analytical Chemistry* 1997, 357, (6), 701-713.

22. Wong, C. S.; Garrison, A. W., Enantiomer separation of polychlorinated biphenyl atropisomers and polychlorinated biphenyl retention behavior on modified cyclodextrin capillary gas chromatography columns. *Journal of Chromatography A* 2000, 866, (2), 213-220.

23. Harner, T.; Wiberg, K.; Norstrom, R. J., Enantiomer fractions are preferred to enantiomer raios for describing chiral signatures in environmental analysis. *Environmental Science & Technology* 2000, 34, 218-220.

24. Asher, B. J.; D'Agostino, L. A.; Way, J. D.; Wong, C. S.; Harynuk, J. J., Comparison of peak integration methods for the determination of enantiomeric fraction in environmental samples. *Chemosphere* 2009, 75, (8), 1042-1048.

25. Brown, T. M.; Sheldon, T. A.; Burgess, N. M.; Reimer, K. J., Reduction of PCB contamination in an Arctic coastal environment: A first step in assessing ecosystem recovery after the removal of a point source. *Environmental Science & Technology* 2009, 43, (20), 7635-7642.

26. Poon, C.; Gregory-Eaves, I.; Connell, L. A.; Guillore, G.; Mayer, P. M.; Ridal, J.; Blais, J. M., Air-vegetation partitioning of polychlorinated biphenyls near a point source. *Environmental Toxicology and Chemistry* 2005, 24, (12), 3153-3158.

27. Yan, S.; Rodenburg, L. A.; Dachs, J.; Eisenreich, S. J., Seasonal air-water exchange fluxes of polychlorinated biphenyls in the Hudson River Estuary. *Environmental Pollution* **2008,** *152*, (2), 443-451.

28. Simcik, M. F.; Zhang, H.; Eisenreich, S. J.; Franz, T. P., Urban contamination of the Chicago/Coastal Lake Michigan atmosphere by PCBs and PAHs during AEOLOS. *Environmental Science & Technology* 1997, 31, (7), 2141-2147.

29. Li, Y. F.; Harner, T.; Liu, L. Y.; Zhang, Z.; Ren, N. Q.; Jia, H. L.; Ma, J. M.; Sverko, E., Polychlorinated biphenyls in global air and surface soil:

distributions, air-soil exchange, and fractionation effect. *Environmental Science & Technology* 44, 2010 (8), 2784-2790.

30. Jamshidi, A.; Hunter, S.; Hazrati, S.; Harrad, S., Concentrations and chiral signatures of polychlorinated biphenyls in outdoor and indoor air and soil in a major U.K. conurbation. *Environmental Science & Technology* 2007, 41, 2153-2158.

31. Bucheli, T. D.; Brandli, R. C., Two-dimensional gas chromatography coupled to triple quadrupole mass spectrometry for the unambiguous determination of atropisomeric polychlorinated biphenyls in environmental samples. *Journal of Chromatography* A 2006, 1110, (1-2), 156-164.

32. Wong, F.; Robson, M.; Diamond, M. L.; Harrad, S.; Truong, J., Concentrations and chiral signatures of POPs in soils and sediments: A comparative urban versus rural study in Canada and UK. *Chemosphere* 2009, 74, (3), 404-411.

33. Guilbeault, B.; Sondossi, M.; Ahmad, D.; Sylvestre, M., Factors affecting the enhancement of PCB degradative ability of soil microbial populations. *International Biodeterioration & Biodegradation* 1994, 33, (1), 73-91.

34. Kurt-Karakus, P. B.; Stroud, J. L.; Bidleman, T.; Semple, K. T.; Jantunen, L.; Jones, K. C., Enantioselective degradation of organochlorine pesticides in background soils: variability in field and laboratory studies. *Environmental Science & Technology* 2007, 41, (14), 4965-4971.

35. Koblickova, M.; Ducek, L.; Jarkovsky, J.; Hofman, J.; Bucheli, T. D.; Klanova, J., Can physicochemical and microbial soil properties explain

enantiomeric shifts of chiral organochlorines? *Environmental Science & Technology* 2008, 42, (16), 5978-5984.

36. Oravec, M.; Simek, Z.; Holoubek, I., The effect of humic acid and ash on enantiomeric fraction change of chiral pollutants. *Colloids and Surfaces A: Physicochemical and Engineering Aspects* 359, (1-3), 60-65.

37. Furukawa, K., Genetic systems in soil bacteria for the degradation of PCB. In Biological degradation and bioremediation of toxic chemicals, Chaudkry, G., Ed. Chapman Hall: London, 1994.

38. Warner, N. A.; Norstrom, R. J.; Wong, C. S.; Fisk, A. T., Enantiomeric fractions of chiral polychlorinated biphenyls provide insights on biotransformation capacity of arctic biota. *Environmental Science & Technology* 2005, 24, (11), 2763-2767.

39. Moeckel, C.; Nizzetto, L.; Strandberg, B.; Lindroth, A.; Jones, K. C., Air-Boreal forest transfer and processing of polychlorinated biphenyls. *Environmental Science & Technology* 2009, 43, (14), 5282-5289.

40. Zhang, D. Q.; Hui, D. F.; Luo, Y. Q.; Zhou, G. Y., Rates of litter decomposition in terrestrial ecosystems: global patterns and controlling factors. *Journal of Plant Ecology-UK* 2008, 1, (2), 85-93.

41. McLachlan, M. S.; Czub, G.; Wania, F., The influence of vertical sorbed phase transport on the fate of organic chemicals in surface soils. *Environmental Science & Technology* 2002, 36, (22), 4860-4867.

42. Jury, W. A.; Spencer, W. F.; Farmer, W. J., Behavior assessment model for trace organics in soil 1. Model description. *Journal of Environmental Quality* 1983, 12, (4), 558-564.

43. Elzein, A.; Balesdent, J., Mechanistic simulation of vertical-distribution of carbon concentrations and residence times in soils. *Soil Science Society of America Journal* 1995, 59, (5), 1328-1335.

44. Zhai, G. S.; Hu, D. F.; Lehmler, H. J.; Schnoor, J. L., Enantioselective biotransformation of chiral PCBs in whole poplar plants. *Environmental Science & Technology* 2011, 45, (6), 2308-2316.

45. Öberg, T.; Bergström, J. G. T., Hexachlorobenzene as an indicator of dioxin production from combustion. *Chemosphere* 1985, 14, (8), 1081-1086.

46. Wania, F.; Shen, L.; Lei, Y. D.; Teixeira, C.; Muir, D. C. G., Development and calibration of a resin-based passive sampling system for monitoring persistent organic pollutants in the atmosphere. *Environmental Science & Technology* 2003, 37, (7), 1352-1359.

47. Wong, C. S.; Pakdeesusuk, U.; Morrissey, J. A.; Lee, C. M.; Coates, J. T.; Garrison, A. W.; Mabury, S. A.; Marvin, C. H.; Muir, D. C. G., Enantiomeric composition of chiral polychlorinated biphenyl atropisomers in dated sediment cores. *Environmental Toxicology and Chemistry* 2007, 26, (2), 254-263.

Chapter 5: Enantioselective Analysis of a PFOS Isomer: Evidence for the Source Contribution of Precursors to a Great Lakes Aquatic Food Web

5.1 Introduction

Perfluorooctane sulfonate (PFOS, $C_8F_{17}SO_3^-$) is a widely studied and environmentally prevalent member of a larger class of xenobiotic compounds called perfluorochemicals (PFCs). PFCs have been widely used in a variety of applications, due to their oil and water repellent properties and their remarkable stability, with historic production peaking at the end of the 20th century in North America and Europe [1]. PFOS has attracted considerable attention as an environmental contaminant in recent years, owing to its global ubiquity [2], ability to bioaccumulate in wildlife [3, 4], and the fact that it has not been reported to degrade, biotically or abiotically, under any environmental conditions. Chronic toxicity studies in monkeys have shown PFOS to cause reduced body weights, increased liver weights, and disruption in serum cholesterol and triiodothyronin [5], while rat studies have shown PFOS to have significant developmental effects [6]. Furthermore, PFOS inhibits gap junction intercellular communication in mammals [7], and disrupts the endocrine systems, reproduction, and development in fish [8]. As a result of these concerns, PFOS was recently added to Annex B of the Stockholm Convention on Persistent Organic Pollutants. Nonetheless, manufacturing of PFOS and its precursors is still permitted for the majority of their historical purposes [9].

PFOS is known to have entered the environment directly by emission through the manufacture and end use of PFOS-containing products, either as an intentional ingredient or residual impurity. However, emissions of perfluorooctane sulfonyl fluoride (POSF)-derived substances that were order-of-

magnitude higher than those of PFOS have been estimated [1]. Such substances are also known as PFOS precursors (hereafter referred to as "PreFOS") and are typically substituted perfluorooctyl sulfonamides having the general formula $C_8F_{17}SO_2NRR'$. These can degrade to PFOS by various pathways, particularly by metabolism. Thus, there is great potential that PreFOS emissions are responsible for some of the PFOS body burden measured in humans and wildlife [10]. For example *N*-ethyl perfluorooctanesulfonamidoethanol (*N*-EtFOSE, $C_8F_{17}SO_2N(C_2H_5)C_2H_4OH$) degrades to PFOS in rat liver slices, via the stable intermediate metabolite perfluorooctanesulfonamide (PFOSA, $C_8F_{17}SO_2NH_2$) [11]. The conversion from PreFOS to PFOS has also been shown *in vivo*, with at least 32% of PFOSA converting to PFOS in exposed rats [12].

Various forms of PreFOS are commonly detected in the environment [10], including in ocean, lake, and river water [13-16], indoor and outdoor air [17, 18], aquatic organisms [15, 19] and birds and their eggs [20, 21]. Moreover, positive correlations between the concentrations of PFOSA and PFOS have been found in numerous biological samples [15, 21, 22], suggestive that PFOSA, and possibly other PreFOS molecules, may be important contributors to body burdens of PFOS in wildlife [10]. However, because most commercially relevant PreFOS compounds have never been analyzed in the environment, and because the biotransformation yield of each is also poorly known, there is great uncertainty in the relative importance of both PFOS and PreFOS in human and environmental exposure scenarios. New analytical methods that could provide empirical evidence, to differentiate direct and indirect (i.e., from PreFOS) source of PFOS

would therefore be valuable, particularly in complex foodwebs where the feeding relationships are difficult to ascertain.

Of 89 theoretical PFOS isomers, 66 have at least one chiral center [23], including several environmentally relevant isomers such as monomethyl-branched isomers 1*m*-, 3*m*-, 4*m*-, and 5*m*-PFOS where "#*m*-" refers to the carbon position of the branched CF_3 group. Wang et al. showed that the biotransformation of a model PreFOS molecule was enantioselective, yielding significantly non-racemic proportions of the starting material after incubation with human liver microsomes [24]. This important result indicated that biotransformation of PreFOS will likely yield non-racemic proportions of product, such as the ultimate metabolite, PFOS. Conversely, if exposure is only to direct sources of PFOS itself, it is anticipated that the enantiomer fraction (EF) will be racemic (0.5), due to the fact that manufactured PFOS enantiomers exist in equal proportion. Consequently, the measurement of the enantiomeric proportions of chiral PFOS isomers in biotic samples might be used to apportion direct versus indirect (precursor) sources of these pollutants. Similar principles have been used to track sources of other chiral environmental contaminants, such as hexachlorocyclohexane (HCH) [25] and polychlorinated biphenyls (PCBs) [26]. The enantiomer separation of 1*m*-PFOS was recently reported, along with enantiomer distributions in human blood [27], however, to date there have been no reports of source apportionment to PFOS in aquatic food webs.

In this study, PFOS concentrations, isomer patterns, and enantiomer fractions (EFs) of 1*m*-PFOS, were determined in various fish and invertebrate

species from Lake Ontario. PFOS concentrations and isomer patterns in Lake Ontario fish have been determined in previous studies [15, 28, 29], but PFOS EFs have never been examined in wildlife. The novel objective of this study was to establish whether there was evidence for non-racemic proportions of 1*m*-PFOS in a well-studied aquatic food web, and if so, to relate the EF to PFOS and PreFOS concentrations or PFOS isomer patterns. The extent to which PreFOS contributes to PFOS concentrations has implications on our understanding of the fate of PFOS in the environment, including the prediction of future PFOS concentrations, the assessment of human and wildlife exposures, and the potential bias of calculated biomagnifications factors. Applying this enantiomer-focused technique may lead to a better understanding of the role precursors play in our ultimate exposure to PFOS.

5.2 Materials and Methods

5.2.1 Materials

The PFOS isomer standard (mixture of branched and linear isomers; >98% purity), the PFOSA standard (> 98% purity), and ^{13}C-labelled PFOS internal standard (>98% chemical purity, >99% $^{13}C_4$, >99% linear) were obtained from Wellington Laboratories Inc. (Guelph, ON, Canada). HPLC-grade solvents, water, tetrahydrofuran, triethylamine, and formic acid were purchased from Fisher Scientific (Ottawa, ON, Canada).

5.2.2 Sampling

Various methodologies were employed for sampling from various locations in Lake Ontario in 2007 and 2008. Additional details are presented in Tables A5-1 and A5-2. Collection methods included gill netting for lake trout (*Salvelinus namaycush*); bottom trawling for alewife (*Alosa pseudoharengus),* slimy sculpin (*Cottus cognatus*), round goby (*Neogobius melanostomus*), and rainbow smelt (*Osmerus mordax*); use of an epibenthic sled for mysid (*Mysis relicta)* and *Diporeia spp*. sampling; and use of a 150 µm net for zooplankton. Surface sediment was collected by Ekman dredge, and water was collected by grab sampling (1 to 10 m depth).

5.2.3 Sample preparation

Individual lake trout were analyzed as whole fish homogenate. All other fish and invertebrate samples were extracted as composite samples of multiple whole organisms. Following homogenization, samples (0.25 to 0.3 g, wet weight) of fish and invertebrate were extracted twice (2×5mL) with acetonitrile by shaking for 10 min, followed by centrifugation at 4000 rpm. The supernatants were combined, blown to dryness under nitrogen and reconstituted in 1 mL methanol.

Sediment was similarly extracted, but with a prior base digestion step. Briefly, 2 mL of 100 mmol/L sodium hydroxide was added to ca. 0.2 g of sediment. The mixture was sonicated for 30 min, then neutralized with 2 mL of 100 mmol/L hydrochloric acid, extracted successively by shaking with 20 mL and 10 mL methanol, and concentrated and reconstituted as above. All samples were

then cleaned up through a preconditioned solid phase extraction column (Waters Oasis WAX, 6 cm^3, 150 mg, 30 μm). Water was similarly extracted and cleaned up using a previously published method [30]. After cleanup, samples were blown down to dryness and reconstituted in 1:1 methanol/HPLC grade water prior to analysis.

5.2.4 Isomer Analysis

PFOS isomers were separated by HPLC and quantified using a previously published method [31]. Instrumentation consisted of an Agilent 1100 liquid chromatograph paired with an API 5000 triple quadrupole mass spectrometer (Applied Biosystems) operating in negative ion mode. Multiple reaction monitoring was employed, using previously reported mass transitions [32]. Quantitation of PFOS and PFOSA isomers were based on their relative response to ^{13}C-labelled PFOS internal standard, spiked prior to extraction to account for any recovery losses. Recoveries of PFOS for fish and water samples were assessed by spiking known concentrations of PFOS into duplicate samples, yielding recoveries (mean±SD) of 101±16% and 120±11% for fish and water, respectively. Due to a lack of branched standards, PFOSA isomer distributions (percent linear) were based on the peak area of the linear isomer relative to the total peak area (sum) of all isomers (based on the 498→78 transition), rather than actual concentrations.

5.2.5 Enantioselective separation and quality assurance

1*m*-PFOS (Figure 5-1A; inset) was chosen as the targeted chiral PFOS isomer because its chiral centre is closest to the sulfonate moiety. The α-position of the chiral centre was desirable because this, presumably, increases the likelihood that the biotransformation of its analogous 1*m*-precursor(s) will be enantioselective, as demonstrated previously for a model 1*m*-PreFOS molecule [24].

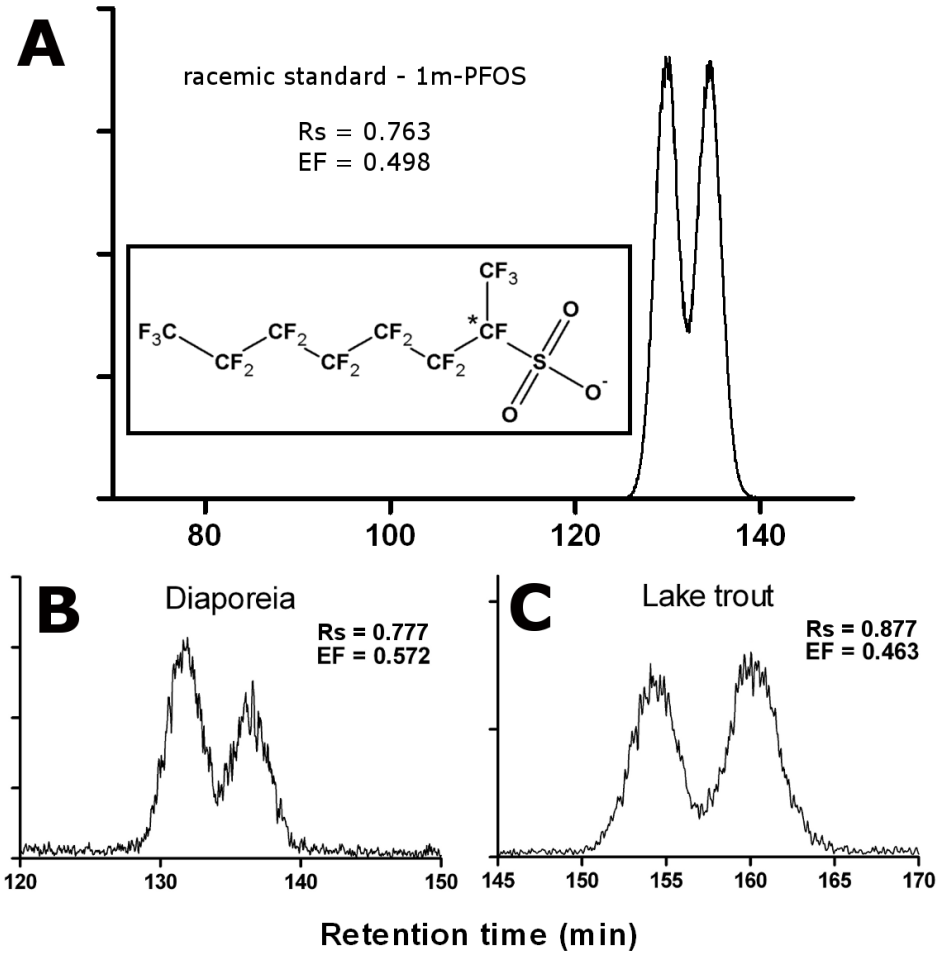

Figure 5-1: *Example chromatograms showing the enantiomer separation and distribution for 1m-PFOS: A) Racemic standard, Inset: Structure of 1m-PFOS with asterisk at chiral center. B) Diporeia, and C) lake trout, from Lake Ontario.*

As previously described [27], 1*m*-PFOS enantiomers were separated on two Chiralpak QN-AX columns (150 × 2.1 mm × 5 µm d_p each) in series, using an isocratic mobile phase of 70% THF, 20% 0.2M formic acid, 10% water, and 0.05% triethylamine at 120 µL/min. Quantification of both 1m-PFOS enantiomers employed the unique MRM transition, 499→419, which is free from interference from other PFOS isomers under our method conditions [31]. For this study, the EF for 1*m*-PFOS was defined as the area of the first-eluted enantiomer, divided by the sum concentration of both enantiomers [33], because the elution order is unknown. Due to limited column lifetime that limited the number of samples that could be analyzed, only samples which showed a minimum signal-to-noise ratio of 20, based on the aforementioned isomer analysis, were selected for enantiomer analysis.

Deconvolution of enantiomer peak areas was performed to determine EF accurately using Peakfit v4.06 software (Systat Software, San Jose, CA) as previously described (Chapter 3) [34], with the exception that the "vary widths" parameter was employed to account for differential peak broadening between the enantiomers, a side effect of the significantly long retention times required for 1*m*-PFOS enantiomer separation. Long retention times also resulted in significantly wide peaks (greater than 5 minutes per peak in most cases). This substantially reduced signal to noise ratios, resulting in a relatively high but adequate on-column detection limit of 4.6 pg (sum of both enantiomers) for 1*m*-PFOS, compared to 0.36 pg with the isomer method.

Adding to the analytical challenge here was that 1*m*-PFOS makes up only about 1.6% of total PFOS in ECF mixtures [35], therefore additional nitrogen evapoconcentration was performed, and injection volumes (20 µL) were doubled (relative to the isomer method) to ensure adequate sample signals. Except where noted, EFs were rejected if the peak signal to noise ratio was less than 10. EFs were considered nonracemic if they were statistically different from the mean EF of racemic standards (based on five injections of 1 ng/mL 1*m*-PFOS standard). Statistical differences among sample groups and standards were determined using ANOVA and the Tukey Honestly-Significant-Difference post-hoc test, with a minimum confidence level of 95%. The integrity of enantiomer signatures was assessed and verified by performing standard addition spikes with a 1*m*-PFOS standard, to rule out the presence of matrix effects. Matrix effects were calculated by subtracting the individual peak areas of each enantiomer after spiking from those areas before spiking, then calculating the EF based on the difference [36]. Samples of lake trout (×2), slimy sculpin, *Diporeia* (×2), and zooplankton samples (×1) were assessed, yielding a range in EFs based on this peak area difference of 0.493 to 0.513 (mean±S.E.= 0.502±0.007, not statistically different from racemic standards alone) for all samples, confirming no significant matrix effects. The 1*m*-PFOS isomer was not detected in any blanks, and therefore EFs were not affected by blank subtraction.

5.3 Results and Discussion

5.3.1 *PFC concentrations and isomer patterns*

PFOS was detected in all samples at similar wet weight concentrations (Table 5-1) to those reported by Houde et al. [28]. Concentrations in lake trout in the current study (2008 sampling) were also not significantly different from those measured in 2004 [29], presumably due to a long residence time of PFOS in Lake Ontario, which may moderate significant changes in usage and emission of PFOS in the region.

Table 5-1*: Concentrations (mean±SD) of PFOS and PFOSA in Lake Ontario aquatic organisms (ng/g wet weight).*

species	n	PFOS concentration	PFOSA concentration
lake trout	10	58±13	0.49±0.18
slimy sculpin	8	141±62	8.8±5.9
alewife	8	29±7	1.7±0.8
goby	8	21±10	1.5±0.5
smelt	10	38±11	3.7±2.3
diporeia	7	100±21	3.5±1.2
zooplankton	8	6.5±1.7	0.20±0.13
mysids	8	7.8±6.1	2.5±1.6

Consistent with previous analyses [15, 28], the highest concentrations of total PFOS were observed in *Diporeia* and slimy sculpin, not in lake trout, the top predator. Martin et al. hypothesised that this phenomenon may be due to possible high concentrations of PFOS, or PreFOS, in sediment; and thus a source to benthic feeders such as *Diporeia*, and in turn, slimy sculpin [15]. Consistent with this hypothesis, in the current study high concentrations of PFOSA were also observed in sculpin and *Diporeia* (Table 5-1). Furthermore, concentrations of PFOSA were strongly correlated to PFOS in some species (Figure 5-2), including

sculpin ($p=0.00050$, $r^2=0.89$) and smelt ($p=0.0030$, $r^2=0.69$), suggesting a link between PFOS and one of its known precursors. No such correlation was observed in any invertebrate species, but a significant correlation was observed when the three invertebrate species were combined for statistical analysis ($p=0.0047$, $r^2=0.32$) – a correlation simply driven by higher concentrations of both compounds in *Diporeia*.

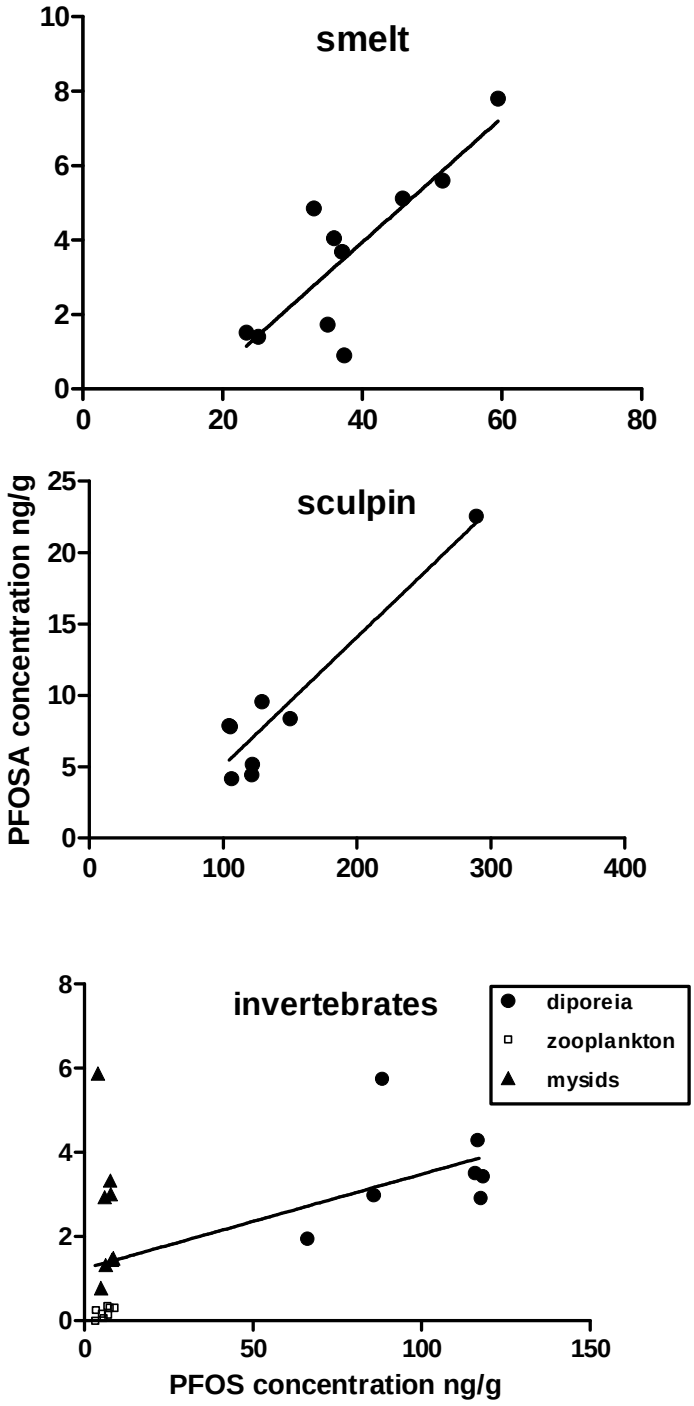

Figure 5-2: *Significant ($p<0.05$) correlations between PFOS and PFOSA concentrations for aquatic organisms in Lake Ontario.*

The PFOS isomer profile we measured in Lake Ontario water (69.8±1.4% linear) was very similar to that known in technical mixtures of PFOS (~70% linear [35]), although somewhat higher than those reported by Houde et al. (43-56% linear) [28]. The linear PFOS isomer was enriched (>90% of total PFOS) in all aquatic species (Figure 5-3), relative to water and were generally consistent for aquatic species sampled primarily in 2002 which showed a dominance (>88%) of the linear isomer [28]. This is most likely explained by the enhanced capability for aquatic organisms to excrete branched PFOS isomers, relative to linear PFOS. Such a phenomenon was recently demonstrated in laboratory-exposed rainbow trout [37]. In humans, highly branched PFOS isomer patterns have been proposed as a marker of PreFOS exposure [10] because branched PreFOS isomers are preferentially biotransformed, relative to linear ones [38]. In aquatic organisms, however, the preferential elimination of branched PFOS likely means that isomer distributions will not be a precise biomarker of PreFOS exposure.

Nonetheless, significant differences in linear PFOS percentage composition were observed across species (ANOVA, $p<0.0001$), suggesting marked differences in either the PFOS elimination capacity among species, or the sources of PFOS via diet, or both. A diet-weighted average for lake trout, based on previously determined diet contributions for Lake Ontario (discussed in more detail later [39]), produced a calculated percent linear for trout diet of 95.9%, similar to the measured 95.3% in whole trout homogenate. As noted above, laboratory-exposed rainbow trout excreted branched PFOS more quickly than linear PFOS [37], but in the field this is difficult to assess because the lake trout

PFOS isomer profile was affected to some extent by the combination of dietary uptake (a highly linear profile) and bioconcentration from Lake Ontario water (highly branched). Thus, it is unclear whether differences in PFOS elimination or sources were responsible for the observed differences in PFOS linear composition among species.

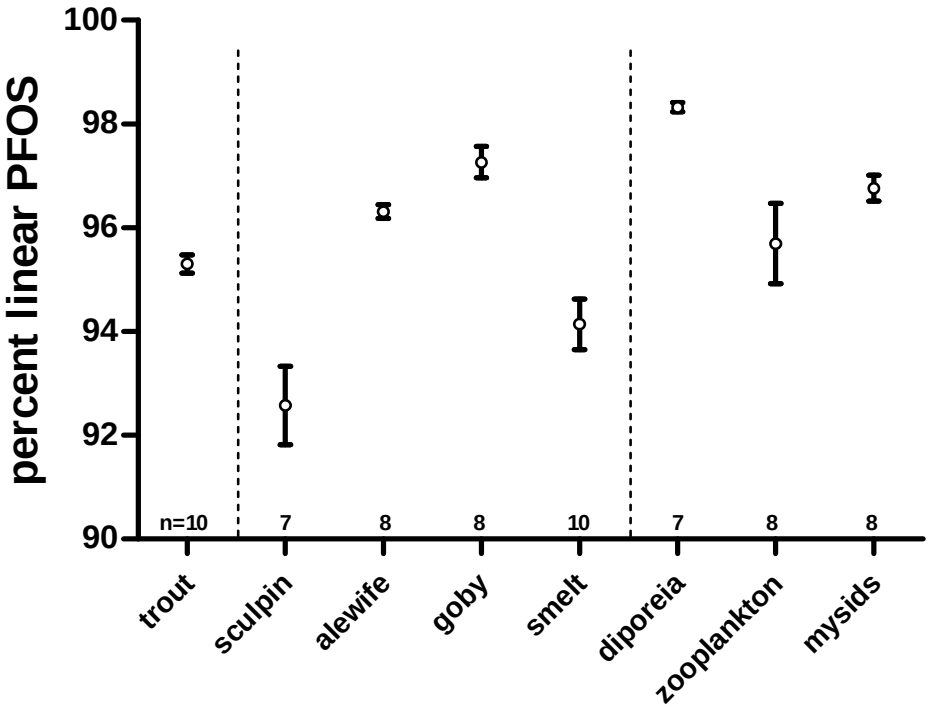

Figure 5-3: *PFOS isomer composition of aquatic species in Lake Ontario, expressed as percent linear (percent n-PFOS). Number of samples analyzed for each is shown as n.*

The isomer distribution of PFOSA (Figure 5-4) was more variable across species than for PFOS, but interestingly, correlations between isomer compositions of PFOS and PFOSA were observed within some species. Most notably, a strong positive correlation ($p=0.0017$, $r^2=0.88$) was observed in sculpin,

suggesting that PFOSA contributed to PFOS concentrations in this species. A weaker but significant association was also found for trout ($p=0.014$, $r^2=0.55$), while no association was found in invertebrates or in other forage fish. Such correlations have not been reported previously, but could conceivably be used as an indicator of precursor exposure, assuming isomer distributions remain unchanged, or at least behave predictably, in the conversion of PreFOS to PFOS.

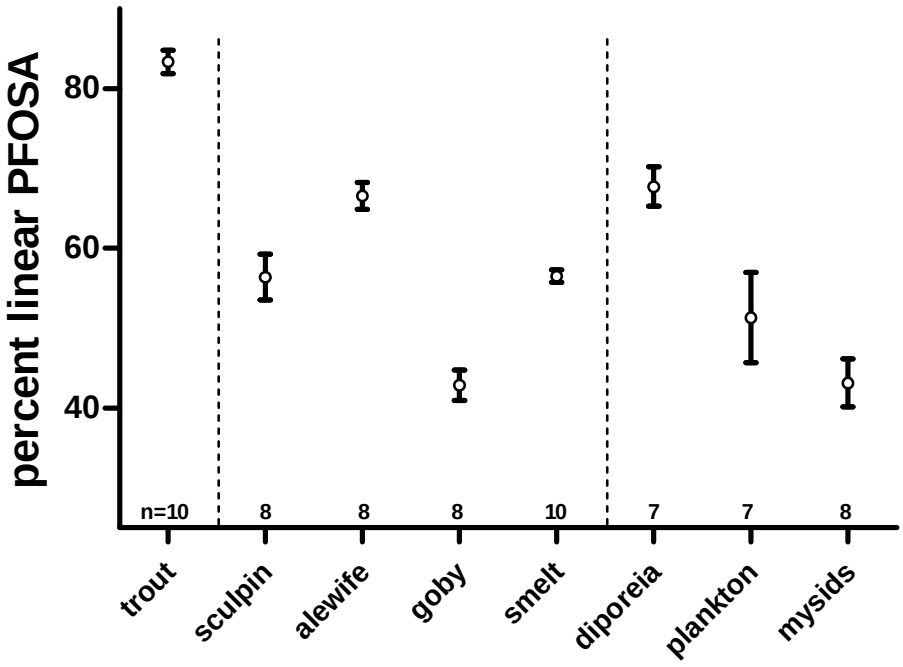

Figure 5-4: *Estimated PFOSA isomer composition of aquatic species in Lake Ontario, expressed as percent linear (percent n-PFOSA).*

5.3.2 *Enantiomer analysis of 1m-PFOS*

With repeated sample injections, degradation in column performance was evident, with steadily decreasing resolutions and a corresponding decrease in retention. Over the entire sample set described here, enantiomer separations of

1*m*-PFOS were achieved with peak resolutions ranging from 0.88 to 0.69 (e.g. Figure 5-1) with a total analysis time ranging from 1.5 to 3 hrs. Standard addition experiments for matrix effect evaluation were performed both early and late in the column's lifetime, therefore the shifting retention times did not bias EF results. It should be noted that, although other PFOS isomers were monitored, no enantiomeric separation of the other major chiral branched isomers (e.g. 3*m*-, 4*m*-, and 5*m*-PFOS) was observed. Concentrations of 1*m*-PFOS, which comprised approximately 0.34% of total PFOS concentrations (mean of all samples in all aquatic species), were strongly positively correlated with the sum concentration of all other PFOS isomers ($p<0.0001$, $r^2=0.56$), suggesting that 1*m*-PFOS and other isomers have a similar source, and that source apportionment results for 1*m*-PFOS may be representative of PFOS sources, in general. Standard EFs were not significantly different from the theoretical racemic value of 0.5, with a mean±SE of 0.499±0.001 (Figure 5-5).

5.3.3 EFs in water and sediment

Enantiomer signatures in a small number of water and sediment samples were studied to assess the behaviour of PFOS enantiomers in the abiotic environment (Figure 5-5). Racemic signatures were observed in both water (EF = 0.498±0.003; n=2) and sediment samples (0.502±0.007; n=3). Racemic signatures in water are expected, as any biotic transformation of PreFOS would likely not contribute significantly to PFOS levels in the bulk water, and abiotic transformation of PreFOS to PFOS would not alter enantiomer distributions.

Racemic EFs in sediment indicate that microbial degradation of PreFOS to PFOS is likely not occurring in sediment, or if it is, the process is not enantioselective. It is most likely that there is no significant biodegradation of PreFOS in sediments, as previous studies found no observable biotransformation of PFOSA [40] or *N*-ethyl perfluorooctanesulfonamidoethanol (NEtFOSE) [41] in anaerobic wastewater sludge treatment. Racemic signatures in water and sediment are important from a source apportionment perspective, since any observation of non-racemic signatures in biotic samples would indicate that these organisms were indeed enantioselectively processing PreFOS (or possibly PFOS, discussed later), and that the nonracemic signatures were not simply due to uptake of non-racemic PFOS resulting from microbial biodegradation of PreFOS.

5.3.4 EFs in invertebrates

In contrast to water and sediment samples, nonracemic signatures were prevalent in biotic samples. All invertebrates had significantly nonracemic 1*m*-PFOS EFs (Figure 5-5), with *Diporeia*, mysids, and zooplankton having mean±S.E. of 0.564±0.004, 0.609±0.022, and 0.447±0.010, respectively. The more extreme and variable EFs for mysids (as marked with an asterisk in Figure 5-5) were based on peaks below the limit of quantitation (signal-to-noise ratios below 10). These are regarded with less confidence, because unacceptable precision in EF measurements ($SD_{EF} \geq 0.01$) occurs at these data conditions [34]. It was notable that the direction of enantioenrichment among invertebrates was different, as zooplankton showed significant enrichment of the E1-enantiomer,

while *Diporeia* and mysids exhibited the reverse trend. This observation suggests that significant differences may exist in the biotransformation pathways among species for the transformation of PreFOS to PFOS, as has been observed for biotransformation of other chiral contaminants in food webs [42]. Nonetheless, all significantly nonracemic EFs for 1*m*-PFOS in invertebrates may be indicative of a precursor source to these species, presumably via enantioselective processing of alpha-branched (i.e. 1*m*-) PreFOS.

The enantioselective processing of halogenated contaminants by invertebrates has been demonstrated previously, with nonracemic signatures for PCBs observed in *Diporeia* and mysids from Lake Superior [43]. While it is often difficult to conclude that nonracemic signatures indicate metabolic activity, rather than an enantioselective excretion processes, a lab study confirmed enantioselective metabolism of *trans*-chlordane in mysids [44]. Thus it is feasible that enantioselective metabolism of PreFOS also occurs in invertebrates.

Further evidence for the influence of PreFOS on the enantiomeric signatures of 1*m*-PFOS came from examining trends in EF with the concentration of PFOSA, a known PFOS precursor. The EFs for mysids, *Diporeia*, and zooplankton were transformed to deviations from racemic (DFR; absolute value of 0.5−EF) [45], to account for the opposite directions of enantioselectivity across these species. DFR was not correlated with PFOS ($p=0.53$) nor PFOSA ($p=0.30$) concentrations; however a significant positive correlation was observed between DFR and the ratio of [PFOSA]:[PFOS] ($p=0.012$, $r^2=0.48$). Furthermore, multiple linear regression analysis confirmed this relationship, with the PFOSA/PFOS ratio

and percent linear PFOS forming a linear relationship with DFR (DFR = -0.622 + (0.00677 × % linear PFOS) + (0.165 × [PFOSA]/[PFOS]; $p<0.001$ for both variables, $r^2=0.51$). Thus, when PFOSA concentrations were high relative to PFOS concentrations (i.e. a potentially greater contribution from precursor sources relative to direct sources), the enantiomer signature of 1*m*-PFOS became more nonracemic, as would be predicted. This may be taken as additional evidence that the presence of precursor sources was indeed reflected in the enantiomer signatures of PFOS. The positive correlation of the PFOS isomer composition with DFR is interesting, as it may suggest that, in these organisms, PreFOS to PFOS transformation favours the linear isomer. However, a similar correlation with PFOSA isomer composition was not observed ($p=0.886$ in MLR analysis).

5.3.5 EFs in fish

All fish had EFs that were closer to racemic than for invertebrates (Figure 5-5), despite invertebrates comprising the base of the food web. Nonetheless, lake trout, the top predator, had a significantly nonracemic EF of 0.467±0.003, suggesting some contribution of a precursor source to these organisms, possibly via their prey. The diet of lake trout in Lake Ontario has changed considerably in the past decade, since the introduction of round goby. The most recent estimates of lake trout diet by mass is 67.9% alewife, 19.9% round goby, 2.4% rainbow smelt, 1.4% slimy sculpin, and 2.4% threespine stickleback [39]. The mean EF in trout was not statistically different than in any of its four studied prey species.

In addition, a diet-weighted (described elsewhere [43]) average EF was calculated to be 0.474, effectively identical to the unadjusted EF. Thus, even though trout have the capacity to metabolize PreFOS to PFOS [46], there was no direct evidence of enantioselective biotransformation in Lake Ontario lake trout. The source of the non-racemic signature was likely from foodweb transfer. No significant correlation of EF with the age of individual lake trout was observed, suggesting that non-age factors, including diet, are the most important determinants of 1*m*-PFOS EFs in this species. All forage fish had non-racemic EFs. That of alewife (EF of 0.471±0.010) closely matched that of zooplankton, its primary food source [47]. The EF of round goby appeared nonracemic (0.470±0.015), and while nominally identical to alewife, was not statistically different from racemic standards, possibly due to the low number of samples available. Round gobies in Lake Ontario primarily feed on chironomid larvae and quagga mussels [48], which were not analyzed here, although zooplankton are also consumed, which indeed had a similar EF to round gobies.

Curiously, the other forage fish examined here had EFs that did not match their known prey. For example, rainbow smelt ingest primarily mysids and *Diporeia*, yet smelt had a racemic EF (0.499±0.017). Similarly, slimy sculpin 1*m*-PFOS was racemic (0.491±0.008) despite its primary food source *Diporeia* [47] having a highly nonracemic EF. Disagreement between the enantiomer compositions of predator and prey are not uncommon. For example, this was observed between *Diporeia* and sculpin for PCB 91 in Lake Superior [43]. There are several possible explanations for this. For example, sculpin may be

metabolizing PreFOS enantioselectively, but in the opposite EF direction of *Diporeia*, thereby moderating its 1*m*-PFOS EF to an approximately racemic signature. Another explanation is that the sculpin may not be eating only *Diporeia*. Analysis of stomach contents from Lake Ontario sculpin in 1992 revealed that a significant portion was unidentifiable [47]. The invasion of non-native zebra and quagga mussels, beginning in the 1990s, has reduced *Diporeia* numbers significantly, and thus sculpin likely consumed other organisms not examined here. Ingestion of other such sediment-dwelling organisms, or possible co-ingestion of racemic sediment, may also be contributing to the racemic signatures in sculpin.

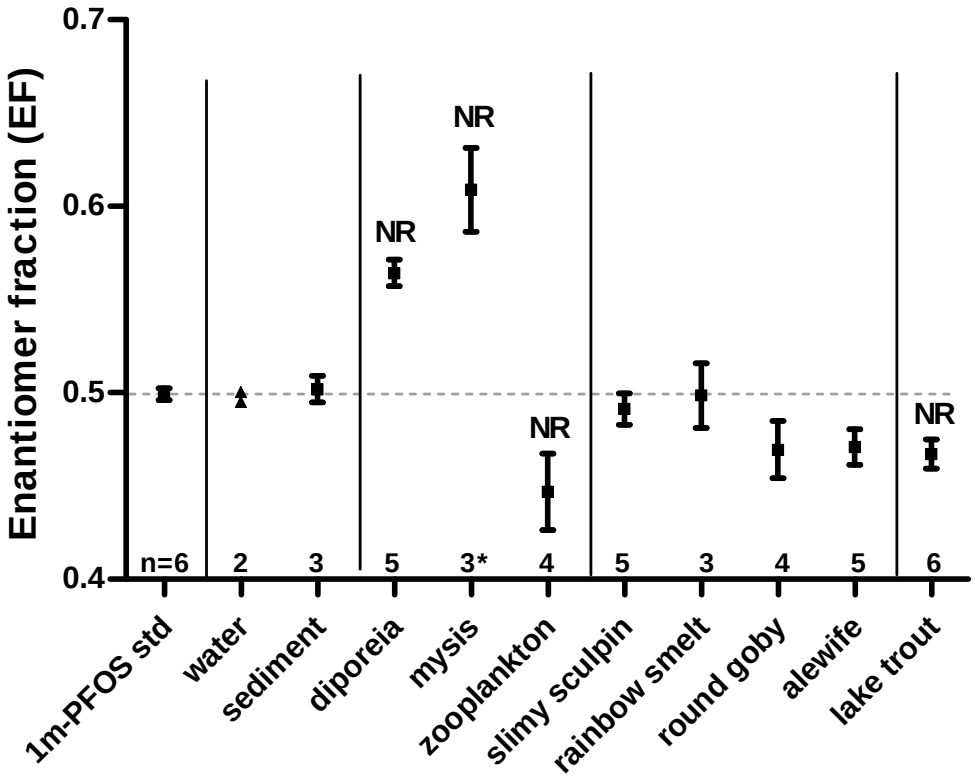

Figure 5-5: *Enantiomer fraction of 1m-PFOS in racemic standards, Lake Ontario water, sediment, and aquatic species. Number of samples analyzed for each is shown as n. Data shown as the mean with standard error represented as error bars (except for water, n = 2). "NR" indicates that the sample group was nonracemic, based on a significant difference with racemic standards. Dashed line indicates the theoretical racemic value of 0.5.*

5.4 Conclusion: Applicability of EFs for precursor source determination

Overall results provide evidence that enantiomer signatures of 1*m*-PFOS can be informative of PFOS sources in a similar manner to source apportionment work for other legacy organohalogen contaminants. Though the data presented here are compelling, we cannot completely rule out the possibility that some of the observed nonracemic signatures are due to enantiospecific absorption or excretion of PFOS, rather than biotransformation of PreFOS. PFOS binds

strongly to serum proteins, such as bovine serum albumin [49], a highly asymmetric biomolecule. While interactions with both the hydrophobic aliphatic tail and hydrophilic sulfonate head group (which is closer to the chiral centre of the 1*m* isomer) play a role in the binding to serum albumins [50], it is unknown whether this binding is stereoselective, and if so, if this would lead to preferential elimination of one enantiomer of 1*m*-PFOS over the other. Excretion of PFOS was not enantioselective in rats [27], but this same phenomenon has not been examined for any aquatic species. The observation of racemic signatures in several organisms (e.g. smelt, sculpin) in the present study suggests that absorption and excretion of PFOS itself are not stereoselective in at least some species. Furthermore, the *in vitro* metabolism of a PFOS precursor was shown to be enantioselective [24] – thus *in vivo* metabolism is also likely enantioselective. Finally, the observed correlations of enantiomer signatures with proportions of PFOSA in this study suggest that EFs are indeed a measure of PreFOS exposure. Further investigation of these phenomena, including laboratory exposure studies with aquatic organisms would aid in the interpretation of environmental EF measurements.

5.5 References

1. Paul, A. G.; Jones, K. C.; Sweetman, A. J., A first global production, emission, and environmental inventory for perfluorooctane sulfonate. *Environmental Science & Technology* **2009,** *43*, (2), 386-392.

2. Giesy, J. P.; Kannan, K., Global distribution of perfluorooctane sulfonate in wildlife. *Environmental Science & Technology* **2001,** *35*, (7), 1339-1342.

3. Tomy, G. T.; Budakowski, W.; Halldorson, T.; Helm, P. A.; Stern, G. A.; Friesen, K.; Pepper, K.; Tittlemier, S. A.; Fisk, A. T., Fluorinated organic compounds in an eastern Arctic marine food web. *Environmental Science & Technology* **2004,** *38*, (24), 6475-6481.

4. Martin, J. W.; Mabury, S. A.; Solomon, K. R.; Muir, D. C. G., Bioconcentration and tissue distribution of perfluorinated acids in rainbow trout *Oncorhynchus mykiss*. *Environmental Toxicology and Chemistry* **2003,** *22*, (1), 196-204.

5. Seacat, A. M.; Thomford, P. J.; Hansen, K. J.; Olsen, G. W.; Case, M. T.; Butenhoff, J. L., Subchronic toxicity studies on perfluorooctanesulfonate potassium salt in cynomolgus monkeys. *Toxicological Sciences* **2002,** *68*, (1), 249-264.

6. Lau, C.; Thibodeaux, J. R.; Hanson, R. G.; Rogers, J. M.; Grey, B. E.; Stanton, M. E.; Butenhoff, J. L.; Stevenson, L. A., Exposure to perfluorooctane sulfonate during pregnancy in rat and mouse. II: Postnatal evaluation. *Toxicological Sciences* **2003,** *74*, (2), 382-392.

7. Hu, W.; Jones, P. D.; Upham, B. L.; Trosko, J. E.; Lau, C.; Giesy, J. P., inhibition of gap junctional intercellular communication by perfluorinated compounds in rat liver and dolphin kidney epithelial cell lines in vitro and sprague-dawley rats in vivo. *Toxicol. Sci.* **2002,** *68*, (2), 429-436.

8. Han, J.; Fang, Z., Estrogenic effects, reproductive impairment and developmental toxicity in ovoviparous swordtail fish (Xiphophorus helleri) exposed to perfluorooctane sulfonate (PFOS). *Aquatic Toxicology* **2010,** *99*, (2), 281-290.

9. UNEP, United Nations Environmental Programme. The 9 new POPs: An introduction to the nine chemicals added to the Stockholm Convention by the Conference of the Parties at its fourth meeting. **2010**.

10. Martin, J. W.; Asher, B. J.; Beesoon, S.; Benskin, J. P.; Ross, M. S., PFOS or PreFOS? Are perfluorooctane sulfonate precursors (PreFOS) important determinants of human and environmental perfluorooctane sulfonate (PFOS) exposure? *Journal of Environmental Monitoring* **2010,** *12*, (11), 1979-2004.

11. Xu, L.; Krenitsky, D. M.; Seacat, A. M.; Butenhoff, J. L.; Anders, M. W., Biotransformation of N-ethyl-N-(2-hydroxyethyl)perfluorooetanesulfonamide by rat liver microsomes, cytosol, and slices and by expressed rat and human cytochromes P450. *Chemical Research in Toxicology* **2004,** *17*, (6), 767-775.

12. Seacat, A. M., Toxicokinetic study of perfluorooctane sulfonamide (PFOSA; T-7132.2) in rats. AR226–0328. **2000**.

13. Ahrens, L.; Barber, J. L.; Xie, Z. Y.; Ebinghaus, R., Longitudinal and latitudinal distribution of perfluoroalkyl compounds in the surface water of the Atlantic Ocean. *Environmental Science & Technology* **2009,** *43*, (9), 3122-3127.

14. Boulanger, B.; Vargo, J.; Schnoor, J. L.; Hornbuckle, K. C., Detection of perfluorooctane surfactants in Great Lakes water. *Environmental Science & Technology* **2004,** *38*, (15), 4064-4070.

15. Martin, J. W.; Whittle, D. M.; Muir, D. C. G.; Mabury, S. A., Perfluoroalkyl contaminants in a food web from lake Ontario. *Environmental Science & Technology* **2004,** *38*, (20), 5379-5385.

16. So, M. K.; Miyake, Y.; Yeung, W. Y.; Ho, Y. M.; Taniyasu, S.; Rostkowski, P.; Yamashita, N.; Zhou, B. S.; Shi, X. J.; Wang, J. X.; Giesy, J. P.; Yu, H.; Lam, P. K. S., Perfluorinated compounds in the Pearl River and Yangtze River of China. *Chemosphere* **2007,** *68*, (11), 2085-2095.

17. Shoeib, M.; Harner, T.; Wilford, B. H.; Jones, K. C.; Zhu, J. P., Perfluorinated sulfonamides in indoor and outdoor air and indoor dust: Occurrence, partitioning, and human exposure. *Environmental Science & Technology* **2005,** *39*, (17), 6599-6606.

18. Jahnke, A.; Huberc, S.; Ternme, C.; Kylin, H.; Berger, U., Development and application of a simplified sampling method for volatile polyfluorinated alkyl substances in indoor and environmental air. *Journal of Chromatography A* **2007,** *1164*, (1-2), 1-9.

19. Kannan, K.; Tao, L.; Sinclair, E.; Pastva, S. D.; Jude, D. J.; Giesy, J. P., Perfluorinated compounds in aquatic organisms at various trophic levels in a Great Lakes food chain. *Archives of Environmental Contamination and Toxicology* **2005,** *48*, (4), 559-566.

20. Kannan, K.; Corsolini, S.; Falandysz, J.; Oehme, G.; Focardi, S.; Giesy, J. P., Perfluorooctanesulfonate and related fluorinated hydrocarbons in marine mammals, fishes, and birds from coasts of the Baltic and the Mediterranean Seas. *Environmental Science & Technology* **2002,** *36*, (15), 3210-3216.

21. Wang, Y.; Yeung, L. W. Y.; Taniyasu, S.; Yamashita, N.; Lam, J. C. W.; Lam, P. K. S., Perfluorooctane sulfonate and other fluorochemicals in waterbird eggs from South China. *Environmental Science & Technology* **2008,** *42*, (21), 8146-8151.

22. Hart, K.; Gill, V. A.; Kannan, K., Temporal trends (1992-2007) of perfluorinated chemicals in Northern Sea otters (Enhydra lutris kenyoni) from South-Central Alaska. *Archives of Environmental Contamination and Toxicology* **2009,** *56*, (3), 607-614.

23. Rayne, S.; Forest, K.; Friesen, K. J., Congener-specific numbering systems for the environmentally relevant C4 through C8 perfluorinated homologue groups of alkyl sulfonates, carboxylates, telomer alcohols, olefins, and acids, and their derivatives. *Journal of Environmental Science and Health, Part A: Toxic/Hazardous Substances and Environmental Engineering* **2008,** *43*, (12), 1391 - 1401.

24. Wang, Y.; Arsenault, G.; Riddell, N.; McCrindle, R.; McAlees, A.; Martin, J. W., Perfluorooctane sulfonate (PFOS) precursors can be metabolized enantioselectively: Principle for a new PFOS source tracking tool. *Environmental Science & Technology* **2009,** *43*, (21), 8283-8289.

25. Ridal, J. J.; Bidleman, T. F.; Kerman, B. R.; Fox, M. E.; Strachan, W. M. J., Enantiomers of alpha-hexachlorocyclohexane as tracers of air-water gas exchange in Lake Ontario. *Environmental Science & Technology* **1997,** *31*, (7), 1940-1945.

26. Asher, B. J.; Wong, C. S.; Rodenburg, L. A., Chiral source apportionment of polychlorinated biphenyls to the Hudson River estuary atmosphere and food web. *Environmental Science & Technology* **2007,** *41*, (17), 6163-6169.

27. Wang, Y.; Beesoon, S.; Benskin, J. P.; De Silva, A. O.; Genuis, S. J.; Martin, J. W., Enantiomer fractions of chiral perfluorooctanesulfonate (PFOS) in human sera. *Environmental Science & Technology* **2011,** *accepted*.

28. Houde, M.; Czub, G.; Small, J. M.; Backus, S.; Wang, X.; Alaee, M.; Muir, D. C. G., Fractionation and bioaccumulation of perfluorooctane sulfonate (PFOS) isomers in a Lake Ontario food web. *Environmental Science & Technology* **2008,** *42*, (24), 9397-9403.

29. Furdui, V. I.; Helm, P. A.; Crozier, P. W.; Lucaciu, C.; Reiner, E. J.; Marvin, C. H.; Whittle, D. M.; Mabury, S. A.; Tomy, G. T., Temporal trends of perfluoroalkyl compounds with isomer analysis in lake trout from Lake Ontario (1979-2004). *Environmental Science & Technology* **2008,** *42*, (13), 4739-4744.

30. Taniyasu, S.; Kannan, K.; So, M. K.; Gulkowska, A.; Sinclair, E.; Okazawa, T.; Yamashita, N., Analysis of fluorotelomer alcohols, fluorotelomer acids, and short- and long-chain perfluorinated acids in water and biota. *Journal of Chromatography A* **2005,** *1093*, (1-2), 89-97.

31. Benskin, J. P.; Bataineh, M.; Martin, J. W., Simultaneous characterization of perfluoroalkyl carboxylate, sulfonate, and sulfonamide isomers by liquid chromatography-tandem mass spectrometry. *Analytical Chemistry* **2007,** *79*, (17), 6455-6464.

32. Riddell, N.; Arsenault, G.; Benskin, J. P.; Chittim, B.; Martin, J. W.; McAlees, A.; McCrindle, R., Branched perfluorooctane sulfonate isomer quantification and characterization in blood serum samples by HPLC/ESI-MS(/MS). *Environmental Science & Technology* **2009,** *43*, (20), 7902-7908.

33. Harner, T.; Wiberg, K.; Norstrom, R. J., Enantiomer fractions are preferred to enantiomer raios for describing chiral signatures in environmental analysis. *Environmental Science & Technology* **2000,** *34*, 218-220.

34. Asher, B. J.; D'Agostino, L. A.; Way, J. D.; Wong, C. S.; Harynuk, J. J., Comparison of peak integration methods for the determination of enantiomeric fraction in environmental samples. *Chemosphere* **2009,** *75*, (8), 1042-1048.

35. Fluorochemical isomer distribution by 19F NMR spectroscopy. US EPA Public Docket AR226-0564.; 1997.

36. MacLeod, S. L.; Sudhir, P.; Wong, C. S., Stereoisomer analysis of wastewater-derived beta-blockers, selective serotonin re-uptake inhibitors, and salbutamol by high-performance liquid chromatography-tandem mass spectrometry. *Journal of Chromatography A* **2007,** *1170*, (1-2), 23-33.

37. Sharpe, R. L.; Benskin, J. P.; Laarman, A. H.; MacLeod, S. L.; Martin, J. W.; Wong, C. S.; Goss, G. G., Perfluorooctane sulfonate toxicity, isomer-specific accumulation, and maternal transfer in zebrafish (Danio rerio) and rainbow trout (Oncorhynchus mykiss). *Environmental Toxicology and Chemistry* **2010,** *29*, (9), 1957-1966.

38. Benskin, J. P.; Holt, A.; Martin, J. W., Isomer-specific biotransformation rates of a perfluorooctane sulfonate (PFOS)-precursor by cytochrome P450

isozymes and human liver microsomes. *Environmental Science & Technology* **2009,** *43*, (22), 8566-8572.

39. Dietrich, J. P.; Morrison, B. J.; Hoyle, J. A., Alternative ecological pathways in the Eastern Lake Ontario food web - round goby in the diet of lake trout. *Journal of Great Lakes Research* **2009,** *32*, (2), 395-400.

40. Sáez, M.; de Voogt, P.; Parsons, J., Persistence of perfluoroalkylated substances in closed bottle tests with municipal sewage sludge. *Environmental Science and Pollution Research* **2008,** *15*, (6), 472-477.

41. Boulanger, B.; Vargo, J. D.; Schnoor, J. L.; Hornbuckle, K. C., Evaluation of perfluorooctane surfactants in a wastewater treatment system and in a commercial surface protection product. *Environmental Science & Technology* **2005,** *39*, (15), 5524-5530.

42. Fisk, A. T.; Holst, M.; Hobson, K. A.; Duffe, J.; Moisey, J.; Norstrom, R. J., Persistent organochlorine contaminants and enantiomeric signatures of chiral pollutants in ringed seals (*Phoca hispida*) collected on the east and west side of the Northwater Polynya, Canadian Arctic. *Archives of Environmental Contamination and Toxicology* **2002,** *42*, (1), 118-126.

43. Wong, C. S.; Mabury, S. A.; Whittle, D. M.; Backus, S. M.; Teixeira, C.; DeVault, D. S.; Bronte, C. R.; Muir, D. C. G., Organochlorine compounds in Lake Superior: Chiral polychlorinated biphenyls and biotransformation in the aquatic food web. *Environmental Science & Technology* **2004,** *38*, (1), 84-92.

44. Warner, N. A.; Wong, C. S., The freshwater invertebrate Mysis relicta can eliminate chiral organochlorine compounds enantioselectively. *Environmental Science & Technology* **2006,** *40*, (13), 4158-4164.

45. Jamshidi, A.; Hunter, S.; Hazrati, S.; Harrad, S., Concentrations and chiral signatures of polychlorinated biphenyls in outdoor and indoor air and soil in a major U.K. conurbation. *Environmental Science & Technology* **2007,** *41*, 2153-2158.

46. Tomy, G. T.; Tittlemier, S. A.; Palace, V. P.; Budakowski, W. R.; Braekevelt, E.; Brinkworth, L.; Friesen, K., Biotransformation of N-Ethyl perfluorooctanesulfonamide by rainbow trout (*Onchorhynchus mykiss*) liver microsomes. *Environmental Science & Technology* **2003,** *38*, (3), 758-762.

47. Kiriluk, R. M.; Servos, M. R.; Whittle, D. M.; Cabana, G.; Rasmussen, J. B., Using ratios of stable nitrogen and carbon isotopes to characterize the biomagnification of DDE, mirex, and PCB in a Lake Ontario pelagic food web. *Canadian Journal of Fisheries and Aquatic Sciences* **1995,** *52*, (12), 2660–2674.

48. Johnson, J. H.; McKenna Jr, J. E.; Nack, C. C.; Chalupnicki, M. A., Diel diet composition and feeding activity of round goby in the dearshore region of Lake Ontario. *Journal of Freshwater Ecology* **2008,** *23*, (4), 607-612.

49. Jones, P. D.; Hu, W.; De Coen, W.; Newsted, J. L.; Giesy, J. P., Binding of perfluorinated fatty acids to serum proteins. *Environmental Toxicology and Chemistry* **2003,** *22*, (11), 2639-2649.

50. Zhang, X.; Chen, L.; Fei, X. C.; Ma, Y. S.; Gao, H. W., Binding of PFOS to serum albumin and DNA: insight into the molecular toxicity of perfluorochemicals. *Bmc Molecular Biology* **2009,** *10*, 12.

Chapter 6: Conclusions and Future Directions

The research presented in this body of work represents several demonstrations of the utility of enantiomer distribution data for a better understanding of the sources and fate of pollutants in the environment. When used appropriately, this information can be a valuable resource to policy makers who are tasked with protecting the health of humans and wildlife, from a regional to global scale. In Chapters 2, 4, and 5, enantiomer data was used to solve source apportionment problems in three different regions in North America, and with two separate classes of contaminant. Chapter 3 highlighted the importance of data handling, when working with and interpreting enantiomer distribution data.

By analyzing samples from the water column of the Hudson River Estuary and the atmosphere above it, the relative importance of fresh and historical PCB contamination to the region was determined. Sources of PCBs to the estuary were apportioned using enantiomer signatures of PCBs in air, water, total suspended matter, phytoplankton, and sediment. PCB congeners 91, 95, 136, and 149 were found to be racemic in the atmosphere of the estuary. However, water, total suspended matter, phytoplankton, and sediment contained nonracemic PCB 95, and to a lesser extent PCB 149. This data indicated that the predominant atmospheric source of these congeners was likely unweathered local pollution and not volatilization from the estuary. The similarity in chiral signatures in the other phases was consistent with dynamic contaminant exchange among them. Chiral signatures in the dissolved phase and total suspended matter were correlated with Upper Hudson discharge, suggesting that the delivery of nonracemic contaminated sediment from the Upper Hudson, not the atmosphere, controlled

phytoplankton uptake of some PCBs. These results indicated that measures to control PCB contamination in the Upper Hudson should be effective in reducing loadings to the estuary's aquatic ecosystem.

Two methods of integrating chromatographic peaks, the common valley drop method (VDM) and the deconvolution method (DM) were shown to have significantly different performance when processing both instrumental and simulated data. The VDM biased EFs by up to +6% to −4% (relative to the 0 to 1 EF scale) for symmetric peaks, and as low as −20% for asymmetric peaks. These biases tended to increase with decreasing resolution and more extreme (nonracemic) EFs. The DM, meanwhile, produced biases that were less than 1% in most cases, including at very low resolutions. The use of environmental calculations that are based on EF, such as biotransformation rate and source apportionment determinations, was shown to be dramatically affected by small errors in EF. These results suggested that a deconvolution-based integration method is preferable for the handling of enantiomer compositions, and should be implemented in future enantiomer-based studies where chromatographic separation is incomplete. Since the vast majority of existing published studies on chiral pollutants do not specify how chromatographic data is processed, caution is advised when comparing and interpreting this data.

Concentrations of PCBs surrounding the Swan Hills Treatment Centre demonstrated a profile typical of a point source, expectedly implicating the incinerator as the cause of PCB contamination to the region. Congener patterns showed a predominance of penta-, hexa-, and heptachlorinated congeners at sites

close to the SHTC, distinct from background sites. Enantiomer analysis of chiral PCBs in air and soil provided evidence for the importance of fresh versus historical releases from the incinerator. This analysis revealed racemic profiles in air for all congeners, while EFs in soil were significantly nonracemic for PCB 95, indicative of significant microbial degradation of this congener in soil. Furthermore, this dichotomy of racemic signatures in air and nonracemic signatures in soil suggested that the primary source of PCBs to the local atmosphere has been recent and continual releases from the SHTC, and not the release of weathered PCBs previously deposited to local soils. EFs for PCBs 95 and 149 were also used to estimate minimum biotransformation half lives of 25 and 97 years, respectively, which suggested an expected gradual decline in the region's PCB load once fresh inputs cease.

Concentrations of PFOS and PFOSA, their isomer profiles, and EFs of 1m-PFOS were determined in aquatic organisms, water and sediment of Lake Ontario to determine the importance of precursors to the aquatic food web's load of PFOS. Concentrations of PFOS and PFOSA were highest in slimy sculpin and Diporeia, consistent with previous studies, and concentrations of the two compounds were correlated in several species. All biotic samples were enriched (>90%) in linear PFOS, providing further evidence of the enhanced capacity of these organisms to eliminate branched PFOS isomers. Racemic 1*m*-PFOS was detected in sediment and water, and some forage fish such as slimy sculpin and rainbow smelt, but significantly nonracemic signatures were found in all invertebrate species as well as lake trout. Furthermore, EFs were found to be

correlated with the relative concentrations of PFOS and PFOSA. Since the transformation of PFOS precursors to PFOS is known to be enantioselective, the observations presented here were strongly suggestive that PFOS precursors do, to some extent, contribute to PFOS in the Lake Ontario foodweb.

By many metrics, efforts to reduce human and wildlife exposure to POPs have been successful, as evidenced by falling concentrations of legacy pollutants such as DDT and PCBs in air, water, and biota over the past three-plus decades. This can be largely attributed to national, and international, or occasionally manufacture-led agreements to stop the production, and eventually the use of the most troublesome POPs. Yet despite this apparent success, at many sites, exposures to POPs exceed levels that risk assessors deem to be safe, highlighting an ever present need to identify sources of contaminant. Evolving global circumstances, including a changing climate, a growing scarcity of water and energy, and the continuous introduction of new chemicals into human use are expected to put even greater pressure on scientists to identify those sources of chemicals that adversely affect human and ecological health. The use of chirality for source apportionment should be regarded as a powerful yet complimentary analytical tool to other environmental assessment techniques to help overcome these challenges.

For compounds like HCH and PCBs, established enantiospecific analytical methods and a good understanding of their environmental behavior have enabled researchers to exploit chirality as an effective marker of air-surface exchange.

Expansion of this technique beyond the research laboratory and into the sphere of routine environmental assessment will likely require successful demonstration in a wider range of compounds. A broader application of enantiomer analysis is hampered by several factors. Clearly, significant improvements in analytical methods are necessary before the study of chiral PFOS isomers can be made in greater detail. The study of the precursor contribution to PFOS concentrations in the arctic would benefit greatly from a similar enantiomer analysis to the one presented in Chapter 5, but the current analytical method is not sensitive enough for an effective analysis at the expectedly low concentrations. Analytical methods for other emerging contaminant classes, such as chiral pharmaceuticals and pyrethroid pesticides, are sufficiently sensitive, but our understanding of the fate of their enantiomers in the environment, including possible enantiomerization, requires further investigation. Furthermore, while the movement of enantiomerically stable legacy contaminants, like PCBs, in the abiotic environment are well understood, the enantiomer distributions of chiral compounds through food webs is often difficult to predict and interpret. A more detailed investigation of chiral contaminants through biological systems, including predator-prey relationships, is warranted to fully take advantage of chirality for source tracking through food webs.

Appendices

Table A-2-1: *Hourly Meteorological data from Newark International Airport, NJ during 14 sampling dates between 1999-2000. WD and WS represent wind direction and wind speed, respectively. VRB indicates a variable wind direction.*

Date	Time	Temp	Rel. Hum.	WD	WS		Date	Time	Temp	Rel. Hum.	WD	WS
	(CST)	(deg C)	(%)	(deg)	(m/s)			(CST)	(deg C)	(%)	(deg)	(m/s)
10/20/99	751	11.1	97	50	3.1		08/23/00	751	20.0	78	200	4.6
10/20/99	851	11.7	93	50	3.1		08/23/00	851	21.1	79	200	5.1
10/20/99	951	11.7	93	330	4.1		08/23/00	951	22.2	71	200	7.2
10/20/99	1051	12.2	90	350	3.1		08/23/00	1051	23.9	64	190	6.2
10/20/99	1151	12.2	90	340	2.1		08/23/00	1151	23.9	62	200	6.7
10/20/99	1251	12.2	90	20	3.1		08/23/00	1251	23.9	64	200	5.1
10/20/99	1351	12.8	87	340	3.1		08/23/00	1351	22.2	76	200	4.6
10/20/99	1451	12.8	87	260	3.6		08/23/00	1451	22.2	76	190	4.6
10/20/99	1551	12.8	83	330	3.6		08/23/00	1551	22.2	76	200	4.6
10/20/99	1651	12.8	77	340	3.6		08/23/00	1651	21.1	87	190	5.1
12/3/99	751	3.9	45	250	4.1		10/25/00	751	13.9	83	20	3.6
12/3/99	851	5.0	39	240	4.1		10/25/00	851	16.7	73	40	3.6
12/3/99	951	6.1	37	260	4.6		10/25/00	951	17.8	73	40	4.1
12/3/99	1051	8.3	31	260	3.1		10/25/00	1051	20.0	66	50	3.1
12/3/99	1151	11.1	26	270	3.1		10/25/00	1151	21.1	61	120	2.6
12/3/99	1251	12.2	25	250	3.6		10/25/00	1251	21.1	64	VRB	2.1
12/3/99	1351	12.8	28	230	3.1		10/25/00	1351	20.6	61	160	4.1
12/3/99	1451	13.3	29	240	3.6		10/25/00	1451	19.4	61	160	5.1
12/3/99	1551	13.3	30	250	3.6		10/25/00	1551	18.9	65	160	3.1
12/3/99	1651	12.8	34	210	2.6		10/25/00	1651	17.8	70	160	1.5
04/19/00	951	8.9	80	10	7.2		10/26/00	751	12.8	100	VRB	1.5
04/19/00	1051	9.4	77	40	5.7		10/26/00	851	13.3	100	VRB	1.5
04/19/00	1151	11.7	66	20	6.2		10/26/00	951	15.0	90	0	0.0
04/19/00	1251	12.8	67	40	6.2		10/26/00	1051	17.8	73	0	0.0
04/19/00	1351	14.4	62	40	5.7		10/26/00	1151	18.9	59	VRB	2.1
04/19/00	1451	15.6	60	60	4.6		10/26/00	1251	19.4	63	210	1.5
04/19/00	1551	16.1	58	80	3.6		10/26/00	1351	20.6	53	150	2.1
04/19/00	1651	16.7	56	40	5.7		10/26/00	1451	20.6	53	160	3.6
							10/26/00	1551	19.4	55	VRB	2.1
04/20/00	851	13.9	62	VRB	2.1		10/26/00	1651	18.3	59	160	2.6
04/20/00	951	14.4	60	VRB	2.1							
04/20/00	1051	15.6	58	110	3.6		10/27/00	751	12.8	96	50	2.6
04/20/00	1151	15.6	60	150	3.1		10/27/00	851	13.9	93	40	2.6
04/20/00	1251	15.6	60	190	3.6		10/27/00	951	15.0	90	80	2.1
04/20/00	1351	16.1	58	130	2.6		10/27/00	1051	16.1	87	10	2.1
04/20/00	1451	14.4	62	130	3.1		10/27/00	1151	17.2	78	360	2.6
04/20/00	1551	13.3	67	160	3.6		10/27/00	1251	18.3	78	VRB	1.5
04/20/00	1651	13.3	67	140	2.6		10/27/00	1351	19.4	68	0	0.0
							10/27/00	1451	20.0	68	110	2.1
04/21/00	751	9.4	90	120	4.6		10/27/00	1551	19.4	71	40	2.6
04/21/00	851	9.4	90	120	4.6		10/27/00	1651	18.3	76	50	2.1
04/21/00	951	9.4	93	120	5.7							

04/21/00	1051	9.4	93	110	7.7		04/24/01	751	20.0	70	240	5.1
04/21/00	1151	8.9	96	100	5.7		04/24/01	851	22.8	62	260	5.1
04/21/00	1251	9.4	93	80	5.7		04/24/01	951	24.4	56	250	5.1
04/21/00	1351	9.4	93	60	3.1		04/24/01	1051	27.2	47	240	7.2
04/21/00	1451	8.9	96	60	7.2		04/24/01	1151	28.9	38	250	8.7
04/21/00	1551	8.3	93	60	8.7		04/24/01	1251	29.4	36	240	11.3
04/21/00	1651	8.3	90	70	9.3		04/24/01	1351	30.6	31	270	9.3
							04/24/01	1451	30.6	32	260	10.3
08/21/00	751	17.2	56	30	5.1		04/24/01	1551	29.4	37	300	11.8
08/21/00	851	18.3	54	20	4.1		04/24/01	1651	23.9	40	280	11.8
08/21/00	951	20.0	45	360	3.6							
08/21/00	1051	21.1	46	20	4.6		04/25/01	751	8.9	48	10	6.7
08/21/00	1151	21.7	44	30	3.1		04/25/01	851	9.4	41	40	7.7
08/21/00	1251	23.3	41	VRB	2.1		04/25/01	951	10.0	38	50	7.2
08/21/00	1351	23.9	40	350	3.6		04/25/01	1051	10.6	36	40	6.7
08/21/00	1451	23.9	42	330	4.1		04/25/01	1151	10.6	36	20	6.2
08/21/00	1551	23.9	40	300	4.1		04/25/01	1251	11.1	35	40	6.2
08/21/00	1651	23.3	40	330	3.6		04/25/01	1351	12.2	33	70	4.1
							04/25/01	1451	12.8	30	70	3.1
08/22/00	751	19.4	66	0	0.0		04/25/01	1551	12.8	29	50	5.1
08/22/00	851	21.7	58	0	0.0		04/25/01	1651	12.2	31	50	3.1
08/22/00	951	23.3	50	VRB	2.6							
08/22/00	1051	23.9	48	240	5.7		04/26/01	751	11.7	37	60	5.1
08/22/00	1151	25.0	47	280	3.6		04/26/01	851	13.3	28	60	5.7
08/22/00	1251	25.0	47	230	4.1		04/26/01	951	13.9	27	40	6.7
08/22/00	1351	25.0	48	230	5.1		04/26/01	1051	14.4	25	90	5.7
08/22/00	1451	25.6	45	240	4.6		04/26/01	1151	15.6	25	90	5.1
08/22/00	1551	24.4	56	180	4.6		04/26/01	1251	15.6	26	20	4.6
08/22/00	1651	24.4	56	160	5.1		04/26/01	1351	16.1	24	VRB	2.6
							04/26/01	1451	15.6	27	150	3.6
							04/26/01	1551	15.0	29	170	5.1
							04/26/01	1651	14.4	26	160	4.6

Table A-2-2: *Sampling dates, locations, and enantiomer fractions of four PCB congeners in air samples from the Hudson River Estuary.*

sampling date YYMMDD	sampling location	Enantiomer fraction			
		PCB 95	**PCB 91**	**PCB 136**	**PCB 149**
010424	CAO	0.492	nd	nd	0.529
010424	CAO	nd	nd	nd	0.525
010426	CAO	0.502	nd	nd	nd
010426	CAO	0.471	nd	nd	nd
000420	HRE	0.471	nd	nd	0.498
000822	HRE	0.500	nd	nd	0.507
001025	HRE	0.497	nd	nd	0.517
001025	HRE	0.487	nd	nd	0.497
001025	HRE	0.501	0.505	0.484	0.512
001026	HRE	0.482	nd	nd	0.514
001026	HRE	0.518	nd	nd	nd
001027	HRE	0.512	0.492	0.512	0.506
001027	HRE	0.499	0.496	0.507	0.495
001027	HRE	0.497	0.503	0.506	0.510
001027	HRE	0.500	0.502	0.493	0.500
010424	HRE	0.484	nd	nd	nd
001025	JC	0.495	0.487	0.501	0.498
001026	JC	0.500	0.488	0.494	0.506
010424	JC	0.504	0.495	0.492	0.498
010425	JC	0.508	nd	nd	0.472
991020	JC	0.495	nd	0.484	0.507
000812	SH	0.500	0.484	nd	0.488
000821	SH	0.494	0.497	0.495	0.507
001025	SH	0.505	nd	0.499	0.496
001026	SH	0.503	0.483	0.494	0.472
001027	SH	0.475	0.467	0.498	0.514
mean		**0.496**	**0.492**	**0.497**	**0.503**
S.D.		**0.012**	**0.011**	**0.008**	**0.014**

Table A-2-3: *Sampling dates, locations, and enantiomer fractions of four PCB congeners in water and phytoplankton samples from the Hudson River Estuary.*

sampling date YYMMDD	sampling location	Enantiomer fraction			
		PCB 95	PCB 91	PCB 136	PCB 149
water					
000420	HRE	0.445	nd	nd	0.527
000821	HRE	0.478	nd	nd	nd
000821	HRE	0.465	nd	nd	0.496
000822	HRE	0.491	nd	nd	nd
000822	HRE	0.483	nd	nd	0.507
000822	HRE	0.469	nd	nd	nd
000823	HRE	0.488	nd	nd	nd
001025	HRE	0.470	nd	nd	nd
001026	HRE	0.488	nd	nd	0.487
001027	HRE	0.462	nd	nd	nd
010424	HRE	0.454	nd	nd	nd
mean		**0.472**	**-**	**-**	**0.504**
S.D.		**0.015**	**-**	**-**	**0.017**
phytoplankton					
000420	HRE	0.464	nd	nd	0.546
000424	HRE	0.474	nd	nd	0.536
001025	HRE	0.472	nd	nd	0.500
001025	HRE	0.481	nd	0.481	0.515
001026	HRE	0.486	nd	nd	0.497
001027	HRE	0.491	nd	nd	0.514
mean		**0.478**	**-**	**0.481**	**0.518**
S.D.		**0.010**	**-**	**-**	**0.020**

Table A-2-4: *Sampling dates, locations, and enantiomer fractions of four PCB congeners in suspended particulate matter and sediment samples from the Hudson River Estuary.*

sampling date YYMMDD	sampling location	Enantiomer fraction PCB 95	PCB 91	PCB 136	PCB 149
suspended particulate matter					
000419	HRE	0.472	nd	nd	0.520
000420	HRE	0.463	nd	nd	0.514
000420	HRE	0.472	nd	nd	0.530
000421	HRE	0.460	nd	0.528	0.523
000821	HRE	0.475	nd	0.501	0.496
000821	HRE	0.494	nd	nd	0.506
000821	HRE	0.468	nd	nd	0.501
000822	HRE	0.478	nd	0.493	0.492
000822	HRE	0.459	nd	nd	0.520
000822	HRE	0.479	nd	nd	0.506
000822	HRE	0.481	nd	nd	0.512
000823	HRE	0.480	nd	0.523	0.494
000823	HRE	0.466	0.487	0.500	0.507
000823	HRE	0.489	0.505	0.507	0.502
001025	HRE	0.480	nd	nd	0.514
001025	HRE	0.480	nd	nd	0.499
001026	HRE	0.484	nd	nd	0.508
001026	HRE	0.460	nd	nd	0.534
001027	HRE	0.476	nd	nd	0.527
001027	HRE	0.496	nd	nd	0.510
001027	HRE	0.501	nd	nd	0.510
001027	HRE	0.465	nd	nd	0.520
010424	HRE	0.455	0.522	nd	0.524
010425	HRE	0.514	nd	nd	0.529
010426	HRE	0.470	nd	nd	0.535
010426	HRE	0.495	nd	nd	0.486
mean		**0.477**	**0.504**	**0.509**	**0.512**
S.D.		**0.014**	**0.017**	**0.014**	**0.013**
sediment					
000419	HRE	0.476	0.499	0.492	0.519
000420	HRE	0.473	nd	nd	0.527
000823	HRE	0.473	0.488	0.511	0.525
001027	HRE	0.477	0.485	0.480	0.524
mean		**0.475**	**0.491**	**0.494**	**0.524**
S.D.		**0.002**	**0.007**	**0.016**	**0.003**

Table A-2-5: *Descriptive statistics for results of sensitivity analysis for enantiomer fraction as a function of Hudson River discharge.*

Averaging (days)	TSM PCB 95		Dissolved Phase PCB 95		TSM PCB 149	
	p-value	r^2	p-value	r^2	p-value	r^2
1	0.0301	0.205	0.0802	0.302	0.386	0.0360
3	0.0295	0.206	0.0668	0.326	0.347	0.0422
5	0.0255	0.216	0.0575	0.345	0.283	0.0547
7	0.0295	0.206	0.0533	0.355	0.299	0.0513
15	0.0440	0.180	0.133	0.233	0.431	0.0298
21	0.0556	0.162	0.0901	0.286	0.287	0.0538
31	0.0434	0.180	0.0666	0.326	0.236	0.0663

Table A-4-1: *Concentration of detected PCB congeners in passive air samples (pg/m^3) in the region surrounding the Swan Hills Treatment Centre during the second sampling season.*

PCB	Sampling site													
	20	19	23	8	22	7a	7b	21	6	1	5	25	17	16
4/10	ND	ND	ND	ND	ND	ND	ND	ND	ND	ND	ND	ND	ND	ND
6	ND	ND	ND	0.11	0.24	0.14	0.15	0.47	ND	ND	ND	1.68	0.37	ND
8	ND	ND	ND	0.51	1.51	0.87	0.83	2.07	0.56	0.63	ND	5.87	1.01	ND
9	2.68	ND	ND	ND	0.24	0.85	ND	0.55	ND	ND	ND	ND	0.90	ND
27/13	ND	ND	ND	0.08	0.18	0.15	0.08	0.20	ND	0.11	ND	0.63	ND	ND
16	0.78	ND	ND	0.81	1.61	1.32	0.92	1.76	0.70	0.52	ND	8.22	1.44	0.73
17	5.46	ND	ND	0.96	2.09	1.44	1.13	2.19	0.61	0.87	ND	8.45	1.79	0.83
18	ND	0.77	ND	1.29	3.10	2.28	1.88	3.75	1.07	1.24	0.99	13.39	3.27	1.23
19	ND	ND	ND	ND	0.22	0.07	0.07	0.37	ND	ND	ND	1.18	ND	ND
22	ND	ND	ND	1.42	4.03	3.35	2.50	2.61	1.28	ND	ND	20.12	ND	ND
24	ND	ND	ND	ND	0.17	0.22	ND	ND	ND	ND	ND	1.09	ND	ND
25	ND	ND	ND	0.89	2.10	2.02	1.49	0.95	1.97	1.07	ND	3.51	3.68	0.67
26	ND	11.73	1.38	2.07	1.90	0.91	1.45	3.57	0.92	19.66	3.56	5.56	3.42	ND
28	ND	ND	ND	ND	12.69	7.98	15.40	11.82	4.12	ND	ND	46.89	5.82	2.15
31/53	2.97	12.89	ND	3.40	7.50	4.76	4.70	8.57	2.18	ND	ND	30.15	5.51	1.16
32	ND	0.82	ND	1.02	1.96	1.39	1.15	2.12	0.67	0.96	ND	11.88	2.18	0.75
33	ND	ND	ND	11.13	6.17	4.13	ND	9.79	2.74	ND	ND	20.60	20.79	1.84
40/37	1.16	ND	ND	ND	ND	ND	ND	ND	ND	ND	ND	15.33	ND	ND
41	ND	ND	ND	0.28	0.94	0.73	0.73	2.00	ND	0.56	ND	3.21	ND	ND
44	1.54	ND	ND	2.18	8.15	6.43	4.81	8.39	1.91	1.58	ND	39.74	3.68	0.92
45	ND	ND	ND	ND	1.17	ND	ND	0.97	ND	ND	ND	3.97	1.40	0.86
46	ND	ND	ND	ND	0.38	0.23	ND	ND	ND	ND	ND	1.47	ND	ND
47	0.56	ND	ND	0.50	1.95	1.43	1.58	1.86	1.86	0.58	ND	8.86	1.73	0.95
48	ND	ND	ND	0.50	0.94	0.88	0.53	0.92	0.35	0.39	ND	4.01	1.04	0.41
49	ND	ND	ND	1.18	4.34	3.57	2.47	4.36	1.27	0.52	ND	22.17	1.73	0.52

Table A-4-1: *continued*

PCB	Sampling site													
	20	19	23	8	22	7a	7b	21	6	1	5	25	17	16
52	ND	0.64	ND	2.36	9.12	6.97	5.38	10.56	1.98	1.37	ND	41.64	4.83	1.79
63	ND	ND	ND	0.22	0.53	0.58	0.41	ND	ND	0.50	ND	3.03	ND	0.62
64	ND	ND	ND	1.06	5.29	4.23	3.07	3.61	1.56	1.00	ND	23.31	ND	ND
67	ND	1.94	2.78	1.44	1.23	3.17	4.14	1.41	ND	ND	ND	8.68	ND	0.85
70	ND	ND	ND	3.34	12.21	10.00	8.02	11.75	2.76	2.24	ND	63.14	3.90	ND
71	ND	ND	ND	0.30	1.71	1.24	1.09	2.26	0.40	0.64	ND	8.01	ND	ND
74	1.69	ND	ND	1.38	5.06	4.22	ND	ND	1.50	2.00	ND	27.38	ND	3.08
75	ND	ND	ND	ND	ND	ND	ND	ND	ND	ND	ND	ND	ND	ND
77/144	ND	ND	ND	0.82	3.35	2.37	1.57	1.30	0.45	ND	ND	12.27	1.29	ND
84/56	ND	ND	ND	2.21	9.24	10.42	7.84	5.80	ND	ND	ND	60.52	9.12	2.68
85	ND	ND	ND	ND	7.48	4.92	3.77	2.65	0.70	ND	ND	31.30	6.49	ND
87	ND	ND	ND	ND	13.84	10.82	7.11	7.39	2.68	ND	ND	65.83	16.96	ND
92	ND	ND	ND	0.84	2.92	ND	ND	ND	ND	ND	ND	ND	ND	ND
95	ND	ND	ND	3.37	14.42	11.32	11.57	12.21	2.21	1.19	ND	67.06	2.60	ND
97	ND	ND	ND	ND	6.65	ND	ND	3.33	ND	ND	ND	47.95	2.44	ND
99	0.87	ND	ND	3.27	11.45	8.34	6.22	7.42	1.70	ND	ND	43.41	5.81	ND
101	2.35	ND	ND	5.67	25.80	18.10	13.79	18.40	4.28	ND	ND	101.46	6.16	ND
105/141	ND	ND	ND	ND	19.42	ND	8.18	6.60	ND	0.93	ND	ND	ND	ND
110	ND	ND	ND	5.85	26.16	18.51	14.42	16.47	4.45	ND	ND	112.65	18.64	ND
118/131	ND	ND	ND	3.16	14.30	13.63	9.25	10.13	1.57	0.91	ND	69.87	6.05	2.01
119/83	ND	17.50	ND	ND	ND	ND	ND	9.53	ND	7.26	ND	ND	ND	5.02
128/185	ND	1.63	ND	ND	6.54	2.74	2.43	ND	1.60	ND	ND	16.66	ND	ND
130	ND	ND	ND	ND	ND	2.09	0.44	ND	ND	ND	ND	2.93	ND	ND
134	ND	ND	ND	ND	2.48	2.78	1.46	ND	0.68	ND	ND	5.96	ND	ND
135	ND	ND	ND	0.99	3.68	2.60	1.26	1.91	0.35	ND	ND	13.63	ND	ND

Table A-4-1: *continued*

PCB	Sampling site													
	20	19	23	8	22	7a	7b	21	6	1	5	25	17	16
136/117	ND	ND	ND	ND	ND	ND	2.00	ND	ND	9.30	ND	ND	ND	ND
138	ND	4.66	ND	4.60	21.46	14.82	10.33	7.86	2.16	1.55	ND	67.20	ND	ND
146	ND	ND	ND	0.35	4.42	3.02	1.41	2.65	ND	ND	ND	16.15	2.46	ND
149	1.68	ND	ND	4.89	17.95	12.09	9.36	10.32	2.01	1.68	ND	69.55	5.99	1.10
151/82	1.26	ND	ND	2.57	13.50	9.66	6.53	7.76	1.63	ND	ND	51.41	9.06	ND
153/132	ND	2.58	ND	5.41	30.63	18.60	13.96	13.84	2.96	1.68	ND	105.18	9.49	2.34
156/172	ND	ND	ND	ND	5.08	ND	ND	ND	ND	ND	ND	7.73	ND	ND
158	ND	ND	ND	0.44	4.95	4.26	ND	ND	ND	ND	ND	12.45	ND	ND
163	ND	ND	ND	ND	ND	ND	ND	ND	ND	ND	ND	26.83	9.58	7.46
164	ND	ND	ND	ND	1.93	2.57	0.44	ND	ND	ND	ND	4.89	ND	ND
170	ND	2.82	ND	2.10	7.51	2.27	2.11	ND	0.41	0.27	ND	12.02	ND	1.67
174	ND	6.73	ND	4.40	6.60	3.51	2.96	5.25	1.43	ND	ND	20.68	ND	ND
177	ND	31.35	ND	1.09	4.90	2.30	3.52	1.79	0.96	ND	ND	9.83	ND	ND
179	ND	1.34	ND	1.04	2.94	2.29	1.77	3.28	ND	0.84	ND	13.23	ND	ND
180	2.85	13.96	ND	9.91	16.42	6.42	5.49	12.09	1.57	1.83	3.41	33.84	7.66	4.36
187	3.13	7.75	ND	5.01	10.41	6.87	4.43	10.01	1.12	2.11	ND	28.59	4.72	3.73
190	ND	ND	ND	1.39	1.73	0.41	ND	1.34	ND	ND	ND	3.46	ND	ND
194	ND	13.91	ND	6.69	3.24	0.58	0.96	6.72	0.74	ND	ND	4.17	ND	ND
199	ND	ND	ND	6.49	3.13	0.89	1.18	6.89	1.26	1.22	ND	4.40	0.55	1.63
202	ND	ND	ND	1.41	0.41	0.48	0.38	1.17	ND	1.41	ND	1.37	ND	ND
203	ND	15.72	ND	5.39	4.20	1.39	1.61	8.36	ND	1.22	ND	6.79	1.42	2.71
208	ND	3.30	ND	1.41	ND	ND	ND	ND	ND	ND	ND	ND	2.31	ND

Table A-4-2: *Concentration of detected PCB congeners in passive air samples (pg/m^3) in the region surrounding the Swan Hills Treatment Centre during the third sampling season.*

PCB	Sampling site											
	19	**11**	**23**	**24a**	**24b**	**8**	**22**	**17**	**25**	**7**	**6**	**1**
4/10	ND	ND	ND	ND	ND	ND	1.11	ND	0.13	ND	ND	ND
6	ND	ND	ND	ND	ND	0.46	0.91	ND	1.76	0.84	ND	ND
8	ND	0.92	0.46	0.87	ND	1.88	4.82	2.07	8.32	4.31	0.42	1.28
9	ND	1.07	ND	ND	1.28	0.42	3.26	ND	3.25	ND	ND	ND
27/13	ND	ND	ND	ND	ND	0.32	ND	0.35	0.86	ND	ND	0.29
16	ND	1.17	0.66	0.76	1.03	1.58	4.27	1.42	6.73	5.07	ND	1.49
17	0.91	1.29	ND	1.55	1.05	2.22	7.49	2.79	9.33	9.49	0.77	2.26
18	ND	ND	ND	1.57	1.15	3.59	11.21	3.59	13.70	14.31	1.11	2.71
19	ND	ND	ND	ND	ND	ND	ND	ND	0.66	0.20	ND	ND
22	1.50	2.21	1.74	1.11	2.16	2.35	9.05	3.77	17.38	11.25	1.89	3.28
24	ND	ND	ND	ND	ND	0.23	1.38	ND	0.72	1.20	ND	ND
25	ND	ND	ND	ND	ND	ND	8.25	1.42	3.90	7.81	ND	0.92
26	ND	0.94	ND	ND	0.81	2.54	2.92	1.42	5.75	4.37	0.60	ND
28	3.99	5.99	4.32	4.60	4.06	9.56	27.94	12.57	41.38	26.53	4.31	11.17
31/53	1.97	2.59	2.22	2.21	1.85	6.52	18.78	7.01	24.67	16.21	1.80	8.42
32	0.88	1.38	1.05	1.07	1.16	2.67	6.65	3.27	10.90	6.00	ND	1.91
33	ND	3.09	2.46	2.50	3.10	3.82	22.60	4.72	17.11	37.26	ND	ND
40/37	1.15	1.60	ND	ND	ND	ND	8.94	ND	8.58	10.51	ND	ND
41	ND	0.75	0.53	0.68	ND	ND	ND	0.95	4.85	ND	0.53	ND
44	1.86	3.64	2.40	2.22	ND	8.20	25.11	7.10	32.23	26.34	2.11	4.77
45	ND	0.80	0.27	ND	ND	0.62	4.14	0.79	3.87	8.40	ND	0.89
46	ND	ND	ND	ND	ND	0.63	1.40	ND	1.42	5.25	ND	ND
47	ND	ND	0.51	0.59	0.77	ND	5.22	1.82	7.03	4.90	0.67	0.76
48	ND	0.73	0.44	0.44	0.50	ND	5.48	1.27	3.54	7.63	0.61	1.07
49	0.94	1.60	1.00	ND	1.33	5.08	15.46	4.10	17.59	14.30	1.49	ND
52	1.19	ND	1.60	2.02	ND	7.49	28.82	7.16	29.89	24.30	1.47	3.39
63	ND	ND	ND	ND	ND	0.49	0.85	0.61	2.77	2.04	ND	ND
64	0.95	1.99	ND	ND	1.96	3.67	21.58	ND	20.69	18.57	1.54	2.73
67	ND	ND	ND	1.37	ND	9.73	0.95	ND	4.04	4.85	ND	0.95
70	1.40	2.67	2.10	2.37	2.23	9.03	36.13	7.01	39.45	25.29	2.31	5.24
71	0.71	ND	0.84	0.78	ND	2.16	3.68	2.08	8.32	8.56	ND	2.12
74	0.70	ND	1.08	1.04	ND	3.03	12.30	0.77	13.40	ND	ND	ND
75	ND	ND	ND	ND	ND	ND	0.95	ND	ND	ND	ND	ND
77/144	ND	0.63	0.32	ND	ND	2.02	5.55	1.14	9.72	6.43	ND	ND
84/56	ND	ND	ND	2.63	ND	8.28	33.97	4.69	46.19	24.08	ND	ND
85	ND	ND	0.45	1.35	ND	4.18	21.03	3.10	21.39	23.57	ND	2.20

Table A-4-2: *continued*

PCB	Sampling site											
	19	**11**	**23**	**24a**	**24b**	**8**	**22**	**17**	**25**	**7**	**6**	**1**
87	ND	ND	ND	ND	ND	9.29	38.20	8.07	ND	39.81	ND	6.07
92	ND	ND	ND	ND	ND	ND	ND	1.70	ND	ND	ND	0.80
95	0.97	ND	1.19	2.49	1.65	9.88	43.96	8.18	44.35	31.30	1.62	2.95
97	0.83	1.14	ND	ND	ND	ND	22.67	4.34	32.82	ND	ND	ND
99	1.23	1.50	0.82	1.62	ND	5.99	41.47	5.85	ND	33.42	1.25	1.96
101	2.41	4.57	2.79	4.36	3.96	13.97	70.87	13.05	71.61	67.15	4.07	6.11
105/141	ND	ND	1.55	2.55	ND	10.07	ND	6.15	54.82	ND	1.97	3.47
110	2.97	3.31	2.81	ND	4.05	ND	120.17	14.46	ND	70.92	ND	ND
118/131	ND	ND	ND	ND	ND	ND	ND	ND	ND	ND	ND	ND
119/83	ND	ND	ND	ND	ND	ND	ND	ND	5.56	ND	ND	ND
128/185	ND	ND	ND	ND	ND	ND	ND	5.10	ND	ND	ND	ND
130	ND	ND	ND	ND	ND	0.27	ND	ND	3.05	ND	ND	ND
134	ND	ND	0.66	ND	ND	1.02	3.89	ND	6.55	ND	1.00	ND
135	0.65	ND	0.47	ND	0.70	2.02	6.15	1.44	ND	5.44	ND	0.66
136/117	4.05	ND	1.54	1.39	1.60	3.15	ND	3.94	12.86	ND	1.69	3.56
138	4.10	ND	7.77	10.67	ND	14.60	52.23	8.62	56.16	40.18	9.98	19.62
146	ND	ND	ND	ND	ND	1.46	8.80	ND	ND	8.36	ND	ND
149	3.83	3.28	2.54	3.23	ND	9.66	45.81	8.67	50.42	40.96	2.77	4.20
151/82	1.56	2.47	1.70	1.78	2.28	7.72	27.60	5.93	42.79	23.30	1.58	2.36
153/132	ND	ND	2.71	3.81	3.43	ND	76.24	ND	79.23	43.34	2.69	5.29
156/172	ND	ND	ND	ND	ND	ND	ND	12.33	16.00	ND	ND	ND
158	ND	ND	ND	ND	ND	1.84	6.51	1.13	6.23	ND	ND	ND
163	ND	ND	ND	ND	60.93	ND	32.60	1.71	9.54	38.90	ND	20.96
164	ND	ND	ND	ND	ND	0.66	ND	ND	3.29	ND	ND	ND
170	1.79	ND	1.72	1.27	ND	5.35	16.37	3.49	18.65	14.73	ND	0.96
174	1.92	1.93	ND	2.10	1.58	ND	ND	4.07	ND	2.20	1.24	1.46
177	ND	1.28	ND	1.69	ND	ND	13.39	ND	ND	10.50	ND	1.64
179	ND	1.46	ND	ND	ND	ND	7.51	ND	ND	ND	ND	ND
180	ND	3.92	3.15	4.53	ND	10.81	32.29	7.69	ND	32.47	ND	ND
187	ND	3.53	ND	2.72	ND	ND	24.06	ND	ND	ND	ND	ND
190	ND	ND	ND	ND	ND	ND	ND	0.82	4.23	4.86	ND	ND
194	ND	ND	1.01	ND	ND	ND	ND	5.02	ND	ND	ND	ND
199	ND	ND	ND	ND	ND	ND	2.39	ND	ND	3.13	ND	ND
202	ND	ND	0.55	ND	ND	0.26	ND	ND	1.48	0.26	ND	ND
203	ND	ND	ND	ND	ND	ND	ND	ND	ND	ND	ND	ND
208	ND	ND	ND	ND	ND	ND	11.06	1.76	0.76	21.61	ND	ND

Table A-4-3: *Concentration of detected PCB congeners in passive air samples (pg/m^3) in the region surrounding the Swan Hills Treatment Centre during the fourth sampling season.*

PCB	Sampling site									
	19	12	23	24	22	22	8	17	7a	7b
4/10	ND	ND	31.16	ND	ND	ND	ND	ND	ND	ND
6	ND	ND	ND	ND	ND	ND	ND	0.25	0.17	ND
8	0.73	0.93	1.29	0.65	0.62	1.10	0.63	4.01	2.29	2.40
9	ND	ND	0.75	ND	ND	ND	ND	ND	ND	ND
27/13	ND	ND	ND	ND	ND	0.17	0.14	0.25	ND	ND
16	0.85	0.62	ND	0.60	0.86	1.28	0.88	2.26	2.10	1.02
17	ND	1.45	2.83	1.22	1.54	2.15	1.37	3.84	3.52	1.73
18	1.57	1.07	1.72	0.82	1.27	1.76	1.43	3.98	3.55	1.85
19	ND	ND	ND	ND	ND	ND	ND	0.48	ND	ND
22	1.56	0.81	ND	1.04	ND	2.58	1.44	4.13	4.14	2.40
24	ND	ND	ND	ND	ND	ND	ND	ND	ND	ND
25	ND	ND	1.22	0.12	ND	0.86	0.65	1.57	0.91	ND
26	ND	0.74	2.79	ND	ND	1.95	0.87	1.31	1.12	0.95
28	5.37	2.40	3.84	4.83	3.06	8.02	4.63	8.55	6.82	4.81
31/53	2.71	1.28	ND	2.27	1.80	4.25	2.58	5.93	4.41	3.01
32	0.85	ND	1.31	0.56	1.13	1.40	0.87	2.61	2.25	1.48
33	ND	1.07	ND	2.78	1.54	5.33	ND	5.63	4.34	2.90
40/37	ND	ND	ND	ND	ND	ND	ND	ND	ND	ND
41	ND	ND	ND	ND	ND	1.29	ND	ND	2.72	ND
44	1.38	1.43	2.30	1.18	1.95	3.56	1.94	6.33	6.43	6.75
45	ND	ND	ND	ND	ND	0.56	ND	1.33	1.26	ND
46	ND	ND	ND	ND	ND	ND	ND	0.63	ND	ND
47	ND	ND	ND	ND	0.62	0.69	ND	ND	1.50	ND
48	ND	ND	ND	ND	ND	0.52	ND	1.00	ND	ND
49	ND	0.60	ND	0.87	1.79	1.65	0.72	3.43	4.05	2.72
52	0.95	1.44	2.23	1.05	1.62	2.68	1.77	6.38	7.84	3.79
63	ND	ND	ND	ND	ND	ND	ND	ND	ND	ND
64	ND	ND	ND	1.85	0.98	3.75	2.67	2.95	4.57	3.08
67	1.22	1.68	3.64	ND	3.18	1.27	ND	ND	ND	3.01
70	ND	ND	2.03	1.21	2.25	3.77	1.80	8.41	6.68	3.03
71	ND	ND	ND	ND	0.50	ND	0.86	1.32	2.11	ND
74	0.68	ND	ND	ND	ND	1.75	ND	3.18	2.50	ND
75	ND	ND	ND	ND	0.57	ND	ND	ND	ND	ND
77/144	ND	ND	ND	ND	ND	ND	ND	1.84	ND	ND
84/56	ND	1.14	9.67	ND	ND	3.96	0.83	ND	5.58	5.74
85	ND	ND	8.15	ND	1.66	1.70	ND	4.26	2.33	2.77

Table A-4-3: *continued*

PCB	Sampling site									
	19	12	23	24	22	22	8	17	7a	7b
87	ND	ND	2.78	ND	2.26	ND	0.91	8.64	5.28	7.20
92	ND	ND	ND	ND	ND	ND	ND	ND	ND	ND
95	0.79	0.55	ND	ND	1.97	2.78	1.25	8.65	7.73	5.62
97	ND	ND	ND	ND	ND	ND	ND	ND	ND	ND
99	ND	ND	ND	ND	1.33	2.09	0.78	5.80	4.36	3.02
101	1.29	ND	ND	1.11	3.43	4.55	1.59	12.28	12.06	6.61
105/141	ND	ND	ND	ND	2.26	3.40	ND	12.39	6.04	3.80
110	1.69	ND	ND	ND	3.98	5.32	1.76	14.38	10.01	6.34
118/131	ND	ND	ND	ND	2.63	ND	ND	8.80	4.89	2.96
119/83	ND	ND	ND	ND	ND	ND	ND	1.06	ND	ND
128/185	ND	ND	ND	ND	ND	ND	ND	8.85	4.29	ND
130	ND	ND	ND	ND	ND	ND	ND	ND	ND	ND
134	ND	ND	2.42	ND	ND	ND	ND	ND	ND	ND
135	ND	ND	2.97	ND	ND	0.42	ND	ND	1.45	0.86
136/117	ND	ND	ND	ND	ND	ND	1.01	3.50	2.66	2.48
138	2.50	0.60	ND	ND	3.33	5.53	ND	16.52	10.14	5.58
146	ND	ND	ND	ND	ND	0.93	ND	ND	0.86	ND
149	9.31	0.85	1.28	ND	2.53	3.75	0.95	8.72	5.56	2.91
151/82	ND	ND	ND	ND	2.51	ND	ND	6.00	4.89	2.51
153/132	ND	0.87	ND	1.38	3.92	5.38	1.99	17.72	8.87	6.16
156/172	ND	ND	ND	ND	ND	ND	ND	6.37	ND	ND
158	ND	ND	ND	ND	ND	ND	ND	5.14	3.62	ND
163	ND	ND	ND	ND	ND	ND	ND	ND	ND	ND
164	ND	ND	ND	ND	ND	ND	ND	ND	ND	ND
170	ND	ND	ND	ND	1.37	1.01	ND	7.90	3.92	1.66
174	ND	5.78	ND	ND	3.84	ND	ND	7.39	2.99	2.03
177	ND	ND	ND	ND	ND	0.82	ND	ND	ND	ND
179	ND	ND	ND	ND	ND	1.49	ND	ND	ND	ND
180	ND	0.90	ND	ND	4.27	3.97	ND	16.10	ND	3.81
187	ND	ND	ND	ND	2.44	2.96	0.79	7.26	2.41	ND
190	ND	ND	ND	ND	ND	1.79	ND	2.68	ND	ND
194	ND	ND	ND	ND	ND	1.96	ND	4.37	ND	ND
199	ND	ND	ND	ND	1.55	0.78	ND	3.37	1.17	0.93
202	ND	ND	ND	ND	ND	ND	ND	ND	ND	ND
203	ND	ND	ND	ND	ND	ND	ND	4.95	ND	ND
208	ND	ND	ND	ND	ND	ND	ND	ND	ND	ND

Table A-4-4: *PCB homologue patterns, as fraction of total PCBs for each homologue group, and total PCB concentration for passive air samples in the region surrounding the Swan Hills Treatment Centre.*

	di	tri	tetra	penta	hexa	hepta	octa+nona	ΣPCBs ng/m^3
				2nd sampling season				
1	0.010	0.344	0.161	0.145	0.214	0.071	0.054	69.8
5	0.000	0.572	0.000	0.000	0.000	0.428	0.000	7.9
6	0.008	0.241	0.202	0.261	0.176	0.082	0.030	67.3
7a	0.007	0.108	0.158	0.347	0.281	0.087	0.012	276.6
7b	0.005	0.133	0.140	0.357	0.258	0.088	0.018	221.7
8	0.005	0.178	0.114	0.189	0.155	0.193	0.166	129.2
16	0.000	0.173	0.185	0.180	0.202	0.181	0.080	54.0
17	0.012	0.243	0.093	0.376	0.192	0.063	0.022	197.2
19	0.000	0.172	0.017	0.115	0.058	0.421	0.217	152.0
20	0.092	0.358	0.131	0.111	0.102	0.206	0.000	28.9
21	0.011	0.154	0.156	0.324	0.170	0.110	0.075	301.3
22	0.005	0.097	0.119	0.339	0.303	0.113	0.025	427.8
23	0.000	0.331	0.669	0.000	0.000	0.000	0.000	4.1
25	0.005	0.116	0.161	0.374	0.257	0.076	0.010	1604.4
				3rd sampling season				
1	0.011	0.224	0.153	0.164	0.419	0.028	0.000	139.9
6	0.008	0.196	0.201	0.167	0.406	0.023	0.000	51.5
7	0.006	0.168	0.169	0.325	0.232	0.073	0.028	892.7
8	0.014	0.159	0.227	0.279	0.247	0.073	0.001	210.8
11	0.031	0.319	0.192	0.166	0.101	0.191	0.000	63.5
17	0.011	0.185	0.149	0.307	0.248	0.071	0.030	220.5
19	0.000	0.234	0.174	0.189	0.319	0.083	0.000	44.5
22	0.009	0.121	0.152	0.368	0.249	0.088	0.013	1066.4
23	0.008	0.211	0.182	0.163	0.327	0.083	0.026	57.4
24a	0.011	0.196	0.147	0.191	0.298	0.157	0.000	75.9
24b	0.012	0.156	0.065	0.092	0.659	0.015	0.000	104.6
25	0.014	0.158	0.186	0.272	0.345	0.023	0.002	961.9
				4th sampling season				
7a	0.013	0.172	0.206	0.303	0.251	0.048	0.006	186.4
7b	0.020	0.165	0.184	0.362	0.200	0.062	0.008	117.9
8	0.021	0.397	0.263	0.192	0.106	0.021	0.000	37.1
12	0.036	0.360	0.197	0.065	0.088	0.255	0.000	26.2
17	0.015	0.136	0.118	0.257	0.293	0.139	0.043	284.7
19	0.022	0.386	0.126	0.113	0.353	0.000	0.000	33.4
22a	0.009	0.154	0.185	0.268	0.200	0.164	0.021	70.6
22b	0.012	0.268	0.195	0.216	0.176	0.109	0.025	106.9
23	0.393	0.162	0.121	0.244	0.079	0.000	0.000	84.4
24	0.027	0.605	0.262	0.047	0.058	0.000	0.000	23.5

Table A-4-5: *Concentration of detected PCB congeners in soil samples (pg/g dry weight) in the region surrounding the Swan Hills Treatment Centre.*

PCB	Sampling site										
	2	**4**	**7a**	**8a**	**10**	**11a**	**13**	**14**	**16**	**19a**	**19b**
4/10	ND	ND	ND	ND	ND	ND	ND	ND	ND	ND	ND
5	0.7	1.4	ND	0.8	ND	30.1	0.4	8.1	ND	2.1	ND
6	ND	ND	ND	ND	ND	ND	ND	1.1	ND	ND	ND
8	ND	ND	ND	ND	ND	ND	ND	ND	ND	ND	ND
9	ND	ND	ND	ND	ND	ND	ND	ND	ND	ND	5.1
27/13	ND	ND	ND	ND	ND	ND	ND	9.5	ND	ND	ND
16	ND	ND	ND	ND	ND	2.7	ND	ND	ND	12.8	ND
17	ND	1.2	ND	ND	ND	ND	ND	ND	ND	ND	ND
18	ND	ND	ND	ND	ND	1.5	ND	ND	ND	6.8	ND
19	0.6	ND	ND	ND	ND	6.8	ND	1.5	ND	ND	ND
22	ND	ND	ND	ND	ND	ND	ND	ND	ND	ND	ND
24	1.8	ND	ND	ND	ND	ND	ND	7.8	ND	ND	ND
25	ND	1.6	ND	ND	ND	ND	ND	ND	ND	ND	ND
26	ND	ND	0.8	ND	ND	ND	ND	ND	528.9	ND	2.2
28	ND	3.2	1.5	ND	ND	ND	0.4	4.8	ND	15.3	8.4
31/53	ND	1.5	1.4	ND	ND	ND	ND	1.6	379.3	ND	ND
32	ND	ND	ND	ND	ND	ND	ND	ND	ND	ND	ND
33	ND	ND	ND	ND	ND	ND	ND	ND	ND	ND	ND
40/37	ND	1.4	1.6	ND	ND	ND	ND	ND	ND	ND	ND
41	ND	ND	ND	ND	ND	ND	ND	2.6	ND	ND	ND
44	ND	4.1	ND	ND	ND	ND	ND	ND	ND	ND	ND
45	ND	ND	ND	ND	ND	ND	ND	ND	ND	ND	ND
46	ND	ND	ND	ND	ND	ND	ND	ND	ND	ND	ND
47	ND	ND	ND	ND	ND	ND	ND	ND	ND	ND	ND
48	ND	ND	ND	ND	ND	ND	ND	ND	ND	ND	ND
49	ND	3.0	3.1	0.9	ND	ND	ND	ND	ND	35.2	ND
52	ND	2.3	ND	ND	ND	ND	ND	1.9	ND	ND	ND
63	ND	ND	ND	ND	ND	ND	ND	ND	ND	ND	ND
64	ND	2.4	ND	ND	ND	ND	ND	ND	ND	ND	5.5
67	ND	ND	ND	ND	ND	ND	ND	3.0	ND	ND	ND
70	ND	ND	10.8	ND	ND	ND	ND	ND	ND	ND	ND
71	ND	ND	ND	ND	ND	ND	ND	ND	ND	ND	ND
74	ND	ND	ND	ND	ND	ND	ND	ND	ND	ND	ND
75	ND	ND	ND	ND	ND	ND	ND	ND	ND	ND	ND
77/144	ND	ND	7.1	ND	ND	ND	0.8	ND	ND	8.2	3.3
84/56	ND	ND	ND	ND	ND	ND	ND	ND	ND	ND	ND
85	ND	ND	12.2	ND	ND	ND	ND	ND	ND	ND	3.8
87	ND	ND	21.1	ND	ND	ND	ND	ND	ND	ND	8.9
92	ND	ND	4.0	ND	ND	ND	ND	ND	ND	ND	ND
95	ND	ND	7.6	ND	ND	ND	ND	ND	ND	8.1	5.4
97	ND	ND	6.4	ND	ND	ND	ND	ND	ND	ND	3.8

Table A-4-5: *continued*

PCB	Sampling site										
	2	**4**	**7a**	**8a**	**10**	**11a**	**13**	**14**	**16**	**19a**	**19b**
99	1.5	ND	15.2	1.8	ND	ND	0.8	ND	ND	ND	7.0
101	ND	6.4	28.7	2.2	3.2	ND	1.7	ND	556.9	13.8	11.1
105/141	ND	ND	73.0	5.1	ND	ND	3.3	ND	ND	ND	21.1
110	ND	ND	ND	3.2	ND	ND	3.2	6.7	ND	36.8	13.0
118/131	ND	ND	ND	ND	ND	ND	ND	ND	ND	ND	ND
119/83	ND	ND	2.5	ND	ND	ND	ND	ND	ND	ND	ND
122/124	ND	ND	ND	ND	ND	ND	ND	ND	ND	ND	1.7
123/109	ND	ND	6.6	ND	ND	ND	ND	ND	ND	ND	ND
128/185	ND	ND	46.4	ND	ND	ND	ND	ND	ND	ND	10.8
130	ND	ND	9.7	ND	1.4	ND	ND	ND	ND	ND	4.9
134	ND	2.1	7.1	ND	ND	ND	ND	ND	636.4	15.5	ND
135	ND	ND	5.5	ND	ND	ND	ND	ND	ND	ND	ND
136/117	ND	ND	9.8	2.0	ND	ND	ND	ND	ND	35.5	ND
137	ND	ND	ND	ND	ND	ND	ND	6.5	ND	ND	ND
138	ND	ND	144.8	8.3	5.1	ND	8.3	16.9	ND	ND	29.4
146	ND	ND	11.0	ND	ND	ND	ND	ND	ND	ND	5.5
149	ND	ND	40.4	3.3	1.9	3.0	2.1	10.2	690.0	ND	17.7
151/82	ND	ND	20.1	ND	ND	ND	ND	ND	ND	ND	13.0
153/132	1.6	ND	105.4	7.0	7.1	5.0	5.6	ND	588.4	36.1	38.9
156/172	ND	ND	38.2	ND	ND	ND	ND	ND	ND	ND	7.0
157	ND	ND	3.8	ND	ND	ND	ND	ND	ND	8.4	ND
158	ND	ND	16.6	ND	ND	ND	ND	ND	ND	7.4	8.0
163	ND	ND	ND	ND	ND	ND	ND	ND	ND	ND	7.1
164	ND	ND	12.7	ND	ND	ND	ND	ND	ND	ND	ND
167	ND	ND	4.3	ND	ND	ND	ND	ND	ND	ND	ND
170	ND	ND	78.2	5.3	2.1	ND	3.6	ND	ND	13.5	12.4
174	ND	1.9	49.4	ND	2.1	ND	2.8	13.6	ND	ND	8.0
175	ND	ND	1.9	ND	ND	ND	ND	ND	ND	ND	ND
177	ND	ND	26.3	ND	ND	ND	3.4	ND	ND	ND	ND
179	ND	ND	13.7	ND	ND	ND	1.5	3.8	ND	ND	7.4
180	ND	8.4	ND	8.0	ND	7.2	8.1	5.9	639.8	50.9	44.9
187	ND	ND	51.2	1.9	2.1	2.4	4.6	ND	455.5	42.9	16.9
189	ND	ND	ND	ND	ND	ND	1.1	3.0	ND	ND	4.4
190	ND	ND	19.3	ND	ND	ND	3.8	ND	ND	ND	ND
191	ND	ND	ND	ND	ND	ND	ND	ND	ND	ND	10.6
194	ND	ND	53.6	ND	1.6	3.8	3.3	ND	ND	24.0	ND
199	0.8	ND	ND	2.1	ND	ND	ND	ND	ND	ND	6.5
202	ND	ND	2.3	ND	ND	ND	ND	ND	452.5	ND	ND
203	ND	ND	ND	ND	ND	ND	3.4	ND	608.0	ND	ND
206	ND	ND	ND	ND	ND	ND	ND	ND	ND	ND	ND
208	ND	ND	2.2	ND	ND	ND	ND	ND	ND	ND	ND

Table A-4-5: *continued*

PCB	Sampling site									
	8b	**22a**	**17**	**25**	**7c**	**6**	**1**	**5**	**22b**	**22c**
4/10	ND	ND	ND	ND	ND	ND	ND	ND	ND	ND
5	18.4	4.1	ND	ND	ND	ND	0.5	0.7	1.2	ND
6	ND	ND	1.7	ND	ND	ND	ND	0.2	ND	ND
8	ND	ND	5.8	ND	2.2	3.8	ND	0.8	3.8	5.2
9	ND	ND	ND	ND	ND	ND	ND	ND	ND	ND
27/13	ND	ND	0.7	ND	ND	ND	ND	ND	ND	ND
16	5.3	ND	4.1	4.8	3.0	ND	ND	0.5	4.0	5.5
17	11.0	3.3	9.3	ND	ND	2.9	ND	ND	7.1	9.4
18	13.3	3.6	9.3	2.9	ND	3.7	ND	0.9	7.4	14.8
19	3.6	2.1	1.3	1.6	ND	ND	ND	ND	ND	ND
22	ND	ND	18.1	7.5	ND	ND	ND	ND	ND	ND
24	ND	ND	4.7	ND	ND	ND	ND	ND	ND	ND
25	ND	ND	7.4	ND	ND	ND	ND	ND	ND	11.2
26	ND	ND	7.9	ND	5.7	1.0	2.3	ND	5.8	5.1
28	29.5	23.7	66.2	7.9	23.7	34.6	ND	ND	ND	176.6
31/53	11.1	16.3	38.9	4.0	14.0	15.0	ND	2.9	15.1	76.3
32	ND	4.0	2.7	ND	ND	ND	ND	ND	3.0	7.3
33	ND	5.3	ND	4.8	ND	ND	ND	ND	ND	ND
40/37	ND	ND	22.5	15.0	21.6	19.8	5.1	4.4	14.4	38.3
41	ND	ND	11.8	ND	27.7	15.5	1.0	ND	4.7	ND
44	12.2	11.1	40.4	15.5	14.4	24.3	ND	3.1	18.5	39.5
45	ND	ND	ND	ND	ND	ND	ND	ND	1.8	ND
46	ND	ND	ND	ND	ND	ND	ND	ND	ND	ND
47	ND	ND	7.6	ND	ND	6.2	ND	ND	ND	ND
48	ND	ND	ND	ND	ND	ND	ND	ND	ND	ND
49	13.1	23.1	33.2	2.6	39.6	41.2	29.3	ND	10.8	37.5
52	21.0	17.6	40.7	ND	59.2	48.2	ND	ND	16.9	30.2
63	ND	ND	7.0	ND	4.0	0.6	ND	ND	ND	8.5
64	ND	13.5	25.9	6.8	25.4	23.7	4.1	3.0	18.6	45.1
67	ND	ND	1.6	8.7	ND	ND	ND	ND	ND	ND
70	ND	ND	104.3	22.2	ND	129.2	ND	7.7	46.4	263.7
71	ND	ND	10.9	ND	38.2	15.0	0.6	ND	2.5	4.7
74	ND	15.4	49.0	ND	ND	ND	ND	ND	ND	127.4
75	ND	ND	ND	ND	19.5	ND	ND	ND	ND	ND
77/144	54.2	22.4	67.3	ND	56.8	72.9	ND	13.8	38.1	143.0
84/56	55.4	ND	ND	38.6	68.2	77.2	ND	ND	ND	ND
85	111.0	38.4	135.7	15.6	126.5	174.8	9.6	27.7	82.9	211.9
87	125.1	66.4	222.5	39.4	ND	255.2	9.1	37.0	105.6	349.4
92	ND	12.1	29.9	ND	70.5	44.8	3.2	5.4	28.0	99.6
95	ND	32.8	75.1	ND	75.5	146.8	4.4	15.5	40.7	161.1
97	24.1	23.7	90.1	18.9	69.0	95.9	2.6	13.7	44.2	114.2

Table A-4-5: *continued*

PCB	Sampling site									
	8b	**22a**	**17**	**25**	**7c**	**6**	**1**	**5**	**22b**	**22c**
99	75.6	44.4	147.8	ND	102.9	162.9	16.4	33.5	90.4	308.9
101	106.7	94.5	245.5	44.7	257.1	274.4	27.1	52.6	147.2	566.0
105/141	483.1	220.2	741.5	148.3	740.0	787.6	60.5	126.4	389.3	ND
110	325.8	144.3	414.1	117.0	ND	532.9	ND	70.5	ND	734.5
118/131	520.7	ND	562.0	ND	786.4	704.3	ND	ND	ND	1246.6
119/83	ND	8.4	ND	ND	15.2	28.7	ND	4.2	15.5	ND
122/124	10.0	4.6	14.9	ND	21.2	28.6	0.7	2.6	8.3	ND
123/109	37.5	15.5	58.3	5.1	48.7	59.3	2.9	10.0	28.5	72.2
128/185	ND	131.6	373.8	111.8	375.0	479.1	37.5	91.2	217.2	875.3
130	52.7	19.7	76.9	9.3	79.3	91.9	3.9	14.7	44.1	202.5
134	49.7	16.2	28.3	ND	38.6	40.6	8.1	6.9	20.7	115.0
135	27.7	21.9	64.3	ND	77.7	87.5	ND	17.1	45.0	175.8
136/117	ND	30.6	63.7	ND	97.9	83.2	19.8	22.1	63.9	ND
137	94.6	15.3	79.2	19.0	66.6	84.8	8.4	19.2	37.7	172.4
138	597.4	648.1	1374.6	ND	1440.2	1588.6	ND	245.9	803.2	3219.6
146	71.3	44.3	156.0	ND	ND	165.1	ND	32.5	ND	366.5
149	248.8	131.6	379.6	70.7	327.8	479.0	32.0	83.1	206.9	734.2
151/82	125.5	79.1	208.4	ND	199.7	270.9	ND	43.9	123.8	409.2
153/132	528.1	302.0	911.8	128.6	1017.4	1059.2	74.7	190.8	443.3	2098.8
156/172	239.7	130.0	358.5	54.4	363.7	398.8	20.8	ND	204.2	837.6
157	30.0	ND	36.6	18.4	ND	55.7	3.8	ND	23.1	107.2
158	59.2	ND	187.6	14.0	201.7	263.2	8.8	27.6	134.0	499.6
163	ND	ND	ND	ND	ND	ND	ND	ND	ND	ND
164	ND	20.4	92.7	ND	94.6	130.1	7.0	16.5	52.7	282.9
167	18.1	15.8	64.2	1.3	55.7	67.3	3.8	10.0	29.3	155.6
170	412.5	265.7	691.8	115.6	772.2	864.0	51.5	147.5	352.7	1817.7
174	223.1	160.3	455.0	70.2	ND	570.8	ND	97.1	373.3	1085.1
175	11.2	4.8	27.6	ND	24.8	39.9	1.3	3.9	9.6	64.4
177	164.6	103.7	263.4	39.5	ND	311.7	ND	53.6	ND	623.8
179	77.3	36.6	95.4	9.9	ND	132.7	ND	24.5	ND	237.1
180	619.7	494.1	1184.7	92.7	1500.9	1457.0	91.0	237.6	591.6	3131.3
187	288.2	156.3	435.5	34.0	ND	511.8	ND	91.7	ND	1019.5
189	ND	13.0	25.7	14.4	13.3	39.5	ND	2.3	ND	77.2
190	101.0	56.3	154.4	ND	185.1	223.9	8.9	38.3	119.3	505.7
191	11.4	14.4	31.4	ND	41.1	53.6	7.6	8.2	8.7	118.7
194	362.7	173.4	385.3	30.2	443.8	457.7	27.8	81.9	249.0	1049.1
199	138.9	95.3	225.6	ND	ND	302.7	16.8	56.8	ND	665.2
202	5.3	6.9	26.4	ND	26.8	39.9	2.7	3.2	14.0	75.4
203	ND	ND	324.9	ND	ND	ND	ND	ND	ND	884.2
206	ND	41.6	99.2	ND	136.3	110.4	ND	21.2	61.1	270.7
208	31.2	5.0	19.8	ND	27.3	19.9	2.1	5.0	ND	48.1

Table A-4-5: *continued*

PCB	Sampling site						
	11b	**23**	**24**	**7d**	**7e**	**7f**	**8c**
4/10	ND	ND	ND	ND	ND	ND	ND
5	22.3	3.3	7.8	2.2	ND	ND	ND
6	ND	1.1	ND	ND	ND	ND	ND
8	ND	ND	4.1	ND	2.4	ND	6.0
9	ND	ND	1.0	ND	ND	ND	ND
27/13	ND	ND	ND	ND	ND	ND	ND
16	3.4	ND	12.7	1.3	ND	4.0	4.3
17	2.3	2.1	13.1	5.6	8.3	5.5	9.7
18	1.3	ND	16.2	3.2	7.1	7.2	9.4
19	5.4	1.4	ND	0.9	ND	ND	ND
22	ND	ND	ND	ND	ND	ND	ND
24	ND	ND	ND	ND	ND	ND	ND
25	ND	ND	ND	3.3	ND	ND	ND
26	0.9	2.5	7.4	ND	3.1	ND	ND
28	1.5	0.8	38.0	ND	90.3	113.3	54.4
31/53	ND	1.2	49.6	9.2	42.0	48.5	32.1
32	ND	ND	6.0	ND	ND	ND	7.4
33	ND	ND	ND	ND	ND	ND	ND
40/37	ND	2.3	16.5	2.2	41.1	36.4	11.4
41	ND	ND	ND	ND	ND	ND	10.5
44	ND	ND	15.6	6.7	36.2	27.0	26.7
45	ND	ND	ND	ND	ND	ND	ND
46	ND	ND	ND	ND	ND	ND	ND
47	ND	ND	ND	ND	ND	10.8	4.5
48	ND	ND	ND	ND	ND	ND	ND
49	ND	ND	60.5	6.7	84.7	99.4	94.5
52	ND	ND	33.6	5.9	84.3	116.5	21.3
63	ND	ND	ND	ND	4.0	ND	9.3
64	ND	2.0	ND	3.3	53.5	35.3	19.4
67	ND	ND	37.8	ND	ND	ND	4.1
70	ND	ND	ND	9.8	142.3	197.4	138.7
71	ND	5.5	23.4	1.7	44.6	9.2	10.9
74	ND	ND	ND	2.8	77.4	92.2	72.2
75	ND	ND	ND	ND	ND	17.8	8.8
77/144	3.6	ND	11.3	6.7	52.6	93.1	69.9
84/56	ND	ND	84.0	ND	ND	ND	ND
85	5.9	ND	27.0	11.7	148.9	198.4	161.4
87	ND	ND	100.3	ND	236.0	309.2	233.0
92	ND	ND	ND	ND	51.4	71.4	51.1
95	ND	ND	ND	8.3	113.4	122.6	84.6
97	6.1	ND	16.1	4.1	95.1	125.5	87.8

Table A-4-5: *continued*

PCB	Sampling site						
	11b	**23**	**24**	**7d**	**7e**	**7f**	**8c**
99	ND	2.9	51.4	11.9	175.3	226.4	163.1
101	ND	4.2	64.5	23.1	312.7	409.3	300.9
105/141	1.7	5.3	262.3	32.5	919.5	1184.5	739.3
110	4.8	4.7	ND	ND	400.2	528.4	401.1
118/131	ND	ND	ND	ND	706.6	878.8	1370.7
119/83	ND	ND	ND	11.8	ND	ND	24.3
122/124	ND	ND	4.1	ND	9.6	10.8	12.0
123/109	ND	ND	14.8	ND	65.7	73.5	70.8
128/185	ND	4.2	99.1	17.3	488.7	637.8	449.8
130	ND	4.7	65.7	4.5	112.6	150.7	93.4
134	ND	5.5	51.4	5.5	43.2	44.2	39.6
135	ND	ND	15.0	ND	74.1	108.4	79.8
136/117	ND	13.7	ND	ND	90.3	116.4	95.1
137	ND	1.9	36.1	4.9	87.5	118.4	84.1
138	8.0	ND	515.9	64.3	1572.6	2117.4	1555.4
146	ND	ND	24.7	ND	181.4	245.0	150.5
149	5.1	ND	134.9	27.2	355.3	429.3	385.3
151/82	5.0	ND	85.1	18.3	219.3	291.3	219.4
153/132	6.8	ND	301.5	70.5	856.2	1165.3	943.5
156/172	ND	ND	147.5	ND	579.6	722.9	433.7
157	ND	ND	ND	ND	134.6	165.3	64.3
158	ND	ND	22.0	13.5	268.5	358.1	271.1
163	ND	ND	ND	ND	ND	ND	ND
164	ND	ND	ND	7.1	143.1	181.6	112.2
167	ND	ND	ND	3.8	80.3	117.7	69.5
170	7.0	11.0	186.7	39.1	865.6	1144.1	831.3
174	13.4	4.6	193.5	48.0	533.2	747.9	ND
175	ND	ND	13.3	ND	52.8	50.4	43.6
177	ND	ND	148.8	ND	360.2	449.6	ND
179	ND	ND	ND	ND	151.2	210.1	ND
180	7.6	ND	419.3	ND	1473.2	2087.8	ND
187	4.1	6.5	165.6	37.3	544.5	750.7	495.1
189	ND	ND	ND	ND	29.0	ND	ND
190	ND	4.3	76.9	8.4	167.8	245.5	231.0
191	ND	ND	ND	8.4	ND	76.5	ND
194	10.9	ND	309.9	25.0	518.9	727.1	497.5
199	ND	ND	52.8	ND	264.0	359.2	ND
202	ND	ND	ND	2.2	46.4	57.3	32.6
203	4.6	ND	ND	ND	498.2	ND	ND
206	8.6	ND	ND	ND	ND	243.5	ND
208	5.0	ND	ND	ND	244.3	25.5	18.3

Table A-4-6: *PCB homologue patterns, as fraction of total PCBs for each homologue group, and total PCB concentration for soil samples in the region surrounding the Swan Hills Treatment Centre.*

Sample site	di	tri	tetra	penta	hexa	hepta	octa+nona	ΣPCBs ng/g dry wgt.
2	0.095	0.343	0.000	0.214	0.237	0.000	0.110	0.01
4	0.035	0.183	0.322	0.156	0.255	0.205	0.000	0.04
7a	0.000	0.004	0.016	0.179	0.685	0.141	0.005	0.98
8a	0.015	0.000	0.018	0.238	0.542	0.190	0.040	0.05
10	0.000	0.000	0.000	0.120	0.862	0.138	0.000	0.03
11a	0.481	0.176	0.000	0.000	0.129	0.214	0.000	0.06
13	0.006	0.007	0.000	0.157	0.442	0.359	0.055	0.06
14	0.085	0.231	0.069	0.062	0.436	0.117	0.000	0.11
16	0.000	0.164	0.000	0.101	0.446	0.198	0.192	5.54
18	0.022	0.247	0.000	0.156	0.383	0.268	0.000	7.04
19a	0.006	0.093	0.094	0.179	0.349	0.315	0.000	0.37
19b	0.015	0.030	0.015	0.219	0.497	0.238	0.018	0.35
11b	0.154	0.102	0.000	0.152	0.312	0.156	0.126	0.15
23	0.046	0.083	0.103	0.178	0.521	0.113	0.000	0.10
24	0.003	0.035	0.046	0.153	0.525	0.240	0.013	4.05
8b	0.003	0.011	0.007	0.283	0.467	0.219	0.026	6.66
22a	0.001	0.014	0.020	0.170	0.552	0.230	0.036	4.10
17	0.001	0.014	0.029	0.223	0.508	0.189	0.057	12.24
25	0.000	0.025	0.052	0.309	0.514	0.133	0.000	1.37
7b	0.000	0.004	0.022	0.227	0.541	0.211	0.018	10.34
6	0.000	0.004	0.023	0.233	0.526	0.201	0.033	14.31
1	0.001	0.004	0.065	0.215	0.505	0.219	0.035	0.62
5	0.001	0.002	0.009	0.186	0.560	0.227	0.040	2.13
22b	0.001	0.008	0.025	0.178	0.623	0.178	0.014	5.43
22c	0.000	0.011	0.022	0.147	0.540	0.229	0.072	26.84
22d	0.000	0.009	0.021	0.211	0.508	0.205	0.066	38.55
7c	0.004	0.040	0.068	0.169	0.619	0.136	0.004	0.58
7d	0.000	0.010	0.038	0.213	0.498	0.192	0.070	15.05
7e	0.000	0.009	0.033	0.216	0.514	0.213	0.036	19.20
8c	0.001	0.010	0.037	0.318	0.550	0.106	0.004	11.52

Table A-4-7: *Enantiomer fractions of chiral PCB congeners in passive air samples, by sampling season.*

Sample site	PCB 95	PCB 91	PCB 136	PCB 149
Sampling Season 1				
5	0.488	ND	ND	ND
6	0.479	ND	ND	0.517
7	0.500	0.491	0.488	0.499
8	0.514	ND	ND	0.512
9	ND	ND	ND	0.478
10	0.511	ND	ND	ND
11	ND	ND	ND	0.484
13	ND	ND	ND	0.503
14	0.460	ND	0.470	0.501
Sampling Season 2				
6	0.519	ND	ND	0.499
7a	0.502	0.512	0.521	0.503
7b	0.504	ND	0.517	0.512
7c	0.504	0.497	0.502	0.506
8	0.497	ND	ND	0.498
21	0.511	ND	ND	ND
22	0.501	0.501	0.521	0.506
25	0.502	0.505	0.493	0.507
Sampling Season 3				
1	0.452	ND	ND	0.499
6	0.418	ND	ND	0.495
7a	ND	ND	ND	0.476
7b	0.465	ND	0.509	0.507
8	0.502	0.507	0.489	0.523
11	ND	ND	ND	0.509
17	0.465	ND	ND	ND
19	ND	ND	ND	0.492
22	ND	ND	ND	0.508
23	0.514	ND	0.488	0.512
24a	0.471	ND	ND	0.495
24b	ND	ND	ND	0.514
Sampling Season 4				
7a	0.507	0.507	0.516	0.504
7b	0.513	ND	ND	0.495
8	0.544	ND	ND	ND
17	0.506	0.481	0.462	0.512
22a	0.507	ND	ND	0.501
22b	0.506	ND	ND	ND

Table A-4-8: *Enantiomer fractions of chiral PCB congeners in Swan Hills soil samples.*

Sample site	PCB 95	PCB 91	PCB 136	PCB 149
1	ND	ND	0.515	0.573
5	0.383	ND	ND	0.504
6a	0.384	ND	ND	0.501
6b	0.462	0.520	0.473	0.510
7a	0.451	0.492	0.477	0.510
7b	0.444	0.489	0.494	0.513
7c	0.443	0.479	0.513	0.518
7d	0.431	ND	0.518	0.523
7e	0.442	ND	0.515	0.525
8a	0.465	0.515	0.495	0.510
8b	0.363	ND	ND	0.485
13	0.442	ND	ND	0.514
16	0.489	ND	ND	0.489
17a	0.436	ND	ND	0.502
17b	0.455	0.487	0.516	0.503
17c	ND	ND	ND	0.482
22a	0.433	0.504	0.492	0.516
22b	0.438	0.501	0.488	0.510
22c	ND	0.490	0.473	0.514
24a	ND	ND	ND	0.549
24b	ND	ND	ND	0.570
25	0.482	ND	ND	0.523
Mean	**0.498**	**0.516**	**0.497**	**0.438**
S.D.	**0.014**	**0.023**	**0.018**	**0.034**

Table A-5-1: *Sampling details for Lake Ontario fish samples. NOTL = Niagara-On-The Lake, PH = Port Hope - Cobourg*

Sample number	Species	Location	Collection date (2008)	Sex/ age (y)	Total Length (cm)	Total Weight (g)	Fork length (cm)
53402	Lake trout	NOTL	09/09	F/3	50	1455.7	45.5
53403	Lake trout	NOTL	09/09	F/7	69	3575.8	64.1
53404	Lake trout	NOTL	09/09	M/6	70.3	4367.6	65
53405	Lake trout	NOTL	09/09	F/6	73	5681	67.1
53406	Lake trout	NOTL	09/09	F/6	62.5	3446.6	58
53407	Lake trout	NOTL	09/09	M/15	68	3293.9	63.5
53408	Lake trout	NOTL	09/09	M/5	69	3418.7	64.5
53409	Lake trout	NOTL	09/09	M/7	72.5	4183.5	67
53410	Lake trout	NOTL	09/09	F/5	59.5	3244.2	55
53411	Lake trout	NOTL	09/09	F/6	66.6	3615.7	63.5
54475	Slimy sculpin	PH	23/09		7.6		5.2
54476	Slimy sculpin	PH	23/09		8		6.5
54477	Slimy sculpin	PH	23/09		8.4		7.4
54478	Slimy sculpin	PH	23/09		8.7		8.3
54479	Slimy sculpin	PH	23/09		9		9.7
54480	Slimy sculpin	PH	23/09		9.7		12.2
54481	Slimy sculpin	PH	23/09		10.4		16
54482	Slimy sculpin	PH	23/09		10.7		21.3
54483	Alewife	PH	23/09		9.4		8.2
54484	Alewife	PH	23/09		14.8		25.4
54485	Alewife	PH	23/09		16.3		31.1
54486	Alewife	PH	23/09		16.7		37.3
54487	Alewife	PH	23/09		17.6		42.2
54488	Alewife	PH	23/09		18.3		46.4
54489	Alewife	PH	23/09		19.3		51.6
54490	Alewife	PH	23/09		20		62.3
54491	Round goby	PH	23/09		7.1		5
54492	Round goby	PH	23/09		9.1		11.1
54493	Round goby	PH	23/09		8.6		9.2
54494	Round goby	PH	23/09		9.5		12.3
54495	Round goby	PH	23/09		10		14.3
54496	Round goby	PH	23/09		15.8		62.4
54497	Round goby	PH	23/09		16.5		80.9
54498	Round goby	PH	23/09		17.3		94.1
54499	Rainbow smelt	PH	23/09		13.3		13.6
54500	Rainbow smelt	PH	23/09		15.4		20.8
54501	Rainbow smelt	PH	23/09		17		30.3
54502	Rainbow smelt	NOTL	11/09		10.8		5.9
54503	Rainbow smelt	NOTL	11/09		12.4		9.7
54504	Rainbow smelt	NOTL	11/09		13.3		12.5
54505	Rainbow smelt	NOTL	11/09		13.8		14.9
54506	Rainbow smelt	NOTL	11/09		14.2		17.1
54507	Rainbow smelt	NOTL	11/09		15.3		21.2
54508	Rainbow smelt	NOTL	11/09		17.8		35.1

Table A-5-2: *Sampling details for Lake Ontario invertebrate samples.*

Sample number	Species	Location	Collection date
INV-1	*Diporeia*	Port Credit	April 10/07
INV-2	*Diporeia*	Port Credit	April 10/07
INV-3	*Diporeia*	Port Credit	April 10/07
INV-4	Plankton	Oswego	Sept. 27/07
INV-5	Plankton	Niagara-On-The-Lake	Sept. 27/07
INV-6	Mysids	Coburg	Oct. 04/07
INV-7	Plankton	Coburg	Oct. 01/07
INV-8	Plankton	Coburg	Oct. 01/07
INV -9	Mysids	Coburg	Oct. 04/07
INV -10	*Diporeia*	Coburg	Oct.04/07
INV -11	*Diporeia*	Port Credit	Oct. 11/07
INV -12	*Diporeia*	Port Credit	Oct. 11/07
INV -13	Plankton	Port Credit	Oct. 11/07
INV -14	Mysids	Niagara-On-The-Lake	Sept. 09/08
INV -15	Mysids	Niagara-On-The-Lake	Sept. 10/08
INV -16	Plankton	Niagara-On-The-Lake	Sept. 11/08
INV -17	Plankton	Oswego	Sept. 16/08
INV -18	Plankton	Oswego	Sept. 16/08
INV -19	Mysids	Oswego	Sept. 16/08
INV -20	Mysids	Oswego	Sept. 16/08
INV -21	Mysids	Coburg	Sept. 22/08
INV -22	Mysids	Coburg	Sept. 22/08
INV -23	Plankton	Coburg	Sept. 24/08
INV -24	Plankton	Coburg	Sept. 24/08

Table A-5-3: *Concentrations (ng/g wet weight) of PFOS isomers, total PFOS, and percent linear in Lake Ontario fish.*

Sample number	*n*-PFOS	*iso*-PFOS	1*m*-PFOS	3*m*-PFOS	4*m*-PFOS	5*m*-PFOS	Total dimethyl	Total PFOS	% linear
lake trout									
53402	67.743	2.203	0.309	0.143	0.333	0.547	1.018	72.151	93.9
53403	67.868	1.635	0.324	0.150	0.271	0.340	0.755	71.193	95.3
53404	76.772	1.615	0.376	0.175	0.278	0.295	0.784	80.120	95.8
53405	47.337	1.167	0.218	0.089	0.155	0.239	0.506	43.679	95.3
53406	56.970	1.415	0.289	0.118	0.202	0.335	0.685	52.724	95.0
53407	61.588	1.403	0.248	0.101	0.202	0.315	0.634	56.619	95.6
53408	53.700	1.258	0.247	0.101	0.174	0.278	0.536	49.462	95.5
53409	68.134	1.530	0.290	0.118	0.225	0.364	0.657	62.674	95.6
53410	48.928	1.118	0.246	0.100	0.171	0.223	0.428	44.995	95.6
53411	45.257	1.086	0.193	0.079	0.173	0.243	0.446	41.726	95.4
slimy sculpin									
54475	110.518	5.445	0.478	0.222	1.214	1.412	2.107	121.482	91.0
54476	96.998	4.558	0.425	0.197	0.992	1.199	1.904	106.383	91.2
54477	110.913	5.465	0.529	0.245	1.180	1.506	2.188	121.780	91.1
54478	110.319	3.864	0.384	0.157	1.035	1.249	1.762	104.576	92.8
54479	109.771	4.972	0.396	0.161	1.095	1.292	2.011	105.403	91.6
54480	160.863	5.216	0.512	0.209	0.949	1.092	2.065	150.095	94.2
54481	316.469	6.544	0.801	0.327	1.303	1.379	2.371	289.177	96.2
54482	146.798	nd	nd	nd	nd	nd	nd	129.081	100.0
alewife									
54483	31.044	0.584	0.155	0.063	0.101	0.136	0.163	28.300	96.5
54484	41.359	0.877	0.220	0.102	0.129	0.193	0.249	43.026	96.1
54485	28.964	0.778	0.155	0.072	0.099	0.088	0.210	30.295	95.6
54486	35.185	0.593	0.207	0.084	0.122	0.133	0.215	32.055	96.5
54487	32.495	0.500	0.156	0.063	0.111	0.122	0.186	29.550	96.7
54488	23.521	0.429	0.140	0.057	0.095	0.105	0.173	21.511	96.1
54489	25.630	0.447	0.150	0.061	0.110	0.115	0.187	23.424	96.2
54490	23.190	0.370	0.103	0.042	0.079	0.079	0.154	21.081	96.7
round goby									
54491	15.115	0.177	0.060	0.028	0.029	0.041	0.041	15.463	97.8
54492	13.067	0.140	0.035	0.014	0.024	0.045	0.052	11.750	97.8
54493	17.211	0.162	0.040	0.016	0.028	0.043	0.082	15.447	98.0
54494	19.861	0.237	0.059	0.024	0.042	0.064	0.088	17.894	97.6
54495	21.278	0.254	0.071	0.029	0.040	0.065	0.099	19.176	97.6
54496	22.425	0.304	0.087	0.035	0.023	0.060	0.083	20.209	97.6
54497	27.573	0.659	0.147	0.060	0.089	0.175	0.222	25.381	95.5
54498	46.687	0.992	0.185	0.075	0.059	0.199	0.341	42.613	96.3
rainbow smelt									
54499	32.685	1.073	0.083	0.038	0.169	0.269	0.742	35.054	93.2
54500	21.599	0.823	0.057	0.027	0.110	0.209	0.607	23.428	92.2
54501	22.992	0.951	0.053	0.025	0.130	0.234	0.713	25.112	91.6
54502	35.311	1.039	0.119	0.055	0.199	0.226	0.569	37.463	94.3
54503	38.792	0.988	0.075	0.030	0.162	0.231	0.597	35.978	94.8
53504	56.151	1.198	0.076	0.031	0.180	0.243	0.638	51.497	95.9
53505	49.641	1.174	0.076	0.031	0.168	0.243	0.685	45.802	95.3
54506	40.294	0.855	0.063	0.026	0.139	0.190	0.580	37.116	95.5
53507	35.011	1.157	0.066	0.027	0.169	0.222	0.870	33.086	93.0
53508	64.677	1.389	0.071	0.029	0.149	0.280	0.876	59.443	95.7

Table A-5-4: *Concentrations (ng/g wet weight) of PFOS isomers, total PFOS, and percent linear in Lake Ontario invertebrates.*

Sample number	*n*-PFOS	*iso*-PFOS	1*m*-PFOS	3*m*-PFOS	4*m*-PFOS	5*m*-PFOS	Total dimethyl	Total PFOS	% linear
LOFWI-1	65.166	0.647	0.000	0.000	0.079	0.090	0.112	66.094	98.6
LOFWI-2	115.920	1.109	nd	nd	0.180	0.175	0.192	117.576	98.6
LOFWI-3	98.963	0.947	0.071	0.029	0.145	0.137	0.190	88.330	98.5
LOFWI-4	3.036	0.065	0.001	0.001	0.011	nd	0.030	3.142	96.6
LOFWI-5	7.699	0.120	0.022	0.009	0.013	0.017	0.044	6.960	97.3
LOFWI-6	8.424	0.163	0.036	0.015	0.040	0.038	0.000	7.652	96.8
LOFWI-7	7.424	0.159	0.029	0.012	0.016	0.015	0.040	6.755	96.6
LOFWI-8	3.730	0.082	0.017	0.007	0.008	nd	0.020	3.392	96.7
LOFWI-9	8.552	0.171	0.030	0.012	0.039	0.036	0.062	7.817	96.2
LOFWI-10	130.209	1.497	0.138	0.056	0.266	0.222	0.304	116.628	98.2
LOFWI-11	95.700	1.170	0.130	0.053	0.165	0.204	0.210	85.803	98.1
LOFWI-12	129.222	1.562	0.134	0.055	0.229	0.268	0.328	115.844	98.1
LOFWI-12.2	132.086	1.585	0.112	0.046	0.185	0.215	0.277	118.232	98.2
LOFWI-14	7.976	0.145	nd	nd	nd	nd	nd	8.122	98.2
LOFWI-15	8.318	0.149	nd	nd	0.029	nd	0.051	8.547	97.3
LOFWI-17	5.561	0.153	0.028	0.011	0.032	0.045	0.060	5.169	94.6
LOFWI-18	5.095	0.256	0.050	0.020	0.046	0.070	0.104	5.621	90.6
LOFWI-19	5.318	0.090	0.019	0.008	0.030	nd	0.050	4.843	96.5
LOFWI-20	4.339	0.076	nd	nd	0.020	0.027	0.044	3.963	96.3
LOFWI-21	6.933	0.092	0.022	0.009	0.025	0.039	0.058	6.304	96.7
LOFWI-22	4.347	0.086	nd	nd	0.023	0.030	0.041	3.980	96.0
LOFWI-23	9.739	0.186	0.039	0.016	0.016	0.025	0.058	8.848	96.8
LOFWI-24	8.185	0.159	0.041	0.017	0.021	0.031	0.058	7.470	96.3

Table A-5-5: *Concentrations (ng/g wet weight) of PFOSA isomers, total PFOSA, percent linear, and the enantiomer fraction (EF) of 1m-PFOS in Lake Ontario fish. A dash (-) indicates that the EF was not measured.*

Sample number	*n*-PFOSA	*br*-PFOSA1	*br*-PFOSA2	*br*-PFOSA3	Total PFOSA	% linear	EF of 1*m*-PFOS
lake trout							
53402	0.37	0.06	0.08	nd	0.52	72.11	0.477
53403	0.44	0.03	0.04	nd	0.51	85.65	0.463
53404	0.31	0.03	0.03	0.01	0.38	81.62	nd
53405	0.54	0.03	0.04	nd	0.54	88.04	nd
53406	0.30	0.02	0.04	nd	0.32	83.46	0.477
53407	0.54	0.06	0.05	0.00	0.57	83.60	nd
53408	0.66	0.04	0.05	nd	0.66	87.97	0.463
53409	0.82	0.08	0.07	nd	0.85	84.48	0.461
53410	0.34	0.03	0.02	nd	0.34	85.94	nd
53411	0.25	0.03	0.03	nd	0.27	80.92	0.461
Slimy sculpin							
54475	2.13	0.90	1.26	0.16	4.45	47.91	0.493
54476	2.13	0.76	1.17	0.12	4.18	50.99	0.480
54477	2.65	0.95	1.46	0.12	5.18	51.07	0.495
54478	4.52	1.74	2.59	0.13	7.89	50.39	0.502
54479	4.73	1.68	2.36	0.13	7.83	53.18	0.486
54480	5.92	1.38	2.24	nd	8.38	62.10	nd
54481	17.25	3.62	4.80	nd	22.57	67.20	-
54482	7.43	1.98	1.47	nd	9.57	68.31	-
alewife							
54483	0.36	0.13	0.14	nd	0.55	57.13	0.465
54484	0.69	0.18	0.15	nd	1.02	67.69	nd
54485	0.74	0.19	0.14	nd	1.07	69.33	-
54486	1.41	0.41	0.39	0.01	1.95	63.54	nd
54487	1.55	0.38	0.36	0.03	2.04	66.53	0.480
54488	1.58	0.43	0.39	nd	2.12	65.74	0.476
54489	1.78	0.40	0.37	nd	2.24	69.69	0.457
54490	2.36	0.45	0.43	nd	2.85	72.82	0.476
round goby							
54491	0.23	0.11	0.20	nd	0.54	42.07	-
54492	0.67	0.47	0.64	nd	1.56	37.47	nd
54493	1.24	0.62	0.83	0.06	2.41	45.16	nd
54494	0.92	0.34	0.44	nd	1.50	53.95	0.508
54495	0.71	0.47	0.67	0.03	1.65	38.07	0.486
54496	0.65	0.32	0.50	0.03	1.32	43.69	0.449
54497	0.68	0.42	0.65	0.04	1.58	38.10	0.472
54498	0.67	0.31	0.50	0.03	1.33	44.29	0.470
rainbow smelt							
54499	0.96	0.37	0.40	nd	1.72	55.48	-
54500	0.87	0.30	0.32	0.03	1.52	57.10	-
54501	0.73	0.31	0.34	0.02	1.40	52.06	-
54502	0.51	0.19	0.20	0.00	0.90	56.28	nd
54503	2.65	0.89	0.99	0.08	4.05	57.54	0.499
53504	3.81	1.16	1.33	0.08	5.61	59.69	0.512
53505	3.38	1.11	1.26	0.07	5.12	58.13	0.481
54506	2.21	0.87	1.05	0.06	3.69	52.79	nd
53507	3.15	1.03	1.25	0.09	4.85	57.05	0.516
53508	5.24	1.63	1.86	0.15	7.81	58.99	nd

Table A-5-6: *Concentrations (ng/g wet weight) of PFOSA isomers, total PFOSA, percent linear, and the enantiomer fraction (EF) of 1m-PFOS in Lake Ontario invertebrates. A dash (-) indicates that the EF was not measured.*

Sample number	*n*-PFOSA	*br*-*PFOSA1*	*br*-PFOSA2	*br*-PFOSA3	Total PFOSA	% linear	EF of 1*m*-PFOS
LOFWI-1	1.39	0.17	0.39	nd	1.95	71.37	n/m
LOFWI-2	2.05	0.24	0.57	0.05	2.92	70.17	n/m
LOFWI-3	4.81	0.52	1.11	0.10	5.75	73.54	0.572
LOFWI-4	nd	nd	nd	nd	nd	-	n/m
LOFWI-5	0.09	0.03	0.04	nd	0.14	57.58	n/m
LOFWI-6	1.44	1.02	1.25	0.08	3.33	38.05	0.604
LOFWI-7	0.13	0.11	0.15	0.01	0.35	33.31	0.456
LOFWI-8	0.10	0.08	0.11	nd	0.26	35.10	nd
LOFWI-9	1.20	0.92	1.19	0.10	3.00	35.22	0.650
LOFWI-10	3.70	0.57	0.48	0.13	4.29	75.81	0.569
LOFWI-11	2.05	0.35	0.91	0.08	2.98	60.39	0.558
LOFWI-12	2.47	0.42	1.02	0.08	3.51	61.88	0.556
LOFWI-12.2	2.38	0.39	1.04	0.10	3.43	60.93	0.567
LOFWI-14	0.50	0.37	0.52	0.07	1.45	34.26	0.573
LOFWI-15	0.52	0.40	0.55	0.02	1.48	34.79	n/m
LOFWI-17	0.10	0.04	0.05	nd	0.17	52.63	0.470
LOFWI-18	0.03	0.02	0.02	nd	0.07	43.45	n/m
LOFWI-19	0.40	0.20	0.28	nd	0.78	45.45	n/m
LOFWI-20	3.49	1.60	1.54	0.05	5.88	52.23	n/m
LOFWI-21	0.78	0.32	0.40	nd	1.32	52.12	nd
LOFWI-22	1.77	0.73	0.81	0.04	2.94	53.01	n/m
LOFWI-23	0.26	0.04	0.05	nd	0.31	74.01	0.423
LOFWI-24	0.22	0.06	0.08	nd	0.31	63.10	0.439

Table A-5-7: *Least squares linear regression correlation statistics between PFOS and PFOSA for two variables: concentration and percent linear.*

	Concentration PFOS versus Concentration PFOSA		Percent linear PFOS versus Percent linear PFOSA	
species	**R^2**	**Significant at p=0.05?**	**R^2**	**Significant at p=0.05?**
Lake trout	0.035	no	0.55	yes, positive
Slimy sculpin	0.89	yes, positive	0.88	yes, positive
Alewife	0.38	no	0.02	no
Round goby	0.01	no	0.06	no
Rainbow smelt	0.69	yes, positive	0.26	no
Invertebrates (combined)	0.32	yes, positive	0.14	no

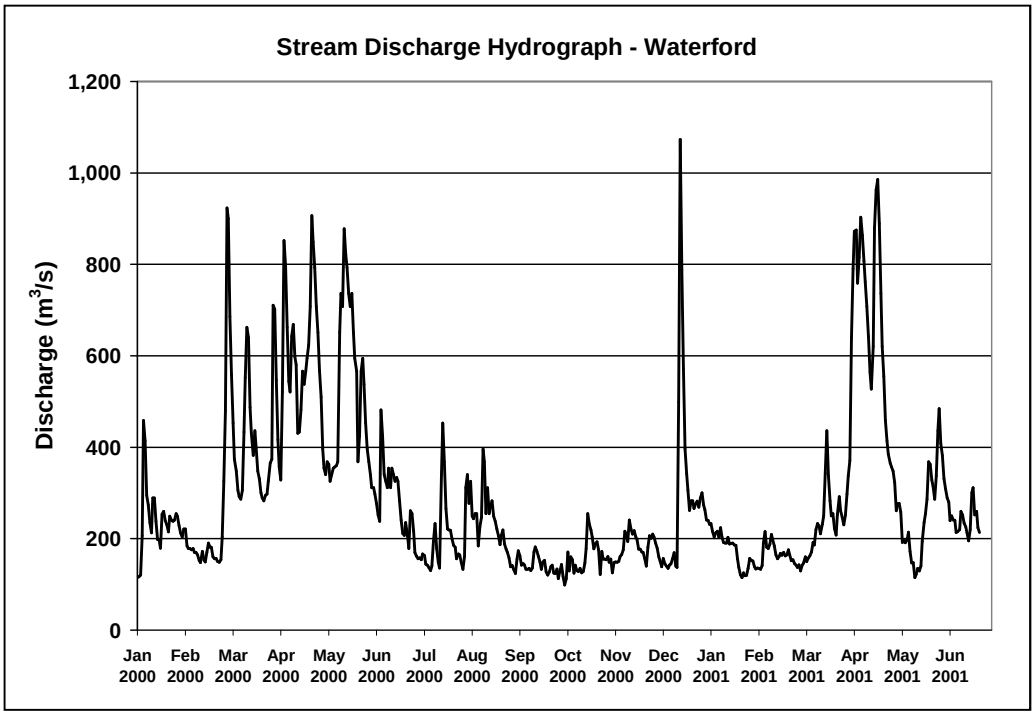

Figure A-2-1: *Stream discharge hydrograph for Hudson River at Waterford (monitoring station #01335755).*

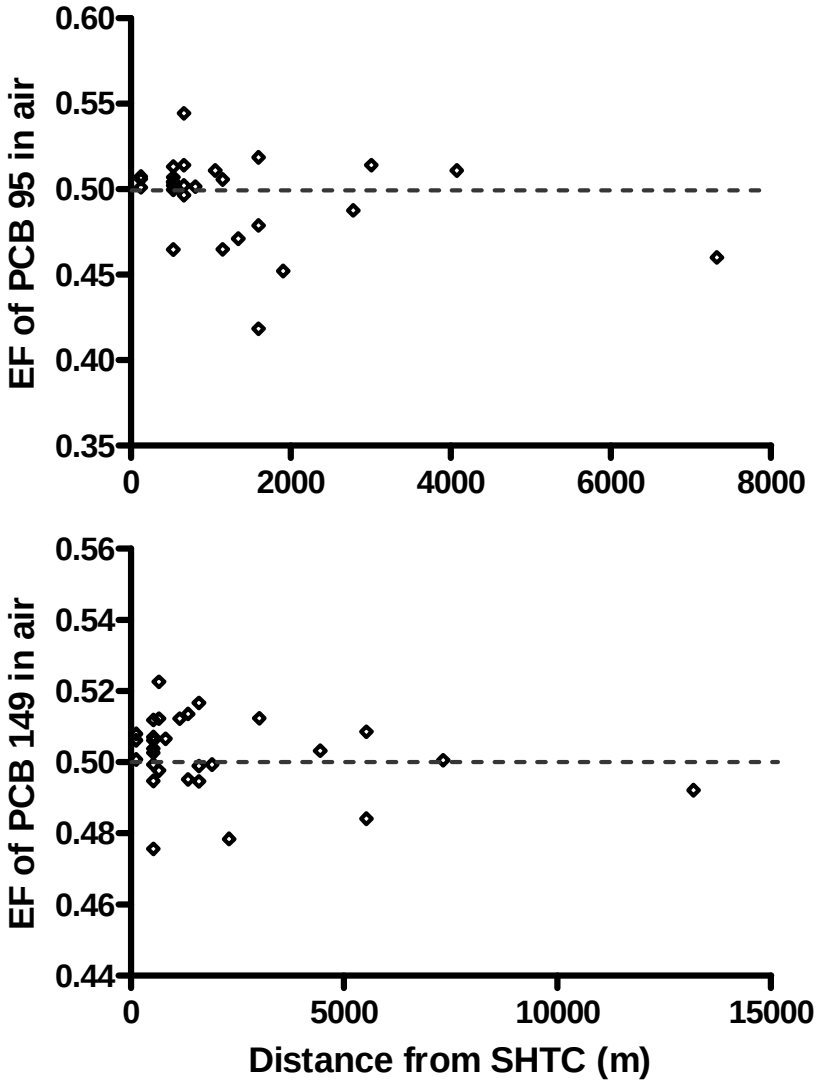

Figure A-4-1: *Enantiomer fraction of PCBs 95 and 149 in air as a function of distance from the Swan Hills Treatment Centre.*